CHARACTERIZATION OF THE 3' TERMINAL 42 NUCLEOTIDE HOST PROTEIN BINDING ELEMENT OF THE MOUSE HEPATITIS VIRUS 3' UNTRANSLATED REGION

A Dissertation

by

REED FINDLEY JOHNSON

Submitted to the Office of Graduate Studies of
Texas A&M University
in partial fulfillment of the requirements for the degree of

DOCTOR OF PHILOSOPHY

May 2003

Major Subject: Medical Sciences

CHARACTERIZATION OF THE 3' TERMINAL 42 NUCLEOTIDE HOST PROTEIN BINDING ELEMENT OF THE MOUSE HEPATITIS VIRUS 3' UNTRANSLATED REGION

A Dissertation

by

REED FINDLEY JOHNSON

Submitted to Texas A&M University
in partial fulfillment of the requirements for the degree of

DOCTOR OF PHILOSOPHY

Approved as to style and content by:

Julian L. Leibowitz (Chair of Committee)	Steve Maxwell (Member)
Van G. Wilson (Member)	Douglas K. Struck (Member)
Cristabel J. Welsh (Member)	Julius Gordon (Head of Department)

May 2003

Major Subject: Medical Sciences

ABSTRACT

Characterization of the 3' Terminal 42 Nucleotide Host Protein Binding Element of the Mouse Hepatitis Virus 3' Untranslated Region. (May 2003)

Reed Findley Johnson, B.S., Kansas State University

Chair of Advisory Committee: Dr. Julian Leibowitz

Mouse hepatitis virus (MHV) is a member of the coronavirus family in the order Nidovirales. The 32 kb genome contains cis-acting sequences necessary for replication of the viral genome. Those cis-acting sequences have been shown to bind host proteins, and binding of those proteins is necessary for virus replication. One of the cis-acting elements is the 3' terminal 42 nucleotide host protein binding element. Previous work has demonstrated that mitochondrial aconitase, mitochondrial heat shock protein 70, heat shock protein 60 and heat shock protein 40 bind to the 3' terminal 42 nucleotide host protein binding element. We demonstrated that RNA secondary structure of the 3' terminal 42 nucleotide host protein binding element is necessary for host protein binding in vitro. We also demonstrated that primary structure of the 3' terminal 42 nucleotide host protein binding element is necessary for viral replication by targeted recombination. DI replication assays infer that the 3' terminal 42 nucleotide host protein binding element plays a role in positive strand synthesis from the negative strand template. Current studies involve the infectious cDNA clone, which will provide definitive answers on the role of the 3' terminal 42 nucleotide host protein binding element in MHV replication.

TABLE OF CONTENTS

Page

LIST OF FIGURES

FIGURE Page

LIST OF TABLES

CHAPTER I

INTRODUCTION

Background

Mouse hepatitis virus taxonomy. Mouse hepatitis virus (MHV) is a member of the family coronaviridae of the recently introduced order nidovirales (20). The other nidovirus family members are the toroviruses and arteriviruses. Corona- arteri- and toro-viruses were organized into the same family because all have a positive sense, single stranded, RNA genome, similar RNA dependent RNA polymerase organization, and a 3' co-terminal nested mRNA structure (14). Arteriviruses are smaller than coronaviruses and toroviruses with enveloped virions containing icosahedral nucleocapsids and measure 50-75 nm in diameter and lack surface projections that are found in corona- and toroviruses (20). Arterivirus genomes are smaller as well, 13-15 kb, examples are porcine reproductive respiratory syndrome virus, equine arterivirus, lactate dehydrogenase elevating virus, and simian hemorrhagic fever virus. The toroviruses, which include bovine torovirus, equine torovirus, human torovirus, Bredavirus, and porcine torovirus, vary from corona- and arteriviruses because toroviruses lack a 5' leader sequence, have a tubular capsid structure, and the M protein, which is functionally similar to coronavirus M proteins, is not glycosylated (14). Toroviruses are pleiomorphic, measure 120-140 nm in diameter, and have surface projections that resemble coronavirus surface projections. Torovirus genomes range in size from 20-25 kb. Coronaviruses are the largest single stranded RNA virus genomes known, the

This dissertation follows the style of Journal of Virology.

genomes range in size from 23-31 kb (14). Coronaviruses have a helical nucleocapsid and are 100-120 nm in diameter and have a “corona” of peplomers, composed of spike protein which acts as the ligand for host cell receptors.

The coronaviruses are made up of 3 distinct groups based upon organization of nonstructural proteins, antigenic properties, and the processing of the spike protein into two halves (14). The group 1 coronaviruses include canine coronavirus, feline infectious peritonitis virus, human coronavirus 229E, and transmissible gastroenteritis virus. The group I coronaviruses may process spike protein into S1 and S2 portions and some species express a hemagglutinin esterase protein in reading frame 2, group 1 viruses also use aminopeptidase N as a receptor for entry into host cells and may have two open reading frames after the nucleocapsid gene (14, 100). The group 2 coronaviruses include bovine coronavirus, human coronavirus OC43, rat coronavirus, and mouse hepatitis virus (MHV). Group 2 viruses process spike protein into S1 and S2 portions and some strains of some species will express a hemagglutinin esterase as a possible co-receptor. Group 3 coronaviruses include infectious bronchitis virus, and turkey coronavirus. Group 3 viruses process spike protein and do not express a hemagglutinin esterase, they also vary from group 1 and 2 due to the presence of open reading frames between genes M and N.

The human coronaviruses are known to cause diarrhea, gastroenteritis, and necrotizing enterocolitis (79, 81, 103). Human coronaviruses have been associated with multiple sclerosis, OC43 and 229E antigens have been located in CNS tissue from

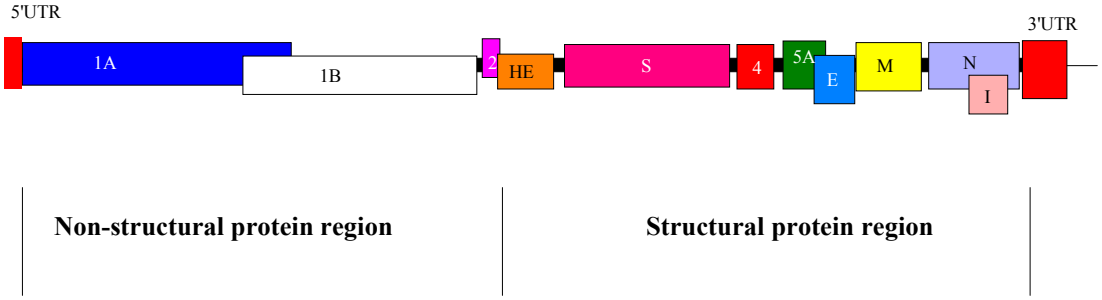

Figure 1. Schematic representation of the MHV genome. The shaded regions indicate the different reading frames for the MHV proteins produced. The rendering is not to scale as the the ORF 1A and IB reading frames comprise nearly 2/3 of the MHV genome. The dark boxes between the reading frames indicate aTRS sequence. The boxes at the termini of the genome indicate the untranslated regions.

human multiple sclerosis patients (13). MHV can cause an encephalomyelitis in mice depending upon the infecting strain and serves as a mouse model for multiple sclerosis (22). Intracerebral inoculation of weanling mice with MHV-JHM results in a demyelinating disease with lesions that can be seen as early as 4 weeks (48).

MHV genome organization. The MHV genome is organized into a 5' non-structural protein region and a 3' structural protein region and acts as a messenger RNA when introduced into a host cell. See Figure 1. The genome is capped, poly-adenylated, and codes for seven mRNA's which are responsible for at least 7 proteins (92). See Figure 2. RNA's 5 and 7 each have two open reading frames (ORF's) (23, 111). Messenger RNA 1, which is genome length, contains two overlapping reading frames ORF 1a and ORF 1b that generate a 740 KDa polyprotein which is then cleaved post- and co-translationally (12). Genes 2 through 7 encode the structural proteins and two nonstructural proteins. Each gene is separated by a short intergenic sequence, the transcriptional regulatory sequence (TRS), which acts as a cis-regulator of transcription. The TRS's precise role in transcription is debated and will be covered in the section on MHV transcription. The genomic TRS regions have a UCUAA nucleotide motif repeated varying number of times depending upon the gene (101). Each of the 7 mRNA's carry a 72nt leader sequence derived from the 5' end of the genome and a co-terminal 3' UTR. Only the 5' unique region of each mRNA is translated.

MHV proteins. The non-structural genes are coded by mRNA 1, which is the full-length infectious mRNA and codes for the RNA dependent RNA polymerase and associated proteins which are co- and post- translationally processed. The coding region

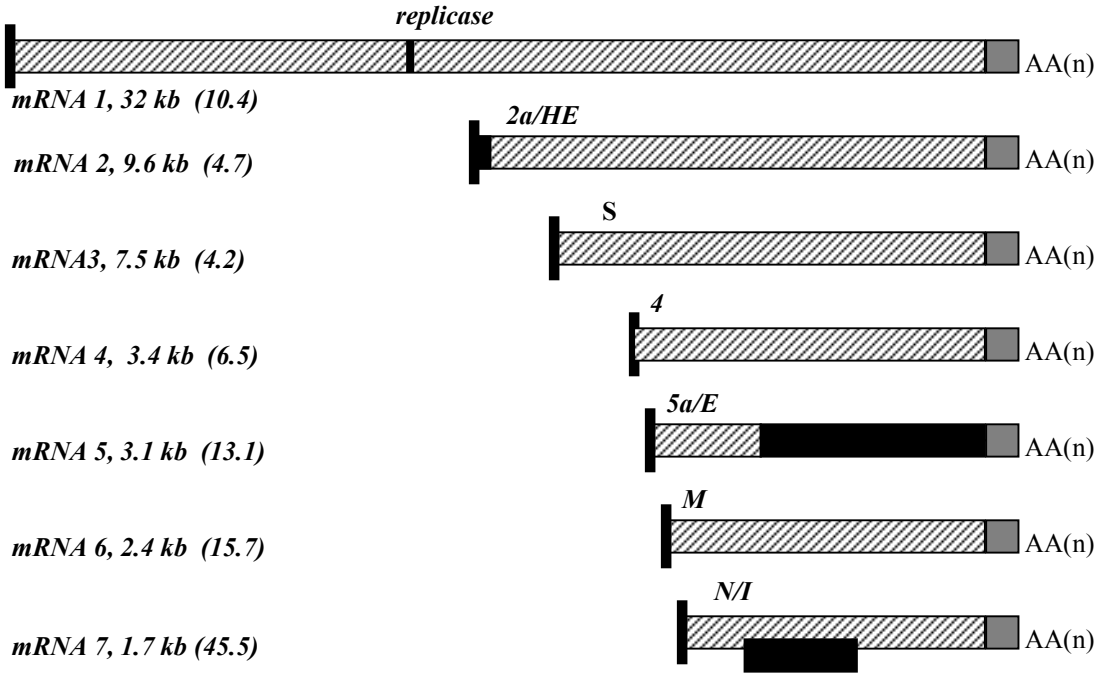

Figure 2. Organization of the subgenomic mRNAís of MHV, protein functions are described in text, sizes and relative molar abundance are listed. The hashed region indicates the ORF of each mRNA, the leader sequence is the dark box at the 5í end of each mRNA. The alternate reading frame of each mRNA is also indicated by a black box. The grey box indicates the 3í UTR that is present on each mRNA. The figure is not to scale.

comprises nearly two-thirds of the genome and is composed of two overlapping ORF's. The –1 frameshift that allows for the switch to ORF 1B is mediated by a pseudoknot and alignment of a 7 nucleotide sequence (12). The polyprotein is thought to function as the RNA dependent RNA polymerase of the virus and as many as 8 functions are associated with the mRNA polyprotein as determined by complementation analysis (96). ORF 1a encodes 2 papain like protease domains and a picornavirus like 3C protease (10). ORF 1b contains a helicase domain and an NTP binding domain and is most likely the core unit of the RNA dependent RNA polymerase (50). See Figure 2 for MHV protein assignments.

Two mRNA's are produced from gene 2 in most MHV strains. The first mRNA, mRNA –2 produces a 30kDa nonstructural protein whose role in the virus lifecycle is not understood (11). The second mRNA is only expressed in some MHV strains. It encodes a hemaggluttinin-esterase (HE), which acts as a secondary receptor and may be involved in tissue tropism. It is not expressed in A59 strain due to a deletion of the initiating methionine (58). A59 is mildly hepato- and neuro- tropic, but it is variably expressed in the neurotropic JHM strain. MHV-3 does not express HE and is predominantly hepatotropic. The variability of expression of hemagglutinin esterase in neurotropic and hepatotropic strains makes it hard to pinpoint a role for HE as a co-receptor or a factor in determining tissue tropism.

The major ligand for the host-cell receptor is the spike protein expressed by mRNA 3. Spike protein binds to CEACAM 1, which is a type 1 membrane spanning protein, of host cells. Spike exists as two portions S1 and S2 that are not covalently

associated (26, 59). S1, which has no membrane spanning region, and resides on the outer surface of a mature virion, is a target for neutralizing antibodies that provide protective immunity (44). S2 also acts as a target for neutralizing antibodies and contains a membrane-spanning portion (16, 18). Antibodies raised to S2 will block syncytia formation in infected cells and lowers virus yield. Lai's group isolated an A59 mutant that had amino acid 159 changed from a glutamic acid to lysine that grew well in tissue culture but its role in a live animal was not fully explored. Weiss's group introduced this mutation into MHV-A59 using Masters' feline infectious peritonitis virus spike protein based targeted recombination system. Studies of the engineered mutant indicate that the Q159L mutation in spike protein decreased hepatotropism and attenuated MHV-A59's ability to induce demyelination, reinforcing the spike proteins role in tissue tropism and disease progression (51).

The fourth mRNA codes for a non-structural protein of undetermined function. The role of the 139 amino acid product of gene 4 in the MHV lifecycle is a mystery, although a knockout virus was produced by targeted recombination. The gene 4 knockout virus exhibited no difference in growth kinetics, had similar CPE, and no change in titer when grown in tissue culture. When the gene 4 knockout virus was introduced in mice there was no apparent change in pathology when compared to MHV-JHM infected mice (73). A second study also using targeted recombination to produce a gene 4-ORF 5a knockout virus showed only a slight decrease in titer in tissue culture cells. Upon challenging mice, mortality due to virus infection was reduced when compared with wild-type infected controls. The 7-day post infection mice however did

exhibit clinical signs of infection suggesting that the 4-5a knockout virus is attenuated in mice (19). Although the specific function of gene 4 is unknown it is apparent that gene 4 plays a role in pathogenicity of MHV-JHM.

The fifth mRNA has two alternate reading frames, ORF 5a and ORF 5b. ORF 5a is not expressed in tissue culture, but may be necessary for infection of an animal. ORF5b is preferentially expressed in tissue culture, and encodes a third membrane protein, E, that is required for formation of virion particles (24, 111). E is an integral membrane protein whose amino terminus is highly hydrophobic and buried in the membrane of virion envelopes, the carboxy terminus extends into the virion and may interact with other viral structural proteins (60). E has also been shown to induce apoptosis in MHV infected 17Cl-1 cells and expression of E protein by recombinant vaccinia virus constructs also induced apoptosis in DBT cells (4).

The sixth mRNA codes for M protein which is a membrane spanning protein required for virion assembly. Some antibodies targeted to M are neutralizing in the presence of complement (25). M protein has been shown to interact with genome associated N protein in pre-Golgi complexes, which is the site of virion assembly and release (69). Work by Nguyen and Hogue demonstrated that BCoV M interacts with HE and S proteins in the ER or IC shortly after protein synthesis begins and suggests M's role in organizing assembly of the virion. However, another study of M protein failed to show an interaction of M with S and E using MHV and Sindbis virus constructs expressing MHV proteins but supported the N and M interaction (69). The data from both studies indicates that M and N interaction is necessary for virus growth and that M

serves as a “central organizer for virion assembly” as suggested by Nguyen and Hogue (70). The difference in results concerning possible interactions of S and HE with M and N could be due to the methodology used and time points post infection studied. Nguyen’s work used BCoV and relied on pulse chase experiments followed by co-immunoprecipitation of M, HE, and S, and immunofluorescence with antibodies to M, HE, and S, while Narayanan et al. used co-immunoprecipitation of M, N, and S from MHV infected cells, and co-infection with Sindbis virus constructs carrying the MHV proteins M, N, and S. Both approaches are feasible and it is likely that the varying results are due in part to the virus used and the time course studied, a period of 1 hour at 15 hours post infection for Nguyen and Hogue versus Narayanan’s work which only gave data for 8.5-9.0 hours post infection, but used MHV. The data suggests that the interactions described in both experiments are reasonable and that M is necessary for structural viral protein interaction although the interaction may be transient. Data to support M and N interaction and its role in virion formation has also come from Kuo and Masters. A deletion mutant of the 2 carboxy terminal amino acids from M was constructed and exhibited M’s requirement for assembly (46). Mutant viruses that were able to grow displayed a 10^3 decrease in viral titer and had small plaque sizes. Revertant viruses that restored titer to near wild type levels were found to have mutations elsewhere in the M gene and also in the N gene but not in the E gene (46).

The seventh and most abundant mRNA is the nucleocapsid protein, which contains two reading frames, the first and predominately used reading frame codes for the nucleocapsid protein, N, which is the most abundant protein in infected cells and

mature virions. N preferentially binds to genome length viral mRNA and has also been shown to bind to M protein to help form an intact virion. N's binding to RNA is determined by its phosphorylation state, when phosphorylated N will bind genomic RNA and when dephosphorylated by specific host cell phosphatases N releases RNA. This release of the RNA may act as one of the initial steps in replication (37). The alternate reading frame encodes a small protein associated with the virion, I. The precise role of I protein has not been identified, but using targeted recombination Fisher et. al were able to demonstrate that mutation of its reading frame did not deleteriously effect viral replication in tissue culture, but did not rule out a role in an infected animal (23).

MHV transcription. Transcription of the 7 MHV mRNA's occurs through a poorly understood mechanism. Currently there are three models that attempt to explain transcription. See Figure 3. The first model is leader-primed transcription (A. in Figure 3), in this model the viral RdRp complex uses genome length complementary RNA as a template for transcription. The leader, a 72 nt RNA has a 3' region that is complementary to the transcriptional regulatory sequence (TRS) on the full length negative strand. The model proposes that the leader anneals to the intergenic regions of each of the genes and transcription proceeds to the 5' terminus of the negative strand. The resulting products are translationally active genomic and subgenomic mRNA's that are 5' and 3' co-terminal (7, 62). This model is supported by the presence of free leader RNA that would serve as a primer to transcription (7). However, another model developed when subgenomic negative strand RNA's were found in infected cells

A. Leader primed transcription

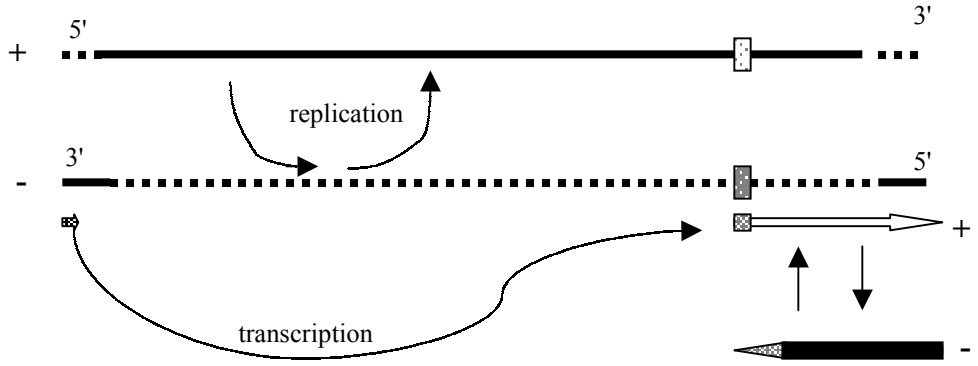

B. Premature termination of transcription

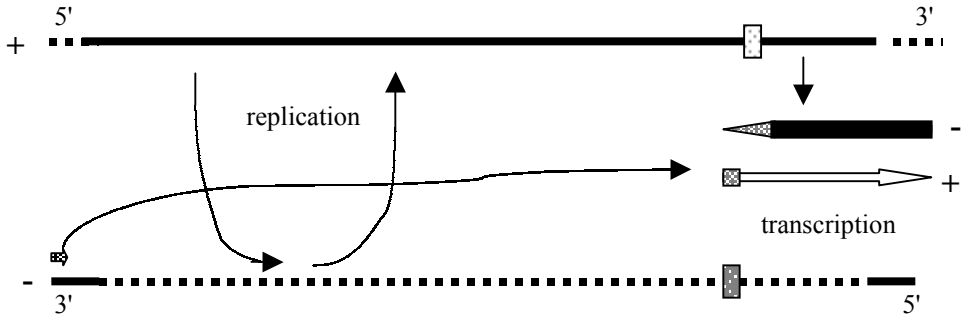

C. Discontinuous transcription

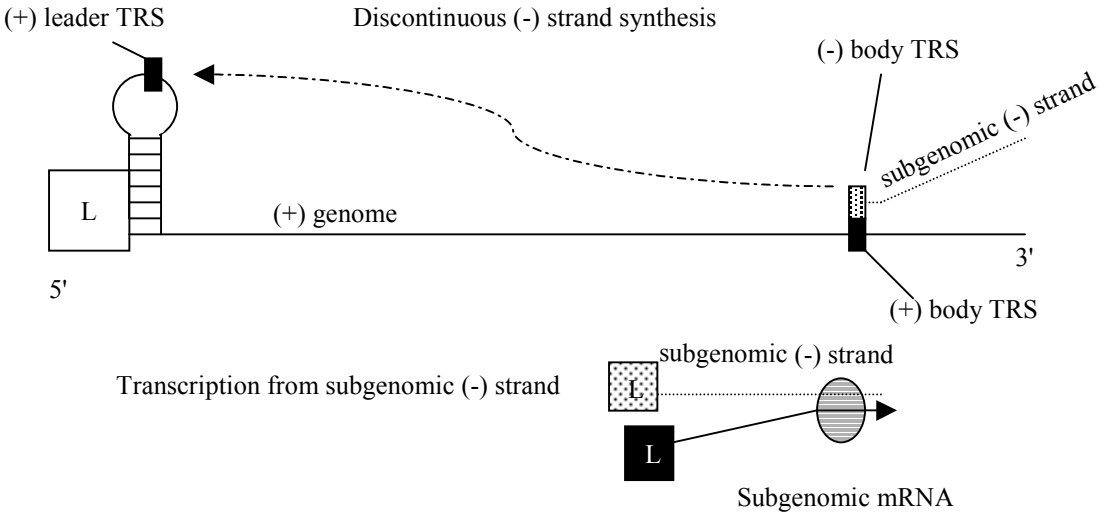

Figure 3. MHV transcription models. Details are covered in the text.

(83, 87). Brian's group identified subgenomic negative strand RNA's in TGEV infected cells by Northern blot analysis of denatured RNase resistant RNA molecules, their time course analysis demonstrates that subgenomic complementary strand RNA's were produced prior to subgenomic mRNA production suggesting a role for the subgenomic complementary strand RNA's as functional templates for mRNA synthesis. This model depends upon premature termination in the generation of full length negative strand RNA's that result in subgenomic negative strand RNA's that contain the 5' and 3' cis-acting elements present in the genome length RNA (B. in Figure 3). These elements could then be recognized by host and viral factors necessary for positive strand synthesis producing positive strand subgenomic RNA's. The resulting subgenomic complementary strand RNA's could then serve as active transcription templates by annealing of the 72 nt leader to the anti TRS in the complementary subgenomic RNA. The RdRp then extends towards the 3' end to produce subgenomic mRNA's.

The third model, discontinuous transcription, uses the negative strand subgenomic length mRNA's as transcription templates for subgenomic mRNA production. In this model (C. in Figure 3) subgenomic complementary RNA's are initiated from the 3' UTR of the MHV genome. The complementary RNA is extended until an intergenic region is reached, the RNA molecule then dissociates and re-associates at the 5' end of the genome where an anti-leader sequence is added, and the complete complementary subgenomic RNA then serves a transcription template. The intergenic regions are thought to serve as transcriptional attenuators rather than transcription start sites as in the leader-primed mechanism. Kinetic data indicates that

subgenomic complementary RNA's are synthesized before subgenomic mRNA's (83, 84, 87). Other support for the discontinuous mechanism comes from a study of temperature sensitive mutants from Schaad and Baric (85). A temperature sensitive mutant of MHV was unable to produce subgenomic complementary RNA's at the restrictive temperature and infection was impaired. Upon switching the infected cells to the permissive temperature the temperature sensitive mutant would produce subgenomic complementary RNA's and mRNA's (85). Regardless of mechanism, the temperature sensitive and kinetic data strongly suggest a role for the complementary subgenomic RNA's to act as active transcription templates to produce viral mRNA's.

Support for the discontinuous model of MHV replication comes from studies of the phylogenetically related arterivirus, equine arteritis virus (EAV). An infectious cDNA of EAV has been developed and studied (102). A point mutant in the replicase gene that converts a serine residue to proline at nucleotide position 7508 from the 5' end was found to be replication competent yet defective in production of subgenomic RNA's. Immuno-fluorescence assays using antibodies to NSP-2 (the EAV RdRp) indicated that the transfected viral RNA's containing this point mutant replicated and translated, and metabolic labeling confirmed the synthesis of genome length positive strand RNA's. Metabolic labeling and RT-PCR of transfected cultures found that subgenomic mRNA's were not synthesized except for a trace amount of mRNA 7 (102). These data alone fail to support discontinuous transcription, but demonstrate that transcription and replication are not coupled. Further study of the EAV infectious clone demonstrated that specific base pairing of the leader 3' sequence to body complementary

mRNA's is required for subgenomic mRNA synthesis (74). Mutagenesis of the leader TRS 3' sequence without a compensatory mutation in the body complement strand yielded viral genomes that still replicated but were transcription defective. The 3' end of the leader TRS is thought responsible for the RNA:RNA interaction and serves as the initiating event in transcription. Sequencing of the lower yield mRNA's indicated that the TRS in the subgenomic mRNA's is derived from the body TRS and not the leader TRS. The only mRNA that was still produced was mRNA 3, but that was transcribed using a different repeat of the 3' TRS sequence. Infectious clones that contained complementary base pairs in the positive sense leader and the complementary TRS strand did not have any defects in transcription or replication supporting the role of proper base-pairing of the leader and the body complement RNA for transcription. These data support the discontinuous model because they show that the subgenomic complementary TRS body sequence is present in the mRNA's produced which supports the model for discontinuous transcription of MHV by giving evidence that the complementary strand RNA is used as a template, and that specific interactions between the 3' end of the leader RNA and the TRS in the complementary subgenomic mRNA's are functional.

MHV replication. MHV replication is thought to occur shortly after entry and uncoating of the virion through production of a full-length negative strand intermediate. Negative strand RNA's have been detected by ribonuclease protection assays as early as one hour 20 minutes post infection (55). The negative strand intermediate then serves as

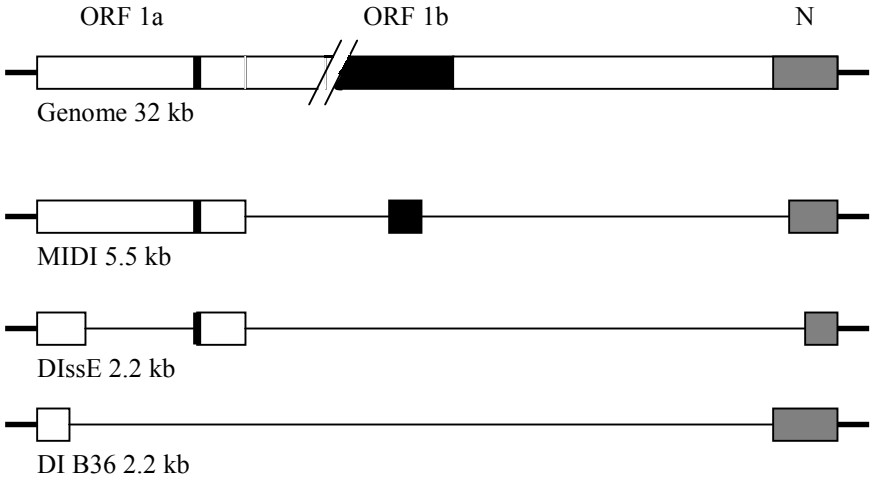

Figure 4. Schematic of defective interfering RNA's MIDI, DIssE, and DI B36, indicating the regions of the genome from which each DI is derived.

a template for the RNA dependent RNA polymerase (RdRp) to generate full length genomic RNAs. The negative strand RNA is probably produced by the RdRp's recognition of loosely identified signals in the 3' UTR of the positive strand genomic RNA, possibly mediated by RNA sequence and/or conformation and interaction of host factors. Using DI replication studies, Lin et al identified the 3' terminal 55 nucleotides as a requirement for negative strand synthesis, but did not further characterize which nucleotides were required or if any host or viral proteins specifically interacted with the 3' terminal 55 nucleotide element (55). After recognition of signals in the 3' UTR, the RdRp produces a full-length negative strand RNA molecule. Replication is thought to occur on smooth membranes of cells, possibly on the intermediate compartment (IC), which is thought to be the release site of mature virions (92). Recent studies have shown replication complexes forming on the smooth membranes of cells including the lysosome, but not specifically on the IC (21)

To date MHV replication has been studied through the use of defective interfering RNA's. DI RNA's are RNA molecules that contain portions of the genome, which are sufficient for replication in the presence of helper (wild type) virus. DI RNA's are thought to originate as a result of recombination events that give rise to RNA molecules of varying sizes and compositions that contain the necessary cis-acting signals for replication. The major DI's used for replication studies are DIssE, MIDI, and B36. See Figure 4. DIssE has been used extensively and has probably provided more data on cis-acting replication signals than the other DI's. DIssE is a 2.2 kb, naturally occurring DI, which was isolated from serial passage of MHV-JHM (61). DIssE is composed of 3

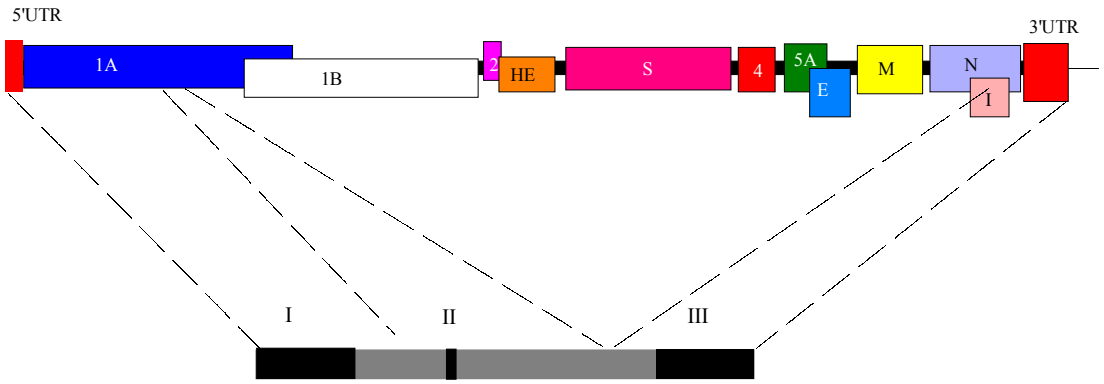

Figure 5. DIssE is derived from the regions of the MHV genome indicated by the hashed lines. The black boxes indicate the regions necessary for replication of DIssE.

regions from the MHV-JHM genome. Region one is from nts 1-864, region II is derived from a 784 nt internal region originating from 3.3 to 4 kb from the 5' end of the genome, and region III is derived from the 601 3' terminal nucleotides. Studies of DIssE mutants have identified several regions required for DI replication: the 5' terminal 474 nts are necessary for replication as is a 58 nt element derived from region II, and the 3' terminal 436 nts are also needed (5, 41, 61). See Figure 5. A recent study of MIDI-C by Spagnolo and Hogue demonstrated that at least 5 A residues in the poly (A) tail are required for replication and the poly (A) tail formation (93).

Studies focusing on the 3' UTR have shown that RNA secondary structure is necessary for replication of DI RNA's. A study of the 5' end of the 3' UTR by Master's lab suggests that a cis-acting 68 nt bulged-stem-loop predicted to contain 6 stem-loop regions is required for DI replication and that secondary structure of the bulged-stem-loop is essential for viral replication (34). Using targeted recombination to generate mutant viruses of the 68 nt bulged stem-loop Hsue et al. demonstrated that primary and secondary structure were important for viral replication (33). Mutations were made in the left arm (or 5' segment of bulged-stem-loop) and the right arm (or 3' segment of the bulged–stem-loop) or both of each of the 6 stem regions and evaluated for their ability to replicate. Those mutants that could not be engineered by targeted recombination were explored by DI replication assays using DI B36. Chemical and enzymatic probing of the 68 nt stem-loop indicated that the original prediction was incorrect and that only 4 stem-loop structures are present. Chemical and enzymatic probing demonstrated that stem-loop A did not exist and that the nucleotides involved in stem A were predicted to be

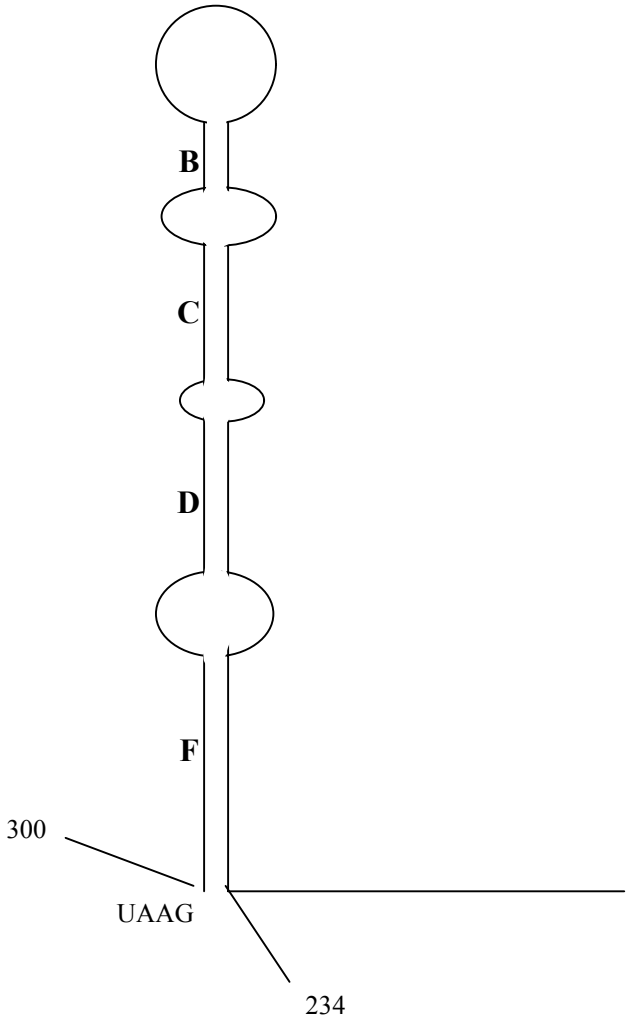

Figure 6. The stem loop structure adjacent to the N gene stop codon. The stem loop is at the 5' end of the 3' UTR. The stem loop regions are indicated by the upper-case letter on the left side of the stem-loop structure and each regions role in replication is discussed in the text. Previous predictions indicate two more stem-loop structures, but chemical and enzymatic probing does not support their formation.

unpaired and form a larger loop than earlier predicted the loop region of stem-loop B in Figure 6. Mutagenesis of stem B showed that primary and secondary structure could be altered with no effect on replication ability of the DI. The primary sequence of stem-loops C and D could be disrupted, but as long as wild type secondary structure was intact the recombinant virus was viable. Stem E was also non-existent based upon chemical and enzymatic probing and is now predicted to be unpaired and is thought to form a large internal loop (between D and F in Figure 6). Mutagenesis of stem F indicated that mutating either the left or right arm was deleterious to replication. Stem F is thought to be critical for forming an RNA:RNA interaction with a pseudoknot structure identified by David Brian's lab (105).

Brian's lab identified a pseudoknot structure in the 3' UTR of BCoV immediately downstream of Masters' 68 nt stem-loop structure (105). An earlier study by Hsue and Masters showed that the 3' UTR's of MHV and BCoV were functionally interchangeable and share high homology (34). Mutagenesis of the nucleotides thought responsible for the RNA:RNA interaction resulted in decreased replication of the DI RNA's studied, supporting the role for a highly conserved tertiary structure, mediated by proper secondary structure to function in viral replication. See Figure 7.

Recently Liu et al used limited ribonuclease digestion and computer modeling to define the secondary structure of the 3' terminal 166 nucleotides (57). Digestion data and computer modeling demonstrate that the 3' terminal 166 nucleotides form multiple stem-loop structures. DIssE mutants were developed that would disrupt base pairing in

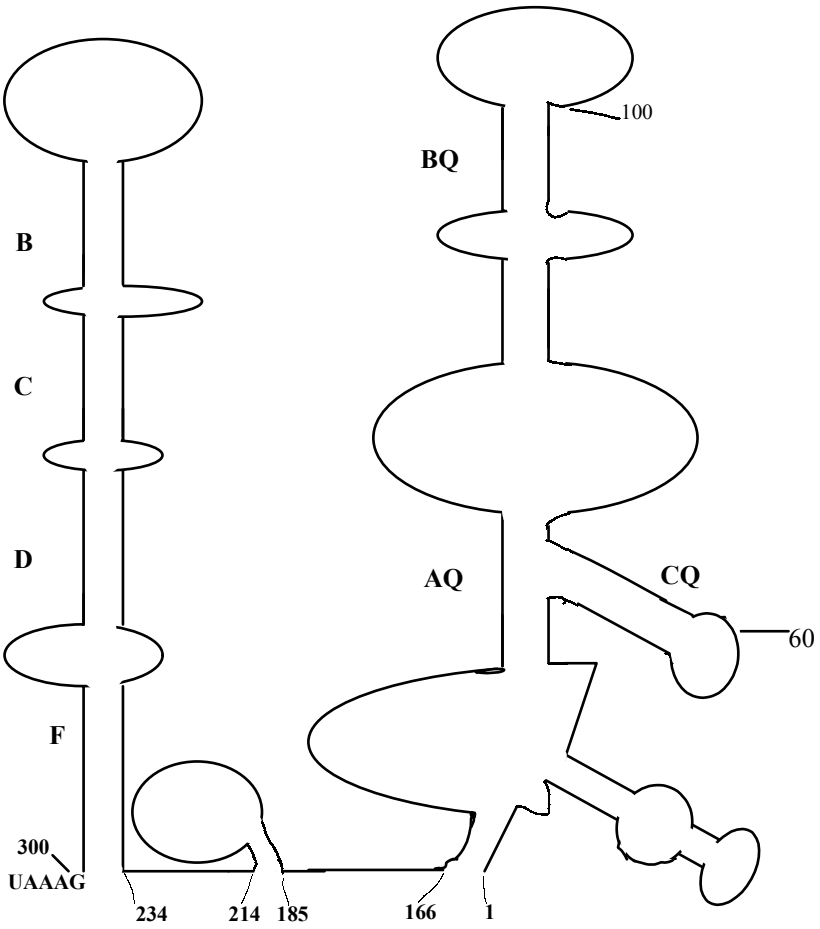

Figure 7. Schematic representation of the defined secondary structures of the MHV 3' UTR including the psuedoknot identified in BCoV. The nucleotide positions are arranged so that position 1 is the first nucleotide 5' to the poly A tail.

the stem sections of the model and tested for effects on DIssE replication. When clustered point mutations were made in either arm of a stem segments AQ and BQ DIssE would not replicate as well and would occasionally recombine to restore wild type primary structure. Mutations in CQ replicated about as well as wild type and were not investigated further. See Figure 7. When compensatory mutations, which should restore base pairing, were introduced DI replication could be restored to near wild type levels and in a couple of individual experiments compensatory mutant DI replication exceeded wild type DIssE replication, supporting a role for RNA secondary structure in MHV replication.

Host proteins have been shown to interact with the regions involved in the secondary and tertiary structures described but not specifically with the proposed stem-loop and pseudoknot structures. Whether or not the RNA structures actually play a role in host protein binding for the 68 nt stem-loop or the pseudoknot has not been tested. Data from Leibowitz's lab indicates that host proteins bind to specific nucleotide motifs within the 3' UTR. Leibowitz's lab identified two host protein binding elements within the 3' terminal 166 nucleotides, secondary structure analysis of this region by computer modeling, limited ribonuclease digestion, and mutagenesis of DI's directed at disrupting RNA secondary structure indicate that secondary structure influences replication (57). Mutation of the protein binding motifs was shown to decrease host protein binding by gel mobility shift RNase T_1 protection assays. When the same mutations were introduced into DIssE for DI replication assays, the mutant DI's did not replicate as well or recombined to restore wild type primary structure, suggesting an importance for host

protein binding to a proper structure (either primary, secondary or both) (56, 109, 110). RNA conformation is not only important for the 3' UTR for replication, but in the internal 58 nucleotide region as well. Work by Repass and Makino indicates that secondary structure of the internal 58 nucleotide region is necessary for replication (78). Mutagenesis of this region, using mutations designed to disrupt predicted secondary structure, indicated that secondary structure of the 58 nucleotide region played a role in DI replication. DI's carrying mutations that disrupted the proposed stem loop structure did not replicate as well as wild type DI's.

The role of host proteins binding to the MHV 3' UTR and the effect of binding on replication has been studied and is the major focus of this dissertation. Previous MHV work has identified 7 proteins that bind to separate regions of the MHV 3' UTR and the proteins do play a role in replication. See Figure 8. Lai's lab has shown that heterogenous ribonucleoprotein A1 (hnRNP-A1) binds to negative strand leader RNA's and in MHV infected cells hnRNP-A1 translocates from the nucleus to the cytoplasm. HnRNP-A1's normal role in the cell is for alternate splicing of cellular RNA's in the nucleus. Using mutant DIs Li et al were able to show that DIs with sequence that demonstrated decrease in hnRNP-A1 binding also showed a decrease in transcription of DI's suggesting hnRNP-A1's role in MHV transcription (53). However, Shen and Masters demonstrated that hnRNP-A1 did not act as transcriptional enhancer, and that a cell line that does not normally express hnRNP-A1 could grow MHV without any deleterious effects (88). Support for hnRNP-A1's role in the MHV lifecycle comes from studying the overexpression of hnRNP-A1 that resulted in accelerated accumulation of

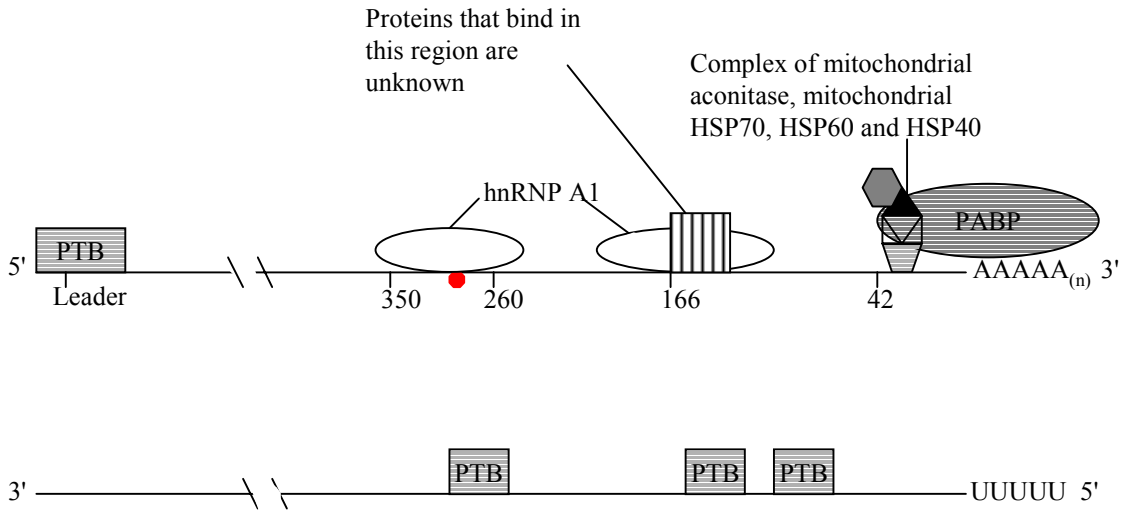

Figure 8. Identified binding sites of known host proteins in the MHV genome and complementary RNA. See text for details for each protein's rol e in the MHV lifecycle. The numbers indicate the approximate nucleotide position each protein or protein complex binds. The dark octagon indicates the stop codon for N gene.

viral RNAs (90). Using a carboxy terminal deletion mutant Lai's lab also showed a dominant negative effect where transcription and replication were inhibited when compared to wild type cells. The carboxy terminus of hnRNP-A1 is thought to be the RNA binding domain (90).

HnRNP-A1 has also been shown to bind to the 3' UTR at positions 90-170 and 260-350 from the 3' terminus excluding the polyA tail (36). This region is complementary to the polypyrimidine tract binding protein (PTB) binding site in the complementary strand RNA. Binding of the hnRNP-A1 to the 5' and 3' UTR's as well as the location of binding suggested a possible role for mediating interaction of the 5' and 3' ends of the genome. Support for the proposed cross-talk comes from using GST fusion proteins of hnRNP-A1 and PTB along with radiolabeled 3' UTR and biotinylated leader. Probes were pulled down by streptavidin columns and the proteins that were pulled down were identified as PTB and hnRNP-A1. Interestingly both RNA probes were needed to extract PTB and hnRNP-A1, either probe alone with both proteins did not pull down the other RNA supporting the necessity of all components to form a complex.

PTB has been shown to bind to the complement of the 3' UTR (5' end of the complementary strand RNA molecule, the putative template for genome replication) PTB binding was shown to alter RNA secondary structure as tested by biochemical probing. PTB was found to bind nucleotides 77-82, 132-136, and 270-305 from the 5' end of the complementary RNA. PTB has also been shown to bind to leader RNA's and may play a role in transcription (52). Recent work by Choi et al demonstrated that

overexpression of PTB reduced transcription of MHV mRNA's, but did not effect translation underlining PTB's role in MHV transcription (17).

Spagnolo and Hogue identified poly (A) binding protein (PABP) as binding to the 3' UTR plus poly (A) tail. They demonstrated that at least 5 A residues of the poly A tail are required for PABP binding, when deleted the protein does not bind and DI replication is impaired, and in some experiments the poly A tail was repaired and replication did occur (93). Spagnolo and Hogue also suggested that PABP may be involved in circularization of the MHV genome. Previous work by Andino's group has shown that PABP interaction is necessary for the circularization of the poliovirus genome, and that circularization is an essential step in the initiation of negative strand synthesis (32). Further work on poliovirus has shown that circularization of the genome is also involved in translation (65, 97). A study by Kuyumcu-Martinez et al. has shown that PABP specifically associated with polysomes is quickly degraded by poliovirus 3C protease (47). Cleavage of PABP by 3C protease may act as a trigger for a switch from translation of genome length RNA to replication, which may not require genome circularization from negative strand templates. It is possible that PABP binding to the MHV poly (A) tail is required for genome circularization and the initiation of negative strand synthesis as seen in poliovirus. It is possible that PABP could be cleaved by one of the many uncharacterized nonstructural proteins produced by MHV or the 3C like protease encoded in ORF 1b, also acting as a trigger for switching from genome length translation to replication from negative strand templates.

Nanda and Leibowitz identified mitochondrial aconitase, mitochondrial HSP70 as well as HSP60 and HSP40 as binding to the 3' terminal 42 nucleotide element within the 3' UTR (67, 68). Two host protein binding elements in the 3' UTR were initially described by Yu and Leibowitz and further characterized by Liu, Yu and Leibowitz. The elements are at positions 166-129 and the 3' terminal 42 nucleotides, and within these two elements is an 11nt motif UGANRGAAGUU (56, 109, 110). Mutagenesis of this motif resulted in decreased replication or recombination that restored wild type sequence in DIssE. Computer based secondary structure modeling of the 3' 42 nucleotide element suggests the formation of a stem-loop structure. Liu's digestion data does not provide any information on the terminal 12 nucleotides, but suggests the formation of a mostly single stranded, bulged-stem-loop structure which differs from the predominantly double stranded model proposed by Yu and Leibowitz (57, 109). The role of secondary structure of the 3' 42 nucleotide element in binding to mitochondrial aconitase, mitochondrial HSP70, HSP60 and HSP40 and the effect of RNA conformation on viral replication has to date not been studied, and is the focus of this dissertation.

Mitochondrial aconitase has a cellular counterpart, the iron regulatory protein. IRP has a 30% amino acid identity and 56% overall amino acid sequence similarity to mitochondrial aconitase (39). IRP is a conditional cytoplasmic mRNA-binding protein which interacts with iron-responsive elements located in the 5' UTR of ferritin mRNA and the 3' UTR of transferrin receptor mRNA and functions to coordinate post-transcriptional regulation of cellular iron metabolism. Iron starvation yields the active

RNA-binding form which binds to IREs of target RNA's; when iron becomes scarce inside a cell the IRPs bind to the IRE in the 5' UTR of the ferritin mRNA which blocks ferritin translation. IRP binding with IREs in the 3' UTR of transferrin receptor mRNA stabilizes this transcript and increases its subsequent translation to increase intra-cellular iron concentration. Given the sequence and structural similarities between mitochondrial aconitase and the iron responsive protein Nanda and Leibowitz demonstrated that iron supplementation increased viral titer at early times post infection and that viral protein expression occurred earlier in infected, iron supplemented cells versus non-supplemented infected cells (68).

The role of secondary structure in replication as well as the specific purpose of host proteins binding to defined regions in the MHV genome is unknown. It is possible that hnRNP-A1's interaction with the negative strand leader and PTB's binding to the positive strand leader may act as an initiation complex for viral replication or transcription. PTB and hnRNP-A1 have been shown to associate in the spliceosome complex so it is possible that PTB recruits leader to hnRNP-A1 to begin transcription of MHV genes, a similar system may be used to recruit host and viral proteins to the 3' UTR to initiate replication. Since the 3' terminal 55 nucleotides are necessary for negative strand synthesis it is possible that mitochondrial aconitase and its associates along with PABP bind to the 3' UTR changing RNA conformation which allows hnRNP-A1 to bind. After or concurrently, the RdRp recognizes a signal either through a protein:protein interaction brought about by hnRNP-A1, PABP, mitochondrial aconitase complex binding, or an unknown host protein. It is also possible that a RdRp:RNA

interaction occurs directly that is mediated through RNA conformational changes from host proteins binding to their specific regions of the 3' UTR. Once the RdRp recognizes its signal in the 3' UTR (either protein or RNA structure) the complementary negative strand is produced and it is possible that PTB binds to help regulate the genome and complementary genome RNA interaction.

The role of RNA secondary structure and the binding of host proteins to RNA secondary structures and their importance in viral life cycles has been described in other virus systems. Hepatitis C undergoes internal ribosome entry site (IRES) dependent translation, disruption of the IRES, which is located in the 5' UTR, leads to a loss in translation and inhibition of viral growth (72). It has been shown that eIF-3 subunit binds the IRES and without this interaction there is no translation of HCV RNA's. An HCV mutant was developed that maintained the wild type IRES secondary structure, but could not be translated. The mutation was in the apical-stem loop of portion IIId of the IRES which binds ribosomal protein S9. See Figure 9. Investigation by enzymatic probing determined that the RNA in the apical stem-loop was not folded properly, when the wild type secondary structure of the apical stem-loop was restored it was found that S9 bound and translation of HCV RNA was restored (72). Hepatitis C studies have demonstrated that the complementary RNA strand's secondary structure is also important for replication of the genome. A study of the HCV region complementary to the IRES region found that complementary IRES does not make a mirror image of the IRES. Disruption of the complementary IRES structure prevents binding of the NS5B (HCV RdRp) and initiation of the production of genome sense RNA molecule (86).

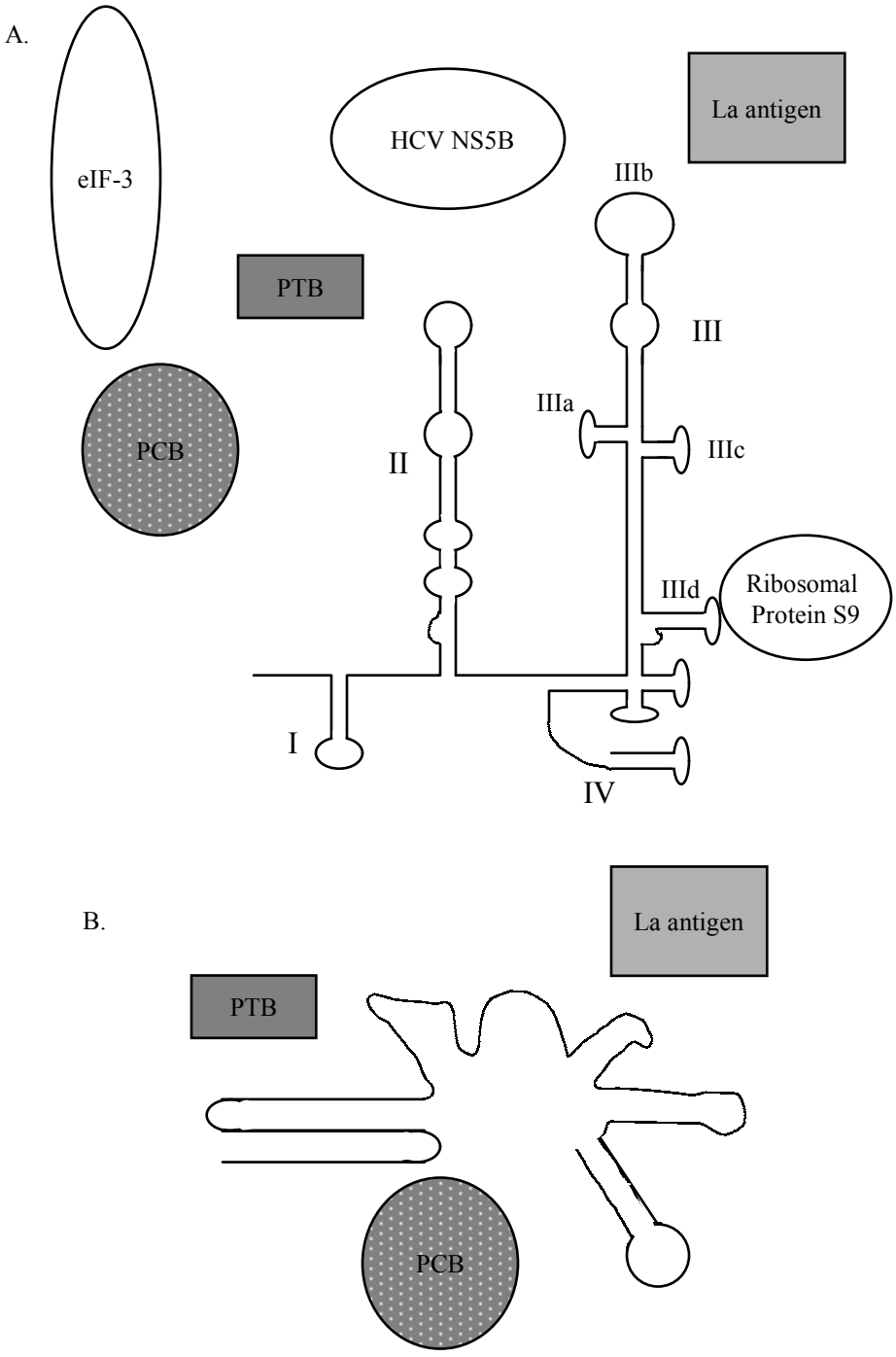

Figure 9. The 5' and 3' UTR's of hepatitis C and the proteins that bind.

The Hepatitis C genome has also been shown to bind many host proteins, although the exact function of each is currently under investigation. See Figure 9. Polypyrimidine tract binding protein (PTB) has been shown by immuno-depletion and in vitro translation assays to be essential for translation of HCV genomes in vitro, and PTB has been shown to associate with the 5' UTR of HCV (2). It has also been demonstrated that the La auto-antigen is required for translation as well (1). Another study has suggested that Poly C binding protein (PCB) interacts with the HCV 5' UTR. This study demonstrated that whole IRES is necessary for binding and extrapolated their data to indicate that secondary structure forms first then serves as a landing site for PCB. The function of PCB's binding to the 5' UTR is unknown (94).

Host proteins binding to the 3' UTR has also been demonstrated for HCV. See Figure 9. It has been demonstrated that La also binds to the 3' UTR and protects HCV RNA from degradation (95). HCV genome is not poly-adenylated, and poly-adenylation is thought to protect cellular RNA's from degradation probably through binding of Poly A binding protein (PABP) and its associated complexes. The mechanism of HCV RNA stability is unknown and work has demonstrated that La, PTB, and heteronuclear ribonucleoprotein C (hnRNP C) bind to regions within the 3' UTR. Studies to determine the function of this binding found that La would protect RNA from degradation, while hnRNP C and PTB did not, and their specific functions remain unclear (29, 95). The secondary structure of the HCV 3' UTR may also be important for replication, disruption of a stem-loop structure in the HCV 3' UTR in an infectious clone construct was viable in chimpanzees, although no infectious virus was produced viral RNA containing the

mutations were detectable at 2 and 5 weeks post inoculation suggesting a role for the 3' UTR in HCV genome stability (49). Lanford et al. also demonstrated that a poly U-UC region deletion was not infectious. It has been shown that PTB binds this poly U-UC region so it is possible that PTB binding may be necessary for replication in vivo.

The importance of proteins binding to the 5' UTR and 3' UTR of other flaviviruses has also been studied, and it has been demonstrated for Japanese Encephalitis Virus that NSP3 and NSP5 bind to the 3' UTR. Both are components of the replicase complex, but their exact role in replication is not known. An RNA secondary structure of West Nile Virus's 3' UTR has been shown to regulate viral RNA translation. A pseudoknot is formed within the 3' terminal stem-loop, and when this stem-loop is mutated or deleted in a West Nile virus replicon no viral proteins are detected (54).

Picornavirus cis-acting sequences have also been extensively studied to determine if RNA conformation, host protein binding, or both influence steps of the virus life cycle. See Figure 10. It has been demonstrated in poliovirus that La, PTB and PCB bind the IRES of the 5' UTR (6). Xenopus laevis oocytes injected with poliovirus genomic RNA and treated with anti-PCB antibodies showed a decrease in translation of polio RNA, demonstrating an in vivo necessity for PCB binding to the IRES of the 5' UTR. It has also been demonstrated that the 5' UTR binds viral proteins 3AB, 3CD, and host proteins EF-1α and an unknown factor of 36kDa. La has also been shown to bind to the 3' portion of the IRES and anti-La antibodies specifically decreased translation of poliovirus RNA (6). Roles for the binding of 3CD and PCB have been demonstrated,

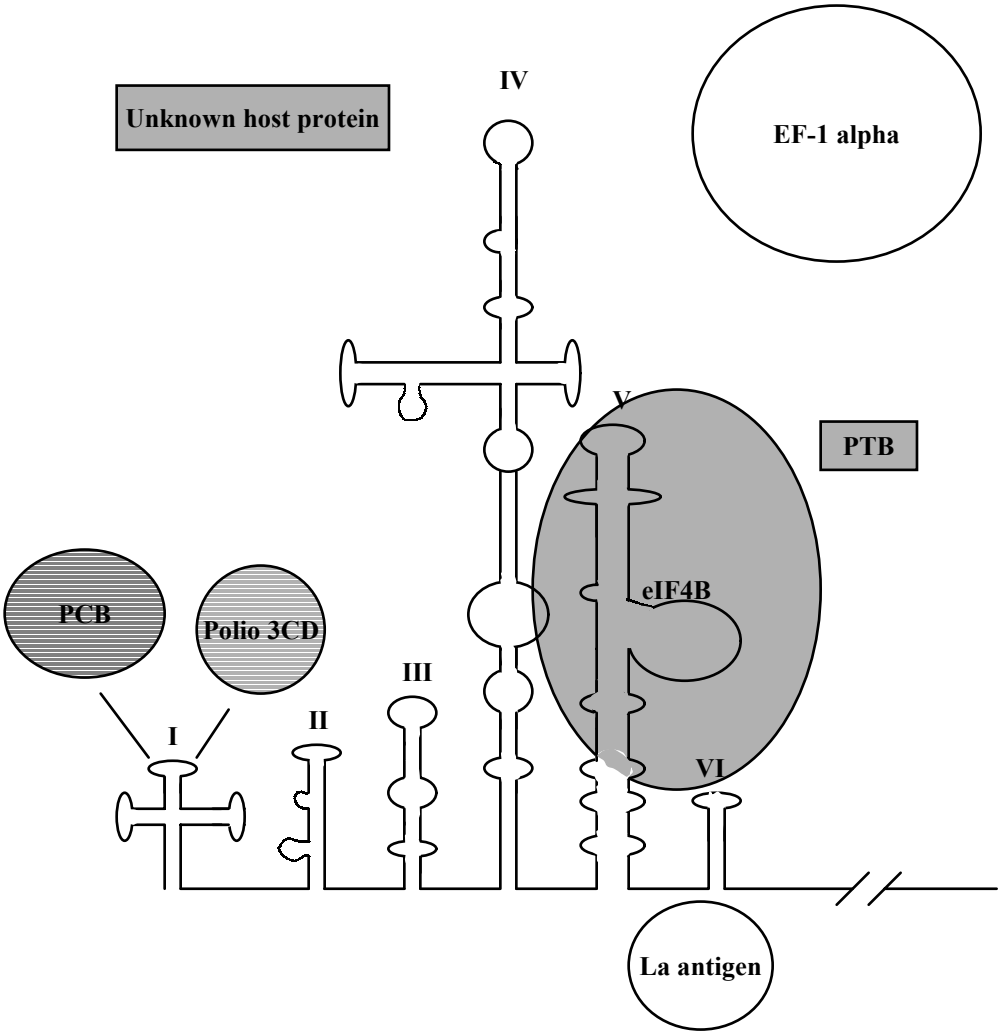

Figure 10. IRES of the poliovirus genome and its associated proteins. For the proteins whose binding region has been identified the protein is shown associating with the IRES in that region. For those proteins, La, PTB, unknown, and EF-1alpha, whose binding sites have not been specifically identified lie near their binding region.

and 3CD and PCB are thought to form a RNP complex at stem-loop B of stem-loop I cloverleaf (27). When PCB binds to the stem loop B it enhances translation of viral RNA's while 3CD binding decreased translation and promoted negative strand synthesis (27). PCB has also been shown to enhance translation of hepatitis A RNA's (31). The data suggest that PCB and 3CD work against one another. It is possible that PCB stabilizes the poliovirus RNA and keeps translation occurring and once 3CD is in a high enough concentration that it competes off PCB, either directly or by binding a second site causing a change in RNA conformation which then releases PCB, or allows another factor or set of factors to bind which cause the switch from translation to replication (27).

Eukaryotic initiation factor 4B has also been shown to interact with the poliovirus IRES and is thought to help form the translation initiation complex at the 5' end of the poliovirus genome (71). eIF4E is part of the cap binding protein along with eIF4G and eIF4A, while eIF4F binds the 18S ribosomal subunit to the 5' end of the mRNA, or in the case of an infected cell the poliovirus genome. eIF4B binds to the 18S ribosomal subunit and ribosome bound eIF4F and stimulates RNA helicase activity. It has been demonstrated that eIF4B binds to domains V and VI of the poliovirus IRES, it forms ribosome initiation complex and was also found to bind to PTB (71).

Proteins which have been shown to bind to the poliovirus 3' UTR are 3AB, 3CD and a 36kDa host protein; mutational analysis demonstrated that decreased binding of protein complexes also decreased replication, possibly through disrupting negative

strand synthesis (64). To the contrary it has also been demonstrated that poliovirus that had its 3' UTR deleted still replicated, but not as well as wild type (99).

Reverse genetics systems for coronaviruses. Recently Master's lab developed targeted recombination, which is a technique that should allow the construction of mutant viruses. Master's lab has been successful in developing two targeted recombination systems; both take advantage of a temperature sensitive MHV A59 mutant, Albany 4 (Alb4) and the DI B36. Albany 4 has an 87 nucleotide deletion that results in a thermolabile, temperature sensitive phenotype. The DI, B36, carries a wild type N gene that acts as a donor to repair the temperature sensitive phenotype and would also carry any mutation into the Alb4 genome that is present in DI B36. Viruses are then selected against by heat treatment and those viruses that survive should be a recombinant carrying any mutation inserted. The other targeted recombination system takes advantage of a cell line produced by Holmes's lab (100). Holmes's lab introduced the feline aminopeptidase N gene into BHK cells so that the BHK cells express the feline aminopeptidase N gene, which is the receptor for Feline Infectious Peritonitis Virus (FIPV). The BHK cells produce infectious virus to equal titer of the normal host cell (100). Master's lab developed a construct based upon B36 that grafts genes 3-6 onto B36's gene 7. Masters et. al then replaced the MHV spike protein (gene 3) with FIPV's spike protein. The construct pFM1 is transcribed and transfected into Alb4 infected L2 cells carrying any mutation inserted into genes 4-7 with it. Recombination takes place and virus carrying FIPV's spike protein in an MHV backbone along with any inserted

mutations is produced. Viruses are then selected by passage onto Holmes's BHK's to propagate recombinant virus (45).

Another approach to reverse genetic systems is cDNA infectious clones. While many of these have been developed and used for other RNA viruses, the large genome size of coronaviruses hampered their development until recently. For example infectious clones exist for equine arterivirus, Hepatitis C virus, mouse hepatitis virus, transmissible gastroenteritis virus, avian infectious bronchitis virus, human coronavirus 229E, West Nile Virus, poliovirus, classical swine fever virus, yellow fever virus, citrus tristeza virus, dengue virus, vesicular stomatitis virus, and others (15, 30, 49, 66, 80, 98, 107, 108, 3, 8, 77, 82, 89, 102, 104).

The first approach in construction of infectious cDNA clones is to engineer full-length cDNA copies assembled from fragments into one plasmid with an RNA polymerase promoter, usually T7. Plasmids carrying the clone are amplified, linearized, transcribed, and transfected into recipient cells that can support growth of the virus. This approach has been used for West Nile virus, dengue virus, citrus tristeza virus, hepatitis C virus, classical swine fever virus, and transmissible gastroenteritis virus (3, 38, 49, 66, 82, 89). The cells are then incubated and wild type virus is harvested.

Another approach for infectious clones is to assemble cDNA fragments into a full-length clone either in plasmids or vaccinia virus constructs under a T7 promoter and transfect cDNA into T7 expressing recombinant vaccinia virus cells. T7 vaccinia drives the transcription of the cDNA to produce infectious virus. This approach has been used

for vesicular stomatitis virus, human coronavirus and infectious bronchitis virus (15, 98, 104).

For some infectious clones stability of the cDNA has been an issue, often deletions of necessary sequence result in a non-infectious cDNA clone (3, 30, 80). Stability issues lead to the third approach of propagating stable cDNA fragments of the virus, assemble the fragments by ligation and transcribe the assembled full-length cDNA. The full-length RNA is transfected into permissive cells, this approach has been used for yellow fever virus, transmissible gastroenteritis virus, and mouse hepatitis virus (80, 107, 108).

Enjuanes's group developed the first infectious clone system for coronaviruses using the first approach (3). They engineered the TGEV genome into a bacterial artificial chromosome with a cytomegalovirus immediate early promoter upstream to the viral coding region. The BAC was then propagated in *E. coli* and purified. BAC's were then transfected into BHK cells and the cytomegalovirus promoter drove transcription of the viral genome and rescue of infectious TGEV particles from the BHK cells. As mentioned previously there was a problem with stability while in *E. coli*, and deletions of gene 1 would result which did not allow virus to propagate. To overcome the instability Enjuanes's group inserted an artificial intron into several regions to stabilize the BAC, the intron was designed to be spliced from the TGEV RNA by the BHK nucleus and infectious TGEV can be recovered (30).

The other coronavirus systems are a variation of the second approach described and take advantage of vaccinia virus constructs which can hold up to 27 kb of non-

vaccinia coding space (15). IBV and human coronavirus 229E have been constructed as infectious clones using this approach (15, 98). IBV is the first group 3 coronavirus constructed into an infectious cDNA clone. The infectious clone was assembled from 3 fragments into a vaccinia virus cDNA propagated, isolated, linearized, and then transfected into a vaccinia susceptible cell line that was infected with T7 expressing vaccinia. IBV was recovered only when IBV N gene expression constructs were co-transfected. Human coronavirus 229E (HCoV-229E) was engineered in a similar fashion (98). Portions of the HCoV 229E genome were assembled from 2 plasmids and a cDNA that was unstable as a plasmid construct into a vaccinia virus vector and grown. After this first construct was generated a third plasmid carrying the 5' UTR and ORF 1a was ligated in position, vaccinia was propagated and DNA was isolated from infected cells. The HCoV-229E region of the vaccinia DNA was excised, in vitro transcribed and transfected into susceptible cells. Infectious virus that could not be distinguished from parental virus, except for engineered markers, was isolated.

The third approach was used by Baric to generate coronavirus infectious clones for TGEV and MHV-A59 (107, 108). Instead of trying to keep the genome together and propagated in *E. coli*, and hope there were no deletions of unstable regions, Baric decided to propagate smaller stable fragments of the genome in *E. coli*, use restriction enzymes to separate the region of interest, assemble the genome in order, transcribe and transfect into recipient cells that would support coronavirus growth (BHK's). TGEV was separated into 6 fragments that could be propagated in *E. coli* and MHV was separated into 7 fragments. The fragments were generated based upon their stability; if a

plasmid was unstable portions of the fragments were rearranged until stable. The fragments were engineered to have Bst XI, Esp 3I, and Bgl 1 sites that recognize specific DNA sequence and leave variable overhangs. The variable overhangs were designed not to disrupt the reading frame of the MHV and TGEV genomes and provide specificity so that the fragments align in proper gene order. The design of the overhangs gives specificity to the junction sites for an in vitro ligation step that joins the genome fragments in correct order without alteration of sequence. To design appropriate ends for ligation some silent mutations had to be introduced in order to engineer the restriction enzyme sites. After assembly of the fragments the cDNA is transcribed and transfected into permissive cells. The infectious clones for TGEV and MHV constructed in this manner have produced progeny virus that are identical to wild type strains. These constructs can then be used to generate mutant viruses that could not be produced using targeted recombination.

Specific Aims

Mouse hepatitis virus contains a 3' UTR that has essential functions in the MHV lifecycle. The purpose of this dissertation is to further define the 3' UTR's 3' terminal 42 nucleotide host protein binding elements role in the MHV lifecycle.

The specific aims were:

1. Investigate the structural requirements of the protein-binding element in the 3' terminal 42 nucleotides of the MHV 3' UTR.
2. Determine the role of the 3' terminal 42 nucleotide host protein binding element in MHV replication.

3. Determine at which step(s) in the MHV-A59 lifecycle the 3' 42 nucleotide host protein binding element functions.

Aim one was accomplished by developing mutants of the 3' 42 nucleotide host protein binding element that disrupted predicted base-pairing and to test the effects of the mutations on host protein binding using gel mobility shift-RNase T_1 protection assays. Compensatory mutations were developed that restored predicted wild type secondary structure and assayed by gel mobility shift-RNase T_1 protection assays to determine if host protein binding was restored. In an attempt to fulfill aim 2 the mutations were then engineered into a targeted recombination system using DI B36 and screened by sequencing in an attempt to produce a mutant virus. Targeted recombination failed to produce a mutant virus, so DI replication assays were attempted to determine the role of the mutations in replication. For 3 of the 6 mutants assayed DI B36 underwent recombination to restore wild type primary structure. The other 3 mutants failed to produce positive strand DI B36. Semi-quantitative RT-PCR demonstrated that the DI B36 mutants produced complementary strand DI B36 at almost equivalent levels when compared to wild type DI B36. The data suggests a role for host protein binding in the production of positive strand RNA, in addition to the requirement for the 3' terminal 55 nucleotides in complementary strand synthesis demonstrated previously (55).

In order to accomplish Aim 3, the mutations developed in Aim 1were introduced into Baric's cDNA infectious clone of MHV-A59 (108). Currently seven mutant viruses are under construction. When completed the mutant viruses will be used to determine

the role of the 3' 42 nucleotide host protein binding element in the MHV lifecycle. The first step will be to sequence the 3' terminal 400 nucleotides of the virus to ensure the intended mutations are present, or determine what alternate sequence could be used for replication. After sequencing, growth curves of the constructed virus will be performed to determine an overall effect on virus production using wild type MHV-A59 as a control. To date two of the viruses have been constructed and sequence data is forthcoming.

CHAPTER II

GENERATION OF THE 3' TERMINAL 42 NUCLEOTIDE HOST PROTEIN BINDING ELEMENT MUTANTS

Introduction

Previous work by Yu and Leibowitz demonstrated that the 3' UTR of the Mouse Hepatitis Virus (MHV) genome contained two host protein binding elements (109). In Yu's work and follow up work by Liu and Leibowitz the elements were defined as the 3' terminal 42 nucleotides and an upstream element consisting of nucleotides 154-129, within these elements is a conserved eleven nucleotide sequence UGARNGAAGUU (56, 109). Replication assays using DIssE wild type and constructs containing mutations within the eleven nucleotide host protein binding motif resulted in restoration of the wild type sequence due to recombination with the helper virus (MHV-JHM), suggesting a role for the 11nt motif in replication. Gel mobility shift RNase T_1 protection assays of probes with the same mutations as DIssE showed a decrease in host protein binding when compared with wild type probe (56, 109).

Other MHV replication studies implicate a role for RNA secondary structure in virus replication. Hsue and Masters found a 68 nucleotide stem loop structure immediately downstream of the stop codon for mRNA 7 that was essential for replication (34). Makino's lab determined that secondary structure at the intergenic region played a role in transcription of MHV RNA's (78). RNA secondary structure has also been shown to be important for replication and translation of other RNA viruses

such as Hepatitis C, poliovirus, and yellow fever virus (1, 8, 9, 27-29, 43, 64, 71, 72, 75-77, 86, 91, 94, 106).

The goal of the current study was to determine if RNA secondary structure played a role in ribonucleoprotein (RNP) complex formation between host proteins and the 3' terminal 42nt element, as determined by gel mobility shift RNase T_1 protection with mutant and wild type probes. The initial development of mutant probes was based upon Yu and Leibowitz's computer predicted secondary structure (109). Computer modeling using Mfold version 3.0 was used to develop second site mutants that restore wild type secondary structure, yet maintain the initial primary structure mutants, and evaluate those mutants for RNP complex formation using gel mobility shift RNase T_1 protection assays.

Materials and Methods

Cells and lysates. 17CL-1 fibroblasts were maintained in DMEM supplemented with 10% calf serum (HyClone Logan UT) with 2mM glutamine (Invitrogen Carlsbad, CA) at 37ºC in a 5% CO_2 environment. Cells were collected by scraping 10 flasks of confluent 17Cl-1 cells into 20-30ml of PBS and centrifuging at 1,000xg for 5 minutes. Cell pellets were resuspended in 2.5ml of hypotonic buffer, consisting of 10mM HEPES (Sigma St. Louis, MO), 1.5mM $MgCl_2$ (Sigma St. Louis, MO), 10mM KCl (Sigma St. Louis, MO), and 0.2mM PMSF (Sigma St. Louis, MO) and incubated on ice for 5 minutes. The non-ionic detergent NP40 (Sigma St. Louis, MO) was added to a final concentration of 0.5%, the cells were vortexed for 30 seconds, incubated on ice for 10 minutes, and then vortexed again for 30 seconds. Lysates were centrifuged at 3,000xg for 10 minutes to

Table 1. Primers used for probe templates

Primer Name	Sequence* 5'-3'
WTA	TAATACGACTCACTATGGGCGAGAGTAAATGAATGAAGT
MT1A	TAATACGACTCACTATGGGCGAGAGTAAcGAATGAAGTTGATCATGGC
MT2A	TAATACGACTCACTATGGGCGAGAGTAAacAATGAAGTTGATCATGG
M24C	TAATACGACTCACTATGGGCGAGAGTAAAactATGAAGT
MT5A	TAATACGACTCACTATGGGCGAGAGTAAAacttaGAGTTGATCATGG
ATW17-20	TAATACGACTCACTATGGGCGAGAGTAAATGAATGAAGTactaCATGGC
ATW	GactaTCTTCCAATT
U3RA	GTGATTCTTCCAATTGGCCATGATCAACTTC
M24CR	GTGATTCTTCCAATTGGCgATGAT
MD10	CAATTGGCCATGATCAAC

*lower case indicates mutant nucleotides

pellet cell nuclei; after centrifugation the supernatant was removed and glycerol was added to a final concentration of 5%. Cell supernatants were then aliquoted into 40 µl portions and stored at -80ºC. A portion of the lysate was set aside for protein quantitation using the Bio-Rad Protein Assay (Bio-Rad Hercules, CA).

PCR and template isolation. PCR was carried out using primers listed in Table 1. Primers were synthesized by Sigma Genosys (Sigma Genosys The Woodlands, TX). The reaction conditions were as follows: 14 cycles of 95ºC for 30 seconds, 55ºC for 60 seconds, 72ºC for 60 seconds, 16 cycles of 95ºC for 30 seconds, 45ºC for 60 seconds 72ºC for 60 seconds, followed by a fifteen-minute incubation at 72ºC. PCR products were then purified by electrophoresis in a 1X TAE, 4% NuSeive GTG agarose (FMC Rockland ME) gel; the amplified fragment was located by ethidium bromide (Sigma St. Louis, MO) staining and excised from the gel with a scalpel and recovered using the Qiagen Qiaquick Gel Extraction Kit (Qiagen Valencia, CA).

Transcription of RNA probes. Transcription was conducted under the following conditions: 20 units T7 RNA polymerase (Promega Madison, WI), 14 U RNasin (Promega Madison, WI), 1.2 mM NTP's, 1X T7 Transcription Buffer (Promega Madison, WI), 250 µCi α^{32}P-UTP (ICN Irvine, CA), 0.08mg/ml acetylated BSA (Promega Madison, WI), 8mM DTT (Promega Madison, WI), 200ng DNA template, and brought to a final volume of 50 µl using diethyl pyrocarbonate (depc) (Sigma St. Louis, MO) treated water. Reactions were incubated at 37ºC for 1 hour and additional reaction mix of NTP's, buffer, DTT, BSA, and enzyme was added for one additional hour. The samples were then treated with 1 unit RQ1 DNase (Promega Madison, WI) for 15

minutes at 37ºC. RNA's were phenol: chloroform: isoamyl (25:24:1) extracted twice, chloroform extracted twice, then loaded on a Microcon 10 centrifugal filter device (Millipore Bedford MA) centrifuged for 30 minutes at 14,000xg, inverted and centrifuged at 900xg for 3 minutes. Probes were quantitated based upon incorporation of α^{32}P-UTP, and 1.4 picomoles of labeled RNA was used for each binding reaction. Unlabelled wild type probe was prepared in the same manner as labeled probe and quantitated based on spectrophotometry at $O.D._{260}$, yeast tRNA was obtained from Sigma (Sigma St. Louis, MO) proteinase K treated, phenol:chloroform extracted, chloroform extracted, ethanol precipitated and resuspended in depc (Sigma St. Louis, MO) treated water to appropriate concentrations.

Gel mobility shift RNase T_1 protection assays. The gel mobility shift RNase T_1 protection assays were carried out as described by Yu and Leibowitz (109). Seven and one-half micrograms of protein was used for each reaction. Reactions were carried out at 22ºC for 20 minutes in 1X reaction buffer consisting of 100mM KCl (Sigma St. Louis, MO), 10mM Tris (Invitrogen Carlsbad, CA) pH 7.6, 5mM $MgCl_2$ (Sigma St. Louis, MO), 1mM DTT (Sigma St. Louis, MO), 500ng Poly (I)-(C) (Boehringer Manheim Indianopolis, IN), 10 μg Heparin (Sigma St. Louis, MO), and 1.4 pmoles of radiolabeled probe in a final volume of 20 μl. After a 20 minute incubation, 0.006125 units of RNase T_1 (Calbiochem -Novabiochem San Diego, CA) per 1.4 pmole of RNA was added to each reaction and incubated an additional 20 minutes at 22ºC. Reactions with unlabeled wild type competitor and non-specific tRNA competitor at 10, 25, 50, 100X molar concentration were carried out in parallel. The complete reaction was loaded onto a 1X

TBE, 6% nondenaturing polyacrylamide gel and electrophoresed for 4.5 hours. Gels were transferred to Whatman 3CHR paper (Whatman Maidstone, UK) and dried at 80ºC under vacuum for 3 hours then exposed to Kodak Biomax MS film (Kodak Rochester, NY) and quantitated with a phosphoimager (Amersham Pharmacia Piscataway NJ). Six gel shift assays of each mutant were used to generate an average binding efficiency, with wild type always set to 100%.

Computer models. The Mfold RNA version 3.0 folding algorithm available at http://www.ibc.wustl.edu/~zuker/rna/node3.html was used to predict secondary structure (112). The following parameters were used for all secondary structure modeling: no folding constraints, RNA sequence =linear, temperature fixed by the program at 37ºC, ionic conditions fixed by the program at 1M NaCl with no divalent cations, percent suboptimatility = 5, upper band = 50, default = window, maximum distance between paired bases set, output at high resolution, format = bases, base number frequency = default, structure rotation angle = 0, and structure annotation by p-num.

UV cross-linking. Gel mobility shift RNase T_1 protection assays to form RNP complexes were carried out as above with the following modifications. After the RNase T_1 digestion step the reactions were exposed to UV light at 254nm in a Hoefer UVC 500 for 30 minutes in an acrylic block chilled to -20ºC at least 3 hours prior to use. 10 units of RNase A (Sigma St. Louis, MO) was added to each cross-linked reaction and incubated at 37ºC for 30 minutes. The samples were then incubated at 100ºC in 2X sample buffer consisting of 50mM Tris Cl (Invitrogen Carlsbad, CA) pH 6.8, 100mM DTT (Sigma St. Louis, MO), 2% SDS (Sigma St. Louis, MO) 0.1% bromophenol blue

(Sigma St. Louis, MO) and 10% Glycerol (EM Science Gibbstown, NJ) for 3 minutes and electrophoresed on a 10% SDS-PAGE gel for 5 hours, dried and exposed to Kodak Biomax MS film (Kodak Rochester, NY).

Results

Gel mobility shift RNase T_1 protection assays and RNA secondary structure predictions. Work by Yu and Leibowitz defined two host protein-binding elements within the 3' UTR of the MHV genome (56, 109, 110). The two elements are located at positions 154-129 and the 3' terminal 42 nucleotides as defined by Yu using gel mobility shift RNase T_1 protection assays. The 3' 42nt element was the smallest probe that formed ribonucleoprotein complexes and sequence analysis of the two elements revealed a shared 11nt motif, UGARNGAAGUU. Secondary structure analysis using Mfold 2.0 indicated that the 3' terminal 42nt host protein binding element formed a small stem loop structure. The nucleotides that compose the 11nt motif form part of the right hand portion of a stem in a bulged stem loop predicted by Yu and Leibowitz (109). The 11nt motif was targeted for mutagenesis by replacing the wild type nucleotides with nucleotides that would not base pair with the wild type nucleotide's pairing partner in Yu's predicted structure. For example mutant MT1A contains a 36U to A mutation, 36U's pairing partner was 15A and the introduction of an A residue should prevent that pairing. Yu's structure also predicts that the 3' terminal 10 nucleotides are single stranded so a mutant deleting those 10 nucleotides was developed, MD10 was designed to test if all that was required was the stem loop formed by the 11nt motif and its pairing partners.

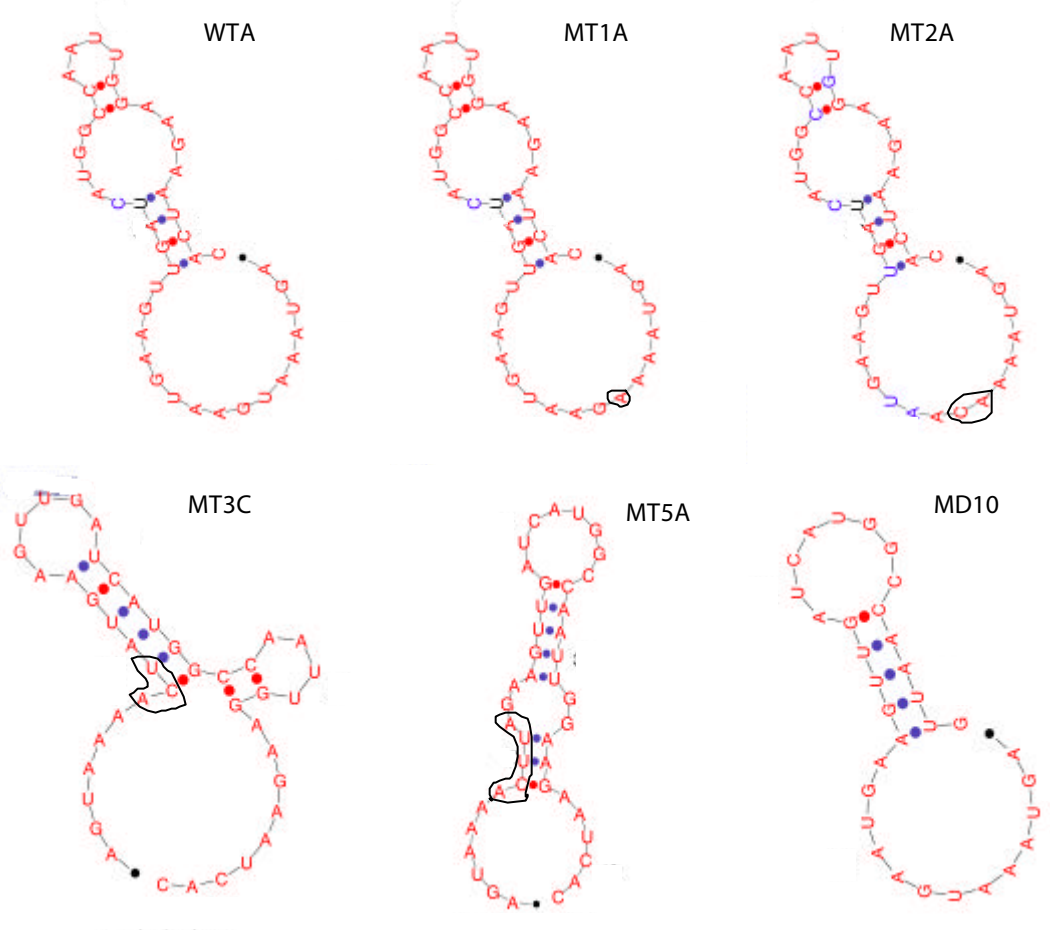

Figure 11. Secondary structure models for the initial set of mutants. Predictions were generated using the Mfold 3.0 RNA folding algorithm. The mutant nucleotides are circled The color of each nucleotide and base pairing indicate the likelihood that the given nucleotide is involved in a particular secondary structure. Red indicates that the structure is likely where blues and blacks indicate that a particular structure for a given nucleotide is less likely.

The more recent version of Mfold (version 3.0) indicated that the secondary structure would be slightly different than that predicted by Mfold 2.0. Mfold 3.0 indicates that nucleotides 27-42 are single stranded with the remaining nucleotides forming a bulged stem-loop structure. See Figure 11. The loop of the wild type predicted structure involves nucleotides 12-15 with nucleotides 10 and 11 pairing with nucleotides17 and 16, the bulge is composed of nucleotides 6-9 and 18-22. Nucleotides 2-5 form a portion of a stem by pairing with nucleotides 26-23 and nucleotide 1 is unpaired. Secondary structure models generated with Mfold 3.0 of probes MT3C, MT5A, and MD10 indicate different secondary structures may have formed. MT3C's most thermodynamically favored model indicates that the nucleotides 36-42 are single stranded with 2 stem-loops forming. The first stem-loop involves nucleotides 29-24 as the loop and nucleotides 30-35 pairing with 18-24 as the stem, the second stem-loop is formed by nucleotides 10,11 and 16, 17 with 12-15 still maintaining a stem-loop structure as in wild type predictions. When MT5A is analyzed with Mfold 3.0 it takes on a different structure, nucleotides 1-6 are single stranded as are nucleotides 36-42; a bulged stem loop is formed by the remaining nucleotides with nucleotides 10, 11 and 30, 31, 32 forming the bulge, nucleotides 17-24 compose the loop and the remaining nucleotides form the stem portions of the predicted structure. Probe MD10 takes on a simple stem-loop structure with nucleotides 11 and 29-42 single stranded, nucleotides 17-24 forming the loop, and the stem formed by 11-16 pairing with 25-29. See Figure 11.

Table 2. Summary of MT binding data

Probe	Sequence*	% Binding	Std Dev	Predicted Effect on 2º Structure
Wild type	5' AGUAAAUGAAUGAAGUUGAUC AUGGCCAAUUGGAAGAAUCAC	100	N/A	N/A
MT1A	5' AGUAAAaGAAUGAAGUUGAUC AUGGCCAAUUGGAAGAAUCAC	68.5	11.3	NONE
MT2A	5' AGUAAAacAAUGAAGUUGAUC AUGGCCAAUUGGAAGAAUCAC	64	21.7	NONE
MT3C	5' AGUAAAacuAUGAAGUUGAUC AUGGCCAAUUGGAAGAAUCAC	6.3	6.1	DISRUPTS
MT5A	5' AGUAAAacuuaGAAGUUGAUC AUGGCCAAUUGGAAGAAUCAC	25.2	5.5	DISRUPTS
MD10	5' AGUAAAUGAAUGAAGUUGAUC AUGGCCAAUUG	44.1	2.5	DISRUPTS

* lower case nucleotides indicate mutations

The 5 mutant probes generated, except for MD10, carried their mutations within the 11nt motif located from position 26 to 36. Mutant MT1A carried a single nucleotide mutation of 36U to A; it maintained wild type secondary structure and bound 68.5% as well as wild type probe. Mutant probe MT2A carried MT1A's mutation and an additional mutation of 35G to C it also maintained wild type secondary structure and bound 64% relative to wild type sequence. Probe MT3C formed RNP complex 6.3% as well as wild type probe, it carries 3 mutations 34A to U, 35G to C, 36U to A and alters its predicted secondary structure. Mutant probe MT5A had mutations in 5 positions within the 11nt motif. The mutations were the same mutations as MT3C with two additional mutations at positions 33A to U and 32U to A. MT5A's secondary structure is altered as well, but its ability to form RNP complexes is elevated when compared to MT3C at 25.2% of wild type. Probe MD10 was a 3' terminal 10 nucleotide deletion, and with this mutation the 11nt motif's primary sequence was intact and RNP complex formation efficiency was reduced to 44.1% of wild type. See Table 2.

In order to determine a role for secondary structure in host protein binding Mfold 3.0 was used to develop second site mutations that were predicted to restore wild type secondary structure and test their effects on host protein binding. Mutant MT3C had the greatest amount of alteration when compared to wild type and had the least amount of binding activity according to the gel shift assay data. A second site mutant was developed for MT3C using Mfold 3.0, and mutant nucleotides were introduced into the MT3C sequence starting at the 3' end and evaluated based upon the secondary structure models generated. When nucleotide 19 was converted from a G to a C residue Mfold

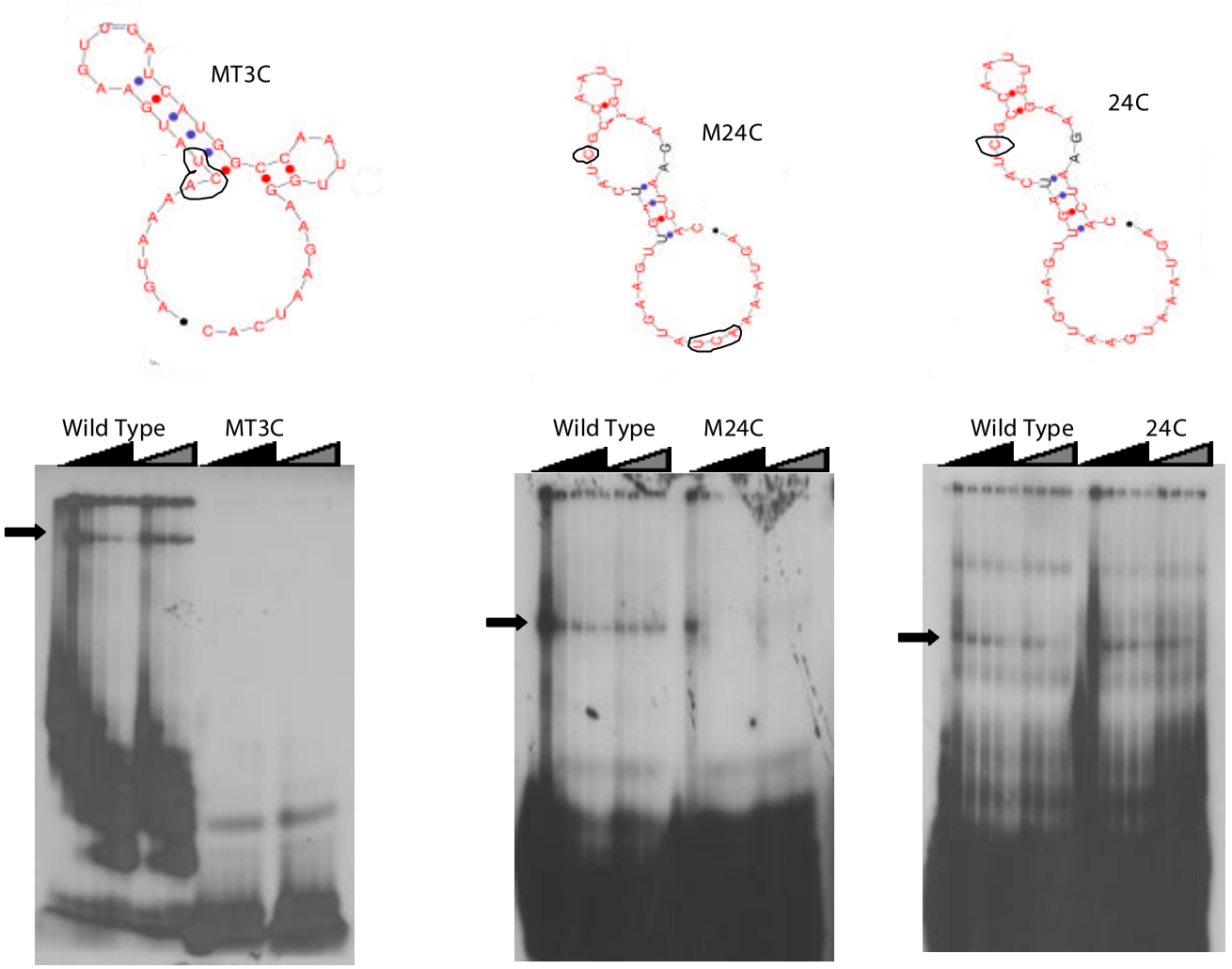

Figure 12. Gel mobility shift RNase T_1 protection assays for the mutants indicated. The mutant nucleotides are circled. The dark triangle represents increasing concentration of wild type competitor RNA and the hashed triangle indicates an increasing concentration of non-specific tRNA competitor. The arrows indicate quantitated RNP complexes and are summarized in Table 3.

Table 3. Summary of MT3C mutants binding activity

Probe	Sequence*	% Binding	Std Dev	Predicted Effect on 2º Structure
Wild type	5' AGUAAAUGAAUGAAGUUGAUC AUGGCCAAUUGGAAGAAUCAC	100	N/A	N/A
MT3C	5' AGUAAAacuAUGAAGUUGAUC AUGGCCAAUUGGAAGAAUCAC	6.3	6.1	DISRUPTS
M24C	5' AGUAAAacuAUGAAGUUGAUC AUcGCCAAUUGGAAGAAUCAC	74.1	8.6	RESTORES
24C	5' AGUAAAUGAAUGAAGUUGAUC AUcGCCAAUUGGAAGAAUCAC	73.5	25.4	NONE

*lower case nucleotides indicate mutations

predicted that it would reform the wild type secondary structure. Based upon Mfold predictions probe 24C was generated and it carries the 19 G to C mutation, maintains wild type secondary structure and has a relative binding efficiency of 73.5% when compared to wild type probe. Probe M24C carries the mutation of MT3C (34U, 35C, 36A versus wild type of 34A, 35G, 36U) and the additional nucleotide 19 G to C mutation. Mfold predicts that M24C takes on the same conformation as wild type and binding efficiency is near equal to the 24C probe at 74.1% of wild type. See Figure 12 and Table 3. These data indicate that wild type secondary structure may play a role in the ability of the 3' terminal 42nt host protein-binding element to bind to host proteins. A similar attempt was made to restore the wild type secondary structure of MT5A but second site mutants of MT5A that restored wild type secondary structure by introducing additional single nucleotide mutations to the sequence could not be identified.

Since the updated version of Mfold predicts a different secondary structure for the wild type sequence more mutations were made in the region of base pairing between nucleotides 23-26 and nucleotides 2-5. Nucleotide 26U is the last nucleotide composing the 11nt motif. Nucleotides 23U, 24A, 25G, 26U were replaced with 23A, 24U, 25C, 26A to make the probe ATW5'. ATW5' disrupts secondary structure with the only base pairing occurring between nucleotides 10-11 and 16-17 with a small loop formed by 12-15. See Figure 13. ATW5' binds 7.2% as well as wild type sequence. Probe ATW3' was generated by converting 2A to U, 3C to G, 4U to A, 5A to U it disrupts secondary structure slightly and binds 4 times as well as wild type sequence. The double mutant, ATW, contains ATW5' and ATW3' mutations, restores wild type secondary structure

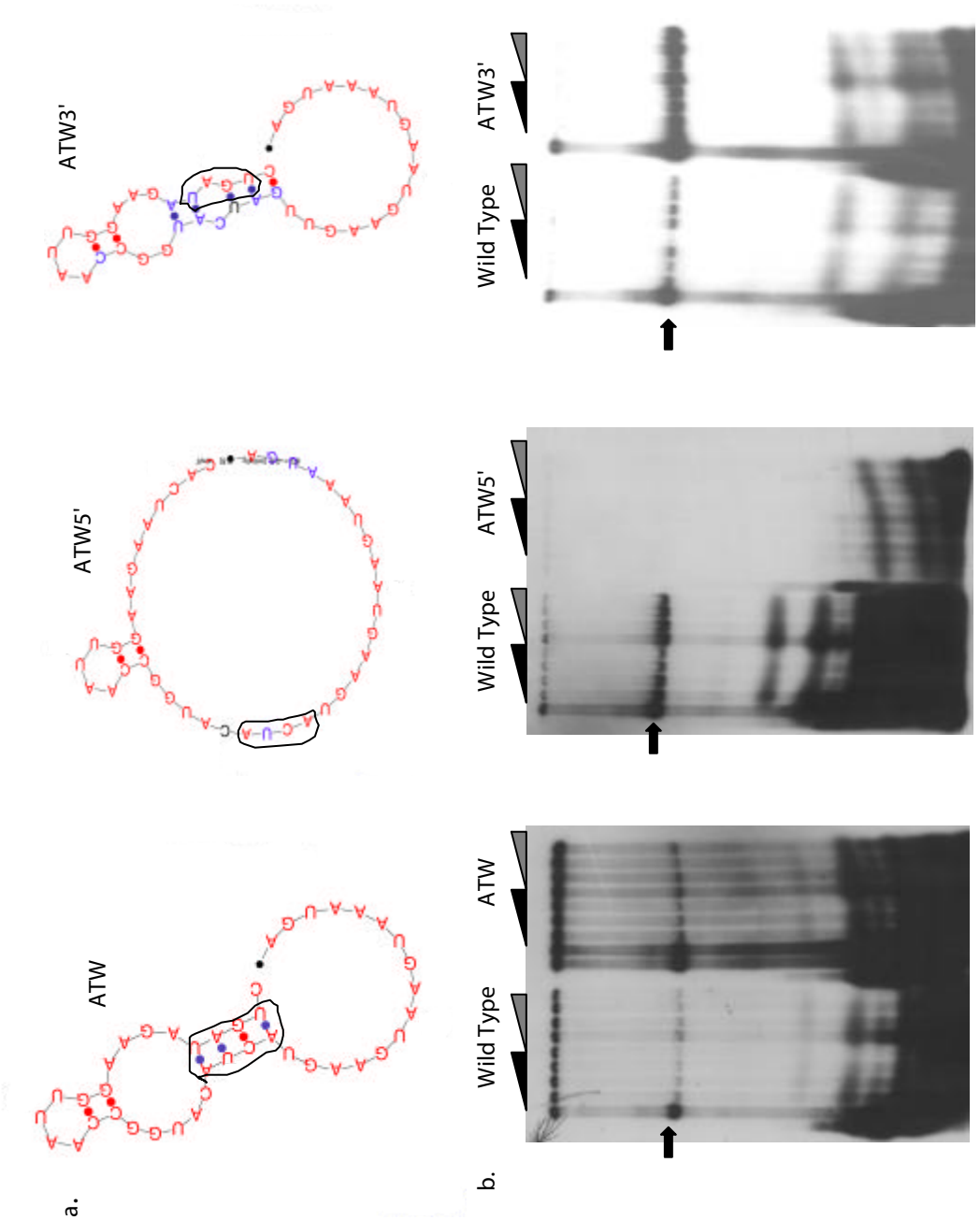

Figure 13. a. Mfold predictions for the indicated probes. The mutations are circled. The color of each nucleotide and base pairing indicate the likelihood that the given nucleotide is involved in a particular secondary structure. Red indicates that the structure is likely where blues and blacks indicate that the structure is less likely. b.Gel mobility shift RNase T_1 protection assays for the mutants indicated. The dark triangle representsincreasing concentration of wild type competitor RNA and the hashed triangle indicates an increasing concentration of non-specific tRNA competitor. The arrows indicate the RNP complexes that were quantitated.

Table 4. Summary of ATW mutants binding activity

Probe	Sequence*	% Binding	Std Dev	Predicted Effect on 2º Structure
Wild type	5’ AGUAAAUGAAUGAAGUUGAUC AUGGCCAAUUGGAAGAAUCAC	100	N/A	N/A
ATW5’	5’ AGUAAAUGAAUGAAGUacuaC AUGGCCAAUUGGAAGAAUCAC	7.2	8.7	DISRUPTS
ATW3’	5’ AGUAAAUGAAUGAAGUUGAUC AUGGCCAAUUGGAAGAuaguC	400	84.4	DISRUPTS
ATW	5’ AGUAAAUGAAUGAAGUacuaC AUGGCCAAUUGGAAGAuaguC	185.8	34.7	RESTORES

*lower case nucleotides indicate mutations

and binds 1.85 times as well as wild type sequence. See Figure 13 and Table 4. The increase in binding for mutants ATW and ATW3' was surprising and it reinforces the concept that both primary and secondary structure play a role in host protein binding to the 3' terminal 42nt host protein binding element.

Wild type, MT1A, MT2A, MT3C, ATW, ATW5', and ATW3' were all predicted to base pair between nucleotides 10-11 and 16-17. Mutations at positions 10-11 and 16-17 were explored using Mfold 3.0 but no compensatory mutations could be identified. Since the base pairing is conserved in mutants with little binding activity as well as those with increased binding activity it could be concluded that this region of secondary structure is not sufficient for host protein binding.

UV cross-linking. Since two of the mutant probes had an increase in binding activity it was prudent to determine if the mutant RNA probes were binding to the same proteins as the wild type probe. UV cross-linking was carried out by using our standard gel shift assay followed by a 30 minute UV cross-link step and RNase A digestion. The reactions were electrophoresed on 10% SDS-PAGE. The gel was dried and exposed to film.

The proteins that bound mutant and wild type probes appear to have the same molecular weight and no additional proteins were resolved. The amount of labeled protein appeared to parallel the signal obtained in gel mobility shift RNase T_1 protection assays. In this context UV cross-linking is not quantitative because the molar ratios of the proteins involved in the complex is unknown and cross-linking of the RNA to the proteins involved in the RNP complex will vary, so measuring relative binding efficiency through this method was not attempted. However, the probes that had

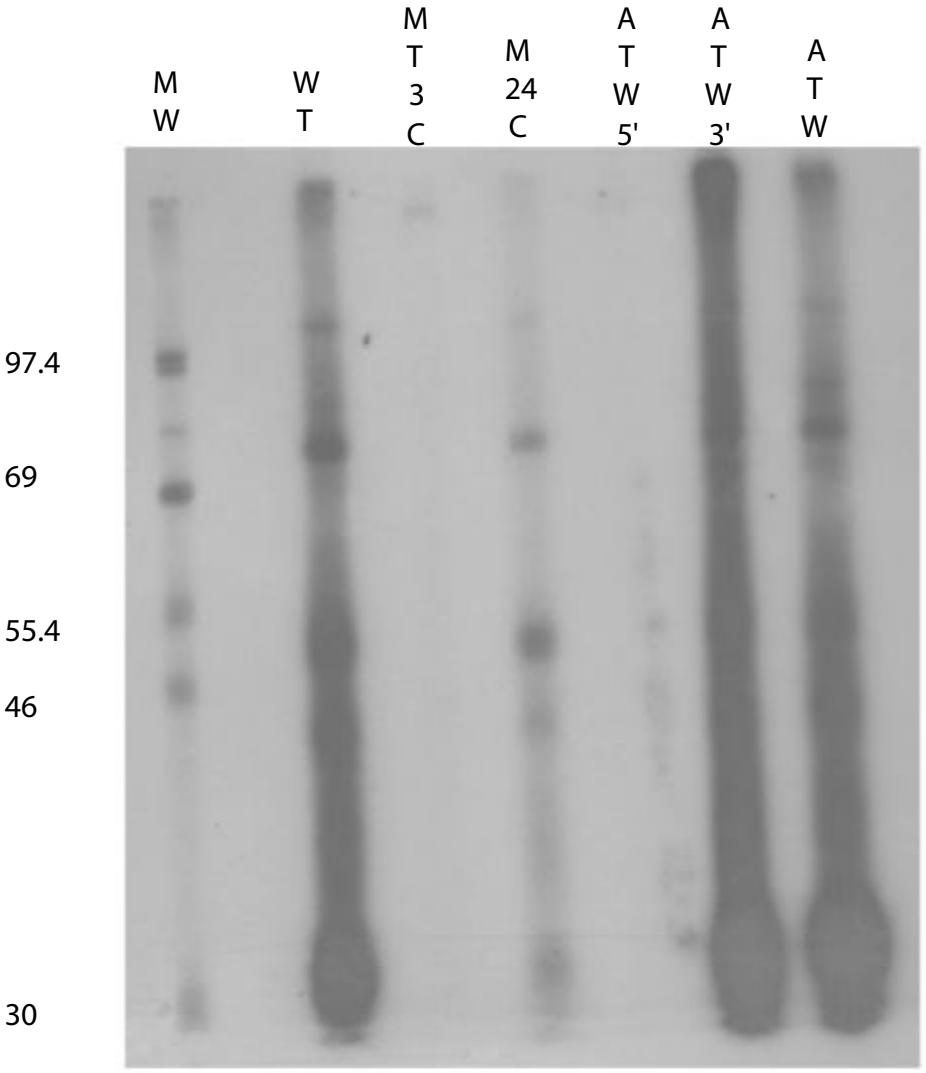

Figure 14. UV cross -linking assay. Probes are identified at the top of each lane. MW is the molecular weight marker WT is the wild type probe; this demonstrates that the probes that formed RNP complexes at higher levels than wild type did not bind any additional proteins.

tremendous decreases in protein binding activity, ATW5' and MT3C, also had decreased amounts of cross-linked protein; probes ATW and ATW3' appeared to cross-link more protein using this assay. See Figure 14.

Conclusions

The goal of the study was to determine if RNA secondary structure was important in the formation of RNP complexes composed of host proteins and the previously identified 3' 42 nucleotide host protein binding element of the MHV 3' UTR. A combination of gel mobility shift RNase T_1 protection assay and computer modeling with the Mfold 3.0 algorithm was used to accomplish the goal. Probes were generated that were predicted to disrupt secondary structure of the 3' 42 nucleotide host protein binding element as predicted by Yu and Leibowitz and assayed for binding to a complex of host proteins. The secondary structure of the mutant probes was also analyzed by computer modeling. Probes MT1A and MT2A maintained wild type secondary structure and had modestly decreased RNP complex formation; this suggests that RNA primary sequence is important for protein binding. Probes MT3C, MT5A, and MD10 all had disruption of their secondary structure and a greater decrease in host protein binding. The decrease in binding alone does not support a role for secondary structure, so Mfold was used to generate compensatory mutations that would restore secondary structure and maintain the original deleterious mutations. Gel mobility shift RNase T_1 protection assays were carried out using the second site mutation alone and in combination with the original mutations. Probe M24C was designed, it contained the MT3C mutations and an

additional compensatory mutation that restored computer predicted wild type secondary structure, as well as host protein binding activity.

The MT3C, M24C and 24C predicted secondary structure and binding data suggest that primary sequence does play a role in host protein binding; the data also support the concept that secondary structure is important for protein binding. When the additional G to C mutation at position 19 is introduced in probe M24C predicted wild type secondary structure is restored and relative binding of the probe increases from 6.3% to 74%. When the G to C mutation is present in otherwise wild type probe its binding efficiency is 73.5% of wild type and its secondary structure is predicted to match wild type. The increase in binding activity in a probe carrying deleterious mutations in conjunction with a second site mutation that restores predicted wild type secondary structure supports a role for RNA conformation in formation of RNP complexes involving host proteins.

Mutants MT1A, MT2A, MT3C, MT5A, and MD10 were all designed based upon predicted secondary structure of the 3' 42 nucleotide host protein binding element using Mfold 2.0 that was available to Yu and Leibowitz (109). The updated Mfold (version 3.0) predicts a different secondary structure for the wild type 3' 42 nucleotides. Probes ATW, ATW3', and ATW5' were developed based upon the current Mfold software that predicts a small stem involving 8 nucleotides (2-5 pairing with 26-23) for the wild type sequence. Probes ATW3' and ATW5' were designed to disrupt the small stem base pairing, while probe ATW was designed to restore protein binding and secondary structure. The data generated with the ATW, ATW3', and ATW5' probes supports the

idea that primary sequence is important for host protein binding, it also argues that secondary structure will affect host protein binding.

The data generated from the gel shift assays and computer predictions also backs up the idea that the 11nt motif present in both binding elements is important for host protein binding. The data generated with the MT1A, MT2A, MT5A, MT3C, M24C, and 24C probes demonstrate that primary sequence is not the only factor involved in host protein binding. The MT1A mutation did not disrupt secondary structure, but decreased binding of host proteins to the probe by 31.5%. The addition of a second mutation (MT2A), also in the 11nt motif dropped binding 36% when compared to wild type probe although it maintained wild type secondary structure. The MT3C mutations were the most informative. MT3C decimated host protein binding to almost zero, 6.3%. When a second mutation was introduced which restored wild type secondary structure but maintained the deleterious MT3C mutation binding increased to 74.1% of wild type, the second site mutation alone had a binding efficiency 73.5% of that of wild type probe. The decreased binding by the double mutant M24C supports the role of the 11nt motif in host protein binding. If primary structure were the only factor involved in host protein binding then one would expect the second site mutant to have a similar binding efficiency as the original MT3C mutant instead of an increase as was observed. If secondary structure was all that was required for binding the restoration of wild type secondary structure would restore host protein binding activity back to wild type level. It is possible that the second site mutant would bind other proteins that give the same appearance in the gel shift assay, but the UV cross-linking experiment rules this out as

the proteins that are cross-linked had the same electrophoretic mobilities with wild type, ATW3', and ATW probes.

When Mfold predicted secondary structure models were compared to data generated by enzymatic digestion of an RNA molecule composed of the 3' terminal 166 nucleotides, the data indicate there are similarities between the Mfold model and biochemical data suggesting the data are accurate for many regions of the RNA (57). Technical difficulties kept Liu et al. from obtaining data on the 3' terminal 12 nucleotides. Analyzing Liu's data by comparing enzymatic probing to the model generated by Mfold for the 3' terminal 166 nucleotides, indicates that nucleotides 42-12 only agree on conformation in 13 of 26 positions of the 31 common nucleotides with 5 ambiguous nucleotides. When the 11nt motif is examined it is found that 4 of the nucleotides agree on conformation between enzymatic probing data and computer predicted models with 3 out of 11 remaining are ambiguous based upon the digestion data. Liu's data upholds the notion that computer predicted models do not always accurately reflect true secondary structure, it must also be noted that this study and Liu's study only analyze a miniscule portion of the MHV genome and that all nucleotides examined may take on a different secondary structure when considered in the context of the MHV genome.

When the predicted secondary structure for the 31 common nucleotides is analyzed on whether or not a particular nucleotide's conformation matches between digestion and modeling data we found that 26 could be evaluated and 5 were ambiguous. Enzymatic digestion data only provides information only on whether or not a given

Nucleotide	Sequence	Digestion	166	WTA
42	A	SS	DS	SS
41	G	SS	DS	SS
40	U	SS	DS	SS
39	A	SS	SS	SS
38	A	SS	SS	SS
37	A	SS	SS	SS
36	U	E	E	E
35	G	SS	SS	SS
34	A	SS	SS	SS
33	A	SS	DS	SS
32	U	E	E	E
31	G	SS	DS	SS
30	A	SS	DS	SS
29	A	SS	SS	SS
28	G	SS	SS	DS
27	U	DS	SS	DS
26	U	E	E	E
25	G	SS	SS	SS
24	A	SS	SS	SS
23	U	DS	DS	DS
22	C	E	E	E
21	A	E	E	E
20	U	SS	DS	SS
19	G	SS	SS	SS
18	G	SS	SS	SS
17	C	DS	SS	DS
16	C	DS	SS	DS
15	A	DS	SS	DS
14	A	SS	DS	SS
13	U	DS	DS	SS

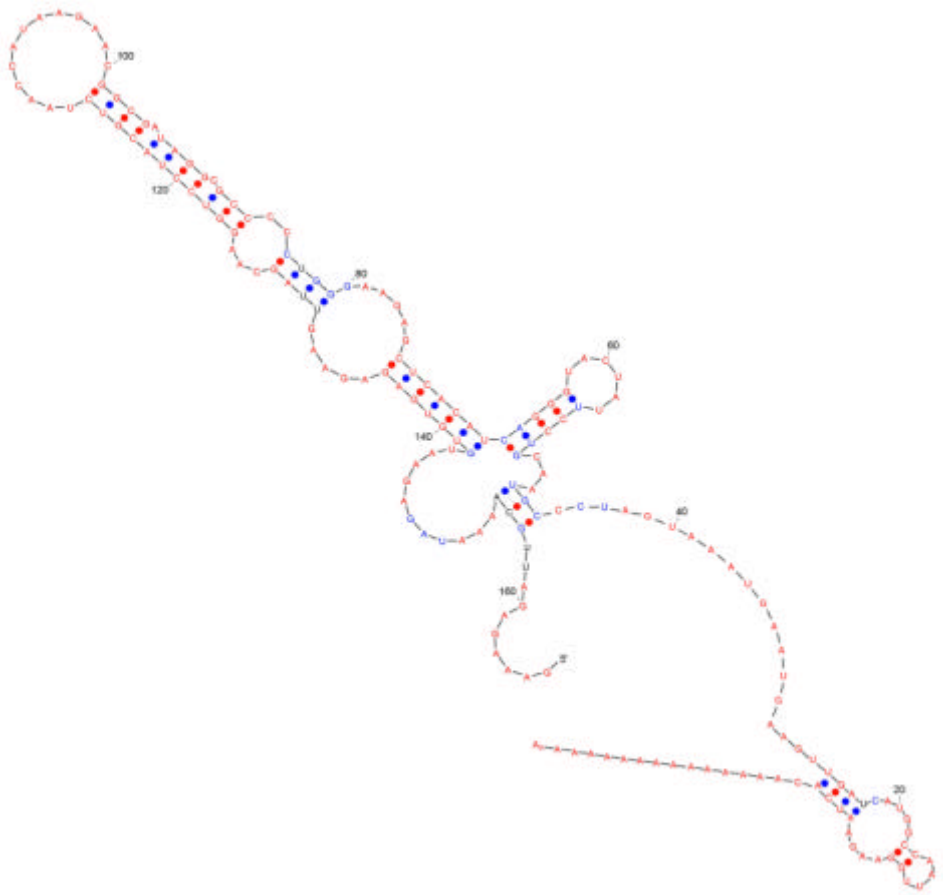

Figure 15. The chart at the left indicates the matches between wild type computer predictions of the 3' terminal 166 nucleotide model and the 3' 42 nucleotide model when compared with digestion data. The predicted secondary structure model has been update to reflect the similarities in secondary structure between the 3' terminal 42 nucleotides and the digestion data.

nucleotide is single or double stranded, it does not give potential base pairing partners. Wild type and mutant Mfold predictions that match wild type predicted structure agreed with digestion data on conformation for 23 of 26 nucleotides. The data analysis allows us to modify the model proposed by Liu et. al.(57). See Figure 15.

Mutant MT3C matched enzymatic probing for 16 of the 31 nucleotides that could be compared, MT5A matched with 22 nucleotides, MD10 matched 24 positions, ATW3' which bound four fold of wild type probe matched in 25 positions, and ATW5' matched in 26 positions, but bound 7.2% as well as wild type probe. The same analysis focusing only on the 11 nt motif indicates that wild type probe, probes with secondary structures similar to wild type, ATW3', and ATW5' all match the digestion data exactly. MT5A matched in 4 positions, MT3C in 3 positions, and MD10 matched in 8 positions.

The data suggests that conformation of individual nucleotides is not the determining factor in host protein binding. It is possible, since the RNP complex is composed of four different proteins in unknown molar ratios, that primary sequence initiates binding of the first protein or complex causing a conformational change which allows binding of subsequent proteins or protein complexes. This may explain the disparity of ATW3' and ATW5', ATW3' bound four fold as well as wild type probe and the predicted secondary structure matches digestion data well, whereas ATW5' barely formed RNP complexes and matches the digestion data better than ATW3'. It is possible that the primary sequence of each is necessary to establish the initial protein binding which then leads to recruitment of the other proteins. ATW5' does not have the initial proper sequence or proper secondary structure. It is also conceivable that ATW5' has the

proper initial signal (the 11nt motif) but the primary and secondary structure of the remaining nucleotides is substantially altered and does not allow for binding of the initial protein complex. Alternatively ATW3' has the correct initial signal (either primary or secondary structure) and takes on a different conformation that allows binding of additional protein complexes giving it a higher relative score in our binding assays.

The data support a role for secondary structure in host protein binding to the 3' 42 nucleotide host protein binding element. In order to investigate an in vivo role for host protein binding it would be necessary to introduce the mutations generated here into a DI construct or into a whole virus.

CHAPTER III

TARGETED RECOMBINATION OF THE MHV 3' 42 HOST PROTEIN BINDING ELEMENT MUTANTS

Introduction

The purpose of this project was to deduce a role for the MHV 3' 42 host protein binding element in the MHV lifecycle. As discussed in Chapter II a role for RNA secondary structure has been proposed as a factor for binding of host proteins to the MHV 3' UTR, but the function of proteins binding to the 3' 42 nucleotide host protein binding element remains unknown. Previously, a study by Lin and Lai demonstrated that the 3' terminal 55 nucleotides are necessary for negative strand synthesis, but their study used CAT reporter assay constructs in an MHV backbone which may not represent a true function for the 3' terminal 55 nucleotides (55). Using selected 3' 42 nucleotide host protein binding element mutants developed in Chapter II we attempted to employ targeted recombination to determine the role of host protein in the MHV life cycle.

Masters developed the targeted recombination technique, which allows for the introduction of mutations into the mRNA 7 region of the MHV genome. Masters developed a defective interfering RNA, B36, that carries the entire MHV mRNA 7 (encoding the nucleocapsid protein) plus the 5' UTR, and a small segment of VSV G protein (42, 63). The temperature sensitive A59 mutant Alb4, which has an 87 nucleotide deletion in the nucleocapsid reading frame of mRNA 7, serves as a recipient for B36 and any mutations it may carry. Alb4 is thermolabile at 40°C, which allows for selection against parental Alb4 when attempting targeted recombination. Alb4's small

plaque phenotype at 39°C, and a wild type plaque size at 34°C also provides a further selection tool to ensure that a plaque purified virus is most likely a recombinant virus. When recombination occurs between B36 and Alb4, the wild type A59 sequence is restored in Alb4 and the resulting recombinant virus is no longer thermolabile or temperature sensitive and will form large plaques at 39°C (63).

The plan was to introduce selected mutations developed in Chapter II into B36 and introduce DI B36 into Alb4 infected cells, select by thermolability, isolate individual recombinants by plaque dilution, screen by RT-PCR for restoration of the 87 nucleotide deletion, and sequence isolated positive strand RNA. Of the 87 isolated viruses screened, 59 were Alb4 and 28 were recombinants. Of those 28 recombinants all contained the wild type sequence regardless of the mutation introduced into B36.

Materials and Methods

Cells and virus. 17Cl-1 cells, a spontaneously transformed NIH 3T3 fibroblast cell line, were maintained at 37°C and 5% CO_2 in DMEM (Invitrogen Carlsbad, CA) supplemented with 10% calf serum (HyClone, Logan UT). L2 cells for plaque purification were maintained at 37°C and 3% CO_2 in DMEM (Invitrogen Carlsbad, CA) supplemented with 10% calf serum (HyClone, Logan UT). L2's for targeted recombination were adapted to grow in suspension; maintained at 37°C and 3% CO_2 in SMEM (Invitrogen Carlsbad, CA) supplemented with 10% calf serum (HyClone, Logan UT). Alb4 virus was generously provided by Dr. Paul S. Masters and a stock was grown for experimental use (42). Seven T-150 flasks of 17Cl-1 cells that were 70% confluent were infected at an M.O.I. of 0.01 at 34ºC until syncytia encompassed greater than 90%

Table 5. Oligonucleotides used for the construction and screening of B36 mutants

Oligo Name	Sequence 5'-3'	Purpose
B36SacI	GAAGAGCTCACATCAGG	TA cloning of Sac I fragment of B36
B36HindIII	CCAGTGCCAAGCTTATGC	TA cloning of Sac I fragment of B36
RJATW3LF	GAAGTTGATCATGGCCAATTGGAAGATAGTCA	Generation of ATW andATW3' mutants
RJATW3LR	TTTTTTTTTTTTTTTTTTTGACTATCTTCCAATTGGCCATGTCAACTTC	Generation of ATW andATW3' mutants
RJATW5LF	GCCCTAGTAAATGAATGAAGTACTACATGGCCAATTGGAAGAATC	Generation of ATW and ATW5' mutants
RJATW5LR	GATTCTTCAATTGGCCATGTAGTACTTCATTCATTTACTAGGGC	Generation of ATW and ATW5' mutants
RJ24CF	GAATGAAGTTGATCATCGCCAATTGGAAG	Generation of MT3C, M24C, and 24C mutants
RJ24CR	GAACCAATTGGCGATGATCAACTTCATTC	Generation of MT3C, M24C, and 24C mutants
RJMT3CLF	CCTGAATGCCCTAGTAAAACTATGAAGTTGATCATGGCC	Generation of MT3C, M24C, and 24C mutants
RJMT3CLR	GGCCATGATCAACTTCATAGTTTTACTAGGGCATTGCAGG	Generation of MT3C, M24C, and 24C mutants
RJMT2ALF	CCTGCAATGCCTAGTAAAACAATGAAGTTGATCATGGCC	Generation of MT2A mutant
RJMT2ALR	GGCCATGATCAACTTCATTGTTTTACTAGGCATTGCAGG	Generation of MT2A mutant

of the cell monolayer, 2-3 days post infection. The virus stock was frozen at -80°C then thawed at room temperature and refrozen. The freeze thaw cycle was repeated twice. After freeze thaw virus stock was sonicated on ice for 3 pulses of 30 seconds at 30% power in a cup probe using a Heat Systems Sonicators Ultrasonic Processor XL (Heat Systems Sonicators Farmingdale, NY), and centrifuged at 2,500xg at 4°C for fifteen minutes. The supernatant was removed and stored at -80°C until use in targeted recombination experiments, a small aliquot was set aside for determining virus titer. Virus titer was determined by 10 fold serial dilution of the virus stock on L2 cells overlayed with 0.8% agarose containing DME 2 for 2 days. Plaque assays were fixed and stained with crystal violet in 80% methanol, 20% water.

Site directed mutagenesis and pB36 mutant construction. Dr. Paul S. Masters kindly provided the plasmid pB36. To ensure that only mutations in the 3' 42 host protein binding element were introduced into pB36 a subcloning strategy to create a mutagenesis template was adapted. See Figure 16. B36 contains a Hind III site directly downstream of the poly (A) tail, and a Sac I site 178 nucleotides upstream of the Hind III site, this fragment was chosen as the mutagenesis template. Primers B36SacI and B36HindIII were used to generate a PCR product for TA cloning using Invitrogen's 2.1 TA cloning kit (Invitrogen Carlsbad, CA). PCR products were generated by 13 cycles of 95ºC for 60 seconds, 50ºC for 30 sec, 72ºC for 90sec, then 16 cycles of 95ºC for 30 seconds, 55ºC for 30 seconds, 70ºC for 60 seconds, then 17 cycles of 95ºC for 30 seconds, 70ºC for 60 seconds followed by a 15 minute extension at 72ºC, using Taq polymerase and its appropriate buffers from Invitrogen Carlsbad, CA (Invitrogen

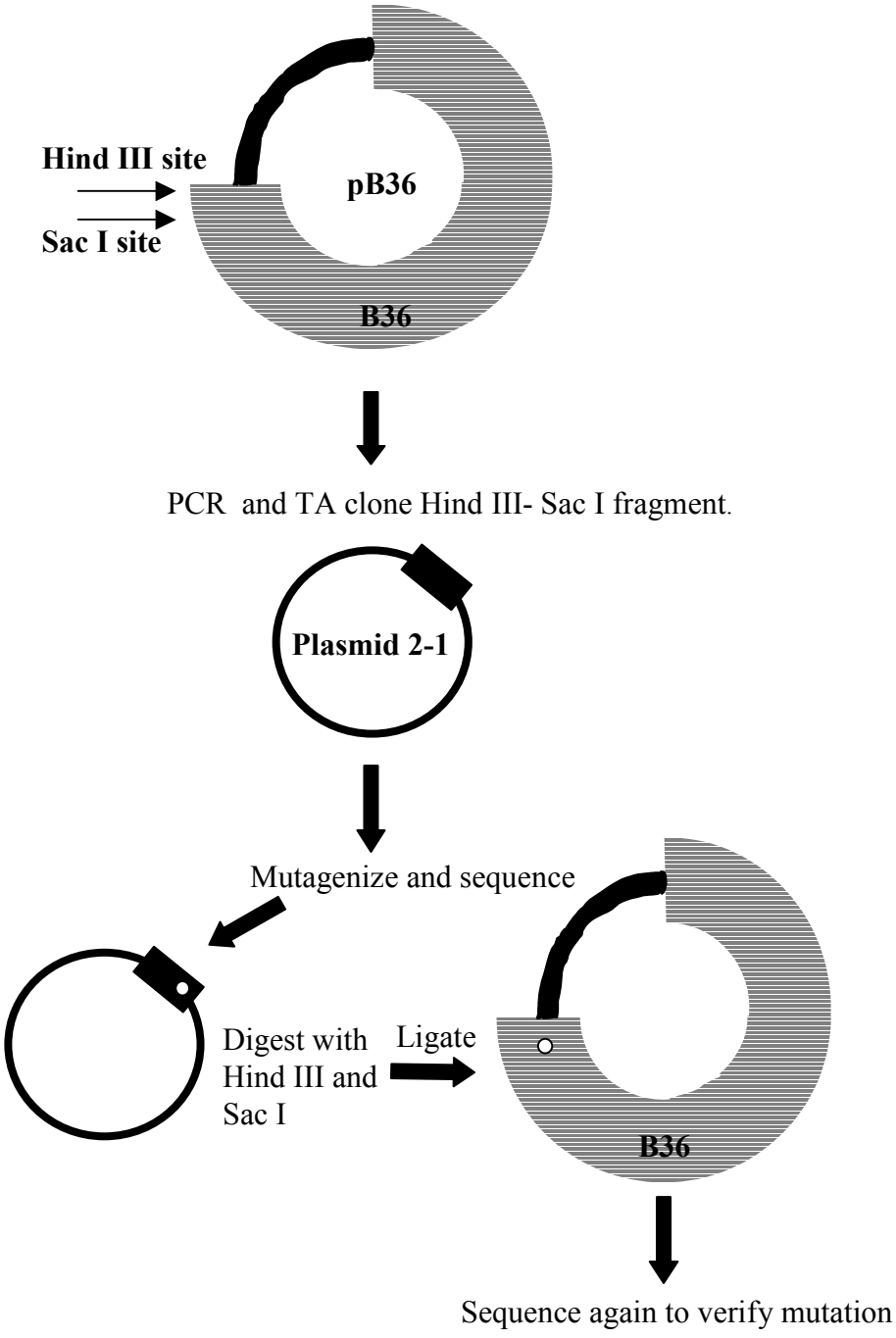

Figure 16. Overview of pB36 mutagenesis.

Carlsbad, CA), 200μM dNTP's (Amersham Pharmacia Piscataway, NJ) and 2 ng of pB36 template and 200nM primers.

The resulting plasmid 2-1 carries the Sac I-Hind III fragment from pB36 and was used as a template for mutagenesis. The mutants MT2A, MT3C, M24C, ATW, ATW5', and ATW3' mutations were introduced into plasmid 2-1 using the QuickChange Site Directed Mutagenesis kit (Stratagene La Jolla, CA) with primers listed in Table 4. After carrying out the procedure for mutagenesis, potential mutant 2-1 plasmids were screened for their intended mutations by sequencing using the T7 primer from the Gene Technologies Lab at Texas A&M University Department of Biology. Sequences were resolved on ABI 377 or 373 sequencing machines (ABI Foster City, CA). Plasmids containing the desired mutant were used for subcloning back into pB36.

The restriction enzymes Sac I and Hind III (Invitrogen Carlsbad, CA) were used to excise the 178 bp fragment that contains the 3'42 nucleotide host protein binding element from mutated plasmid 2-1 for subcloning into pB36. Ten micrograms of mutant 2-1 was digested and 5 μg of wild type pB36 was also cut for receipt of the mutant fragment using Sac I (Promega Madison, WI) and Hind III (Invitrogen Carlsbad, CA). The digested products were then gel purified using the Qiaquick Gel Extraction kit (Qiagen Valencia, CA). Ligations were carried out using T4 DNA ligase and Invitrogen's recommended procedure (Invitrogen Carlsbad, CA). 20 μl reactions were assembled using the Sac I-Hind III digested pB36 fragment and Sac I-Hind III digested 2-1 mutant fragment and incubated at 24°C for 1 hour and then transformed into Top10F cells (Invitrogen Carlsbad, CA). Potential pB36 mutants were selected and sequenced

using primer 5666 (5'GTAGTGCCAGATGGGTTA) (Sigma Genosys The Woodlands TX); colonies containing the desired mutation were amplified and glycerated stocks were maintained. Plasmid pB36 was purified using the Midi Prep Plasmid Purification Kit (Qiagen Valencia, CA).

In vitro transcription. To generate DI RNA's B36 mutants were linearilized using Nsi I (New England BioLabs Beverly, MA) and gel purified. 200ng of template was used in each reaction mix which consists of: 1X transcription buffer (Promega Madison, WI), 100μM ATP, CTP, GTP, UTP (Amersham Pharmacia Piscataway, NJ), 0.8mg/ml acetylated BSA (Promega Madison, WI), 8mM DTT (Promega Madison, WI) 20U RNasin RNase inhibitor (Promega Madison, WI), and 1.6 μM 7-methyl GTP cap analog (New England BioLabs Beverly, MA) in a 50 μl volume and incubated for 2 hours at 37°C. After 2 hours 10 units of RQ1 DNase was added to each reaction and incubated an additional 15 minutes at 37°C to digest template DNA. Each transcription reaction was phenol:chloroform : isoamyl alcohol (25:24:1) extracted twice, chloroform extracted twice and loaded onto a microcon10 microconcentrator (Millipore Bedford, MA) and centrifuged at 14,000xg for 30 minutes. The cartridge was removed and 100 μl of depc (Sigma St. Louis MO) treated H_20 was added, the cartridge was inverted and centrifuged again at 1,000xg for 3 minutes. The purified RNA was ethanol precipitated and quantitated by spectrophotometry at $O.D._{260}$.

Targeted recombination. Targeted recombination was conducted by infecting $2.5x10^5$ L2's at an M.O.I. of 1 with Alb4 for 2 hours for each B36 mutant and wild type B36 control. At the end of 2 hours L2's were washed the twice with Ca^{2+} and Mg^{2+} free PBS

(Invitrogen Carlsbad, CA) followed by addition of 400ul of Ca^{2+} and Mg^{2+} free PBS and 1μg of DI RNA for each DI. Electroporation reaction consisting of DI RNA, Alb4 infected L2's, and PBS was electroporated using two consecutive pulses of 0.8 KV, maximum resistance, and 25 μF in a 0.2cm gap cuvette (Bio-Rad Hercules, CA) using the Gene Pulser II (Bio-Rad Hercules, CA). Each electroporation reaction received 500μl of DME10 immediately after electroporation and the whole of each suspension was overlayed onto individual T-75 flasks of 75% confluent 17Cl-1 cells and incubated at 34°C until syncitia enveloped roughly 80-85% of the monolayer. The cells were then frozen at -80°C thawed, refrozen twice, and sonicated on ice for 3 pulses of 30 seconds at 30% power, peak envelope power 100 watts, in a cup probe using a Heat Systems Sonicators Ultrasonic Processor XL (Heat Systems Sonicators Farmingdale, NY). The resulting suspension was then centrifuged for 15 minutes at 2,500xg at 4°C. The supernatant was removed and stored at -80°C for subsequent selection of recombinant viruses.

Heat treatment of potential recombinant viruses. To determine the optimal conditions for eliminating as much parental Alb4 as possible, $1.0x10^6$ pfu of A59 and Alb4 were heated to 40ºC for 12, 24, 48, and 72 hours. Heat treated virus was assayed by serial 10-fold dilution on L2 cells overlayed with 0.8% agarose and DMEM 2% serum, incubated for 2 days at 34ºC, and stained with crystal violet. Twenty-four hours gave the best results, 70% of Alb4 was eliminated and 40% of A59 was eliminated. In time points past 24 hours the amount of A59 that was heat inactivated substantially

increased and equaled the amount of Alb4 eliminated. Twenty-four hours at 40ºC was adapted as the standard conditions for all of the targeted recombination experiments.

Plaque purification of recombinants. One-milliliter aliquots of harvested virus were heat inactivated for 24 hours at 40°C to reduce non-recombinant Alb4 levels in the virus suspension. The heat-treated aliquot was then plated at serial 10 fold dilutions on L2 monolayers and overlaid with 0.8% agarose and DMEM 10% serum. Two replicates were made, one incubated at 39°C and the other incubated at 34°C for 48 hours as a control. Plaques isolated from the 39°C portion were then extracted with a pasteur pipette and placed in 1ml of DME 2% serum. 500µl of each isolate was inoculated to a 60mm Nunc tissue culture dish (Nalgene Roskilde DE) 65% confluent with 17Cl-1cells and incubated at 34°C. Isolated virus was then grown until syncytia involved 90-95% of the monolayer. The media was then drawn off the monolayer and stored at -70°C, the monolayer was washed once with dPBS and total cellular RNA was isolated using the RNeasy mini kit (Qiagen Valencia, CA).

RT-PCR and sequencing of isolated virus. RT-PCR was carried out using the primer 17TG with the sequence 5' TTTTTTTTTTTTTTTTG, which should select any mRNA with a C residue 5' to the poly (A) tail, including viral RNA. RT reactions were carried out by following Invitrogen's protocol for SuperScript II RNase H^- Reverse Transcriptase (Invitrogen Carlsbad, CA). Five hundred nanograms of 17TG was incubated with 1 µg of total RNA with 1.2mM dNTP's in a volume of 12 µl, incubated at 65°C for 5 minutes and chilled on ice for 2 minutes. Following the first incubation step, Invitrogen's 5X 1^{st} strand buffer was added to 1X concentration with 10 µM DTT

and depc water in a volume of 19µl, this mix was incubated at 42°C for 2 minutes then 200 units (1µl) of SuperScript II was added and incubated at 42°C for 50 minutes (Invitrogen Carlsbad, CA). The RT was heat inactivated at 70°C for 15 minutes. PCR was carried out on one microliter of RT product using the primers B36For (5'TAGTACTCTACCTGGTTTT) and B36Rev (5'ATTGCAGGAATAGTACCC). PCR conditions were 34 cycles of 95ºC for 30 seconds, 40ºC for 60 seconds and 72ºC for 60 seconds, followed by a final extension for 15 minutes at 72ºC. B36For and B36Rev, flank the 87 nucleotide deletion, B36For is identical to the upstream primer used by Masters et al. (63). B36Rev is located downstream of the primer Masters et al. used. Our primer generates a slightly larger product, these primers were used because we wanted to avoid the artifactual product of smaller size noted by Koetzner and Masters (63). We were unsuccessful and the artifactual band persisted in our experiments as well. When a recombination event occurred a 542bp fragment was produced and when a non-recombinant had been isolated a 455bp fragment was produced. PCR products were resolved on 2% agarose gels run with a Phi-X 174 Hae-III marker (Invitrogen Carlsbad, CA) to determine if the isolated virus was a recombinant or a parental Alb4. Positive PCR reactions (larger 542bp band) were used as templates for sequencing reactions. PCR for sequencing reactions was carried out using the B36For and 17TG primers under the conditions used for screening. A total of 4 PCR reactions were combined and gel purified using the Wizard PCR purification kit (Promega Madison, WI) quantitated and sequenced using the primer 5666 (5'GTAGTGCCAGATGGGTTA), and the Big Dye

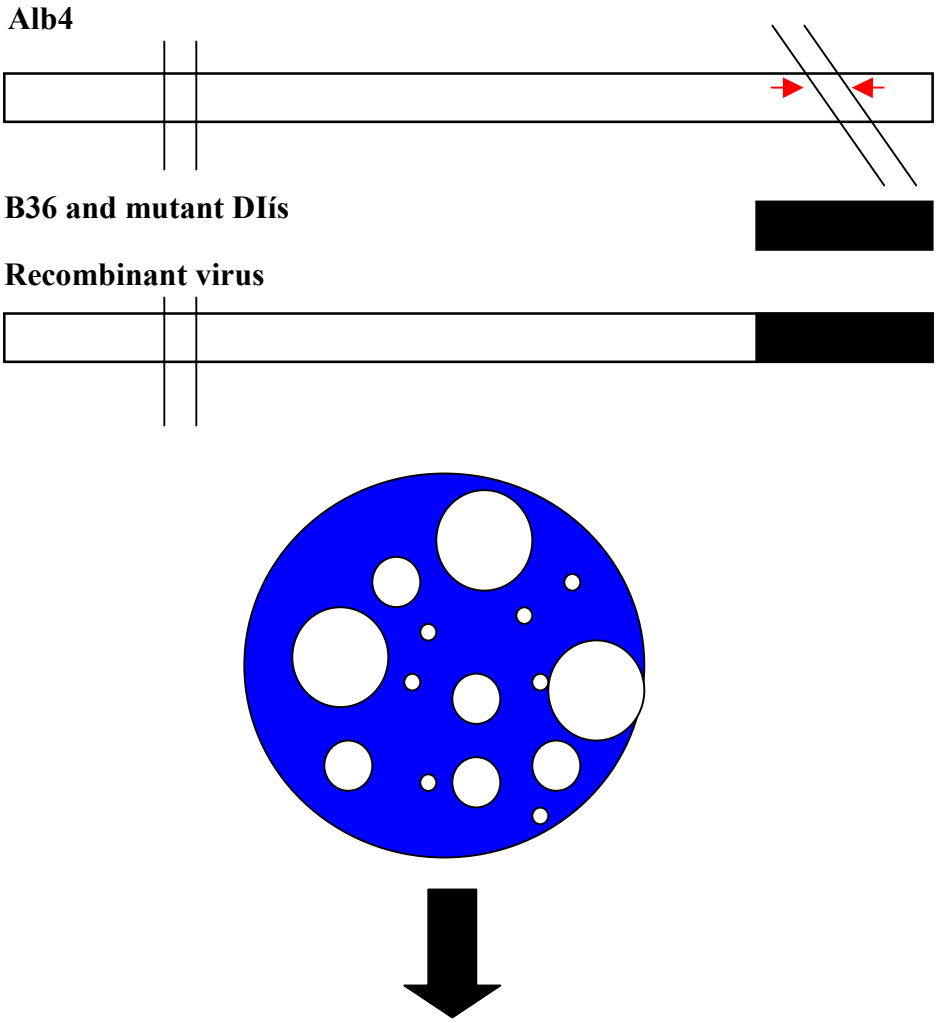

Figure 17. Overview of the selection process for Alb4 recombinants. The red arrows indicate the primers used for screening selected plaques.

Terminator kit (ABI Foster City, CA). The program Sequencher (Gene Codes Corporation Ann Arbor MI) was used to evaluate the sequences.

Results

Construction of DI B36 mutants. Construction of the DI-B36 mutants began with site-directed mutagenesis of a subcloned fragment of pB36. Introducing the mutations into a subcloned piece of B36 followed by restriction fragment exchange was chosen as a mutagenesis strategy rather than directly introducing mutations into pB36. This avoided the need to sequence the entire B36 insert. Sublconing allowed us to make 1 template to carry out our mutagenesis, sequence 3-4 potential mutants and subclone the fragment back into parental pB36 and sequence the 3' terminal 350 nucleotides to ensure our mutation was present.

Targeted recombination. Targeted recombination was carried out as described in Materials and Methods and the procedure is overviewed in Figure 17. After isolation, individual plaques were named based upon the experiment number, the mutation they were expected to carry, and the size of the plaque (small, medium, or large). See Figure 18. Plaque sizes varied from 5 mm down to what looked like pinheads less than 1.0mm. Alb4 is reported to produce 1.0-1.5 mm plaques at 39ºC and A59 wild type size plaques of 3.0 to 3.5 mm at 37ºC (42). Small plaques were judged at anything smaller than 1.5 mm, medium plaques ranged from 1.5-3.0 mm, and large plaques were 3.0 mm and greater. Cultures of individual viruses were grown and RNA was extracted from the infected cells. Isolated RNA was reverse transcribed and PCR was performed on the cDNA; if found to be a recombinant, a large 542 bp band versus a smaller 455 bp Alb4

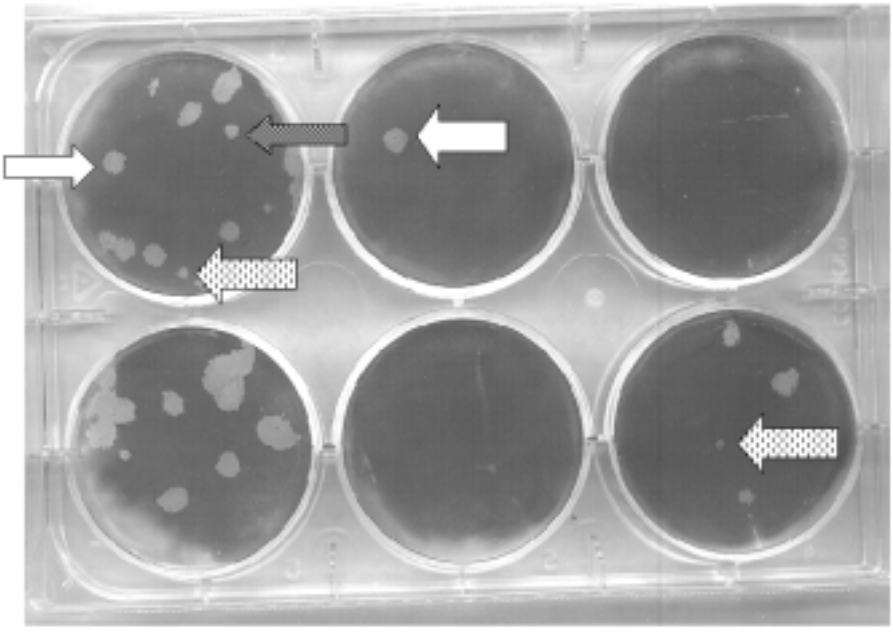

ATW5' **A59** **B36**

Figure 18. Plaque dilution of ATW5', B36, and A59 controls. The large white arrows indicate what were considered large plaques, the hashed arrow indicates a medium plaque, and the dashed arrow indicates a small plaque. The large plaques were picked from the ATW5' well, screened by RT-PCR and sequenced. The small plaque in the B36 well is most likely an Alb4 non-recombinant, and the A59 is an example of wild type (large) plaque size.

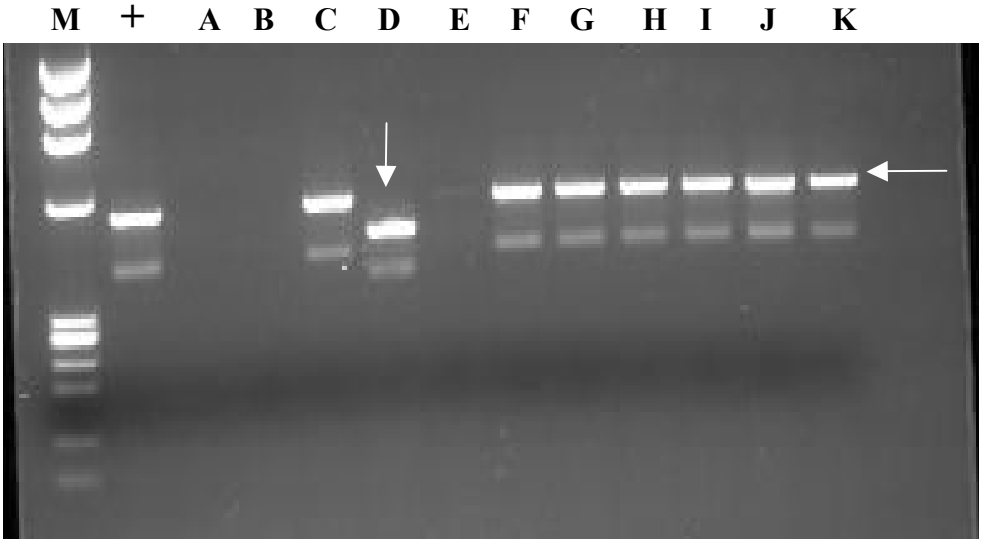

Figure 19. RT-PCR of potential mutant recombinants. The white vertical arrow indicates an Alb4 virus used as a control, the horizontal arrow indicates the larger band of interest which represents a recombinant virus. Lane M is the Phi-X HaeIII marker, Lane + is the pB36 PCR control, Lane A is the no RT control, Lane B I s the no RNA control, Lane E through K represent ATW5' potential mutant recombinant viruses.

band, it was sequenced. See Figure 19. The smaller band in PCR screening assays was common to all experiments and is noted by Koetzner et al. as well (63). In most cases medium and large plaques were recombinant viruses, and small plaques were Alb4 that survived the selection process. Only 4 out of 20 small plaques screened were recombinant, viruses. All recombinant plaques were sequenced and found to be wild type; this indicated an even number of recombination events had occurred and that under these conditions the mutations that we introduced could not be recovered. The results are summarized in Table 5.

Conclusions

Targeted recombination failed to introduce the mutations ATW, ATW5', ATW3', MT2A, MT3C, M24C into the deletion mutant Alb4 to produce a mutant recombinant virus. The restoration of wild type sequence in all selected viruses indicates an even number of crossovers occurred during recombination to restore the wild type primary structure. The data do not exclude the possibility that the mutations introduced were lethal to the virus, the data only indicate that using this technique that the even number crossover recombinant viruses that were isolated and sequenced were favored and any mutant virus that did replicate, replicated below our level of detection.

One possible explanation for not recovering mutant virus is that the heat treatment of the virus and the temperature used for plaque isolation (39°C) favored survival of recombinants containing an even number of crossovers and thus the wild type sequence. The isolated viruses were grown at 34°C to reduce the possibility of overlooking a mutant recombinant virus that was temperature sensitive. Unfortunately

Table 6. Summary of targeted recombination data

Mutant	Number of Plaques Screened		Number of Recombinants	Number of Revertants to Wild Type
ATW	11	7		7
ATW3'	3	3		3
ATW5'	25	10		10
MT2A	11	1		1
MT3C	20	3		3
M24C	17	4		4

this mainly selected Alb4 virus that had not been killed in the heat treatment, 59 out of 87 total plaques as screened by RT PCR. Based upon plaque size 67 large and medium plaque phenotype potential recombinant viruses were screened by RT-PCR, of the 67 plaques screened 24 were recombinants. In order to avoid missing a small plaque phenotype recombinant mutant virus 20 small plaques were also screened by RT-PCR and 4 of them were identified as recombinants. Unfortunately in all cases the recombinants isolated restored wild type sequence. It is also possible that the mutant recombinants were so impaired in one or many steps of replication, that the rarer even number recombinants were able to out compete the mutant recombinants in the initial stages of infection, thus selecting against the mutant recombinants and allowing only survival of the even numbered wild type recombinants. In order to investigate this possibility it was decided to use B36 as a DI in replication experiments of $^{32}PO_4$ labeled DI transfected helper virus (A59) infected cells. Those experiments are discussed in Chapter IV. To address the lethality of mutations an infectious cDNA clone of MHV-A59, which has only recently become available from Ralph Baric, was used to incorporate our mutations and is discussed in detail in Chapter V.

Master's lab has developed another targeted recombination system that uses a construct, pFMHV, that carries genes 3-7 of MHV-A59 but the MHV spike protein has been replaced with the spike protein from Feline Infectious Peritonitis Virus (45). The recombinant virus is grown on BHK cells expressing the feline Aminopeptidase N protein, which were developed by Kathryn Holmes' lab (100). Aminopeptidase N serves as the ligand for feline spike protein and BHK cells expressing Aminopeptidase N

grew FIPV to equal titer as the normal host cells. The restriction of the spike protein allows for better selection of recombinants than the DI B36 based system, because practically all of the background is removed. We chose to use the DI B36 based system even though selection would be more difficult because the pFMHV at roughly 8.7 kb is nearly 4 times the length of DI B36 increasing the likelihood of recombinants derived from an even number cross-over event with wild type sequences. Given the results generated it is doubtful that the feline system would have yielded advantageous results.

Even with the FIPV system Masters' lab has had only moderate success in generating virus with mutations in the 3' UTR. To investigate the role of the 68 nt stem-loop structure Masters attempted to introduce clustered point mutations using the B36 system, for the fifteen mutants they screened they were able to generate nine with the B36 system, the remaining six they tried to obtain using the feline system. None of the six mutations could be generated using the B36 or FIPV targeted recombination systems. When the six mutations were explored with DI B36 in replication assays all six recombined to restore wild type sequence (33).

CHAPTER IV

DI B36 REPLICATION ASSAYS OF THE 3'42 NUCLEOTIDE HOST PROTEIN BINDING ELEMENT

Introduction

To determine the role of the 3'42 nucleotide host protein binding element in MHV replication mutant probes were developed and tested for their effect on host protein binding. Six of the probes assayed did not bind as well as wild type and two of the probes bound better than wild type. To test the effects of the mutants in vivo, targeted recombination was used to attempt to create a mutant virus as discussed in Chapter III. Unfortunately the viruses recovered in targeted recombination experiments underwent an even number of recombination events that restored wild type sequence, regardless of the mutant DI RNA used as the donor. The goal of the project was to determine the role of the 3' 42 nucleotide host protein binding element in the virus life-cycle, since a mutant virus could not be constructed, DI RNA replication assays were adapted to at least determine what role, if any, the 3' 42 nucleotide host protein binding element has in replication. DI B36 has been shown by Masters (42, 63) to function as a DI RNA in the same manner as DIssE (40, 41, 61) when transfected into virus infected cells.

B36 and the B36 mutants developed in Chapter II were used in DI RNA replication experiments, mutants MT2A, MT3C, and M24C recombined to restore wild type sequence in all experiments attempted. Mutants ATW, ATW5', and ATW3' did not

replicate and when sequenced were found to maintain their mutations. Mutants ATW, ATW5', and ATW3' all produced negative strand RNA's, in relatively equal amounts when compared to wild type B36 using semi-quantitative PCR. However the mutants failed to produce positive strand RNA's that could be detected by the DI RNA replication assay. The data suggest a role for the 3' 42 nucleotide host protein binding element in production of positive strand RNA's.

Materials and Methods

Cells and virus. 17Cl-1 cells, a spontaneously transformed NIH 3T3 fibroblast cell line, were maintained at 37°C and 5% CO_2 in DMEM (Invitrogen Carlsbad, CA) supplemented with 10% calf serum (HyClone, Logan UT). L2 cells were maintained at 37°C and 3% CO_2 in DMEM supplemented with 10% calf serum (HyClone, Logan UT). A59 was used as helper virus for all experiments.

Transcription of DI RNA's. DIssE was used as a transfection control (61). The B36 DI RNA's used in this experiment are the same DI RNA's used in Chapter III and their construction is described therein. Transcription reactions were carried out using the mMessage mMachine kit from Ambion Austin, TX (Ambion Austin, TX) following the manufacturer's instructions except for purification of DI RNA's. Purification of DI RNA's was carried out as in Chapter III.

B36 DI replication assays. The method established by Masters' lab was used with extensive modifications (63). 17Cl-1 and L2 cells were grown on monolayer to confluency. 17Cl-1 cells were washed, trypsinized, centrifuged, and resuspended in DME10 and seeded onto six well cluster plates (Corning Corning NY) at a density of

$1.0x10^6$ cells/ well in 3 ml of DME10 prior to preparation of the L2 cells. The 17Cl-1's were washed twice with DME2 2 hours after being plated onto the 6 well cluster plate and fed with 2 ml of DME2 just prior to electroporation of the L2 cells. L2 cells were prepared for electroporation by the following method: L2 cells were trypsinized, washed in DME10% serum, counted, centrifuged at 1,000xg, the media was aspirated and cells were resuspended in DME2 to a concentration of $1.0x10^6$ L2 cells/ml. For each DI RNA $1.0x10^6$ L2 cells were infected at an M.O.I. of 3 for 2 hours. After 2 hours of infection L2 cells were centrifuged at 1,000xg and resuspended in 10 ml Ca^{2+}, Mg^{2+} free PBS (Invitrogen Carlsbad, CA) and centrifuged again at 1,000xg this wash procedure was repeated 2 times. For each DI RNA plus a mock transfected control 1.0 $x10^6$ L2 cells per DI RNA were electroporated with 5 μg of DI RNA or without RNA for the mock transfected control at maximum resistance, 0.8KV and 25μF for 2 pulses 5 seconds apart. The electroporated cells were then resuspended in 1 ml of DME2 and overlayed onto the 17Cl-1 cells.

The overlayed-infected-electroporated cells were incubated until syncytia consumed roughly 65% of the monolayer usually 8-10 hours post infection. At this point the DME2 was removed and replaced with 2 ml phosphate free DMEM (Invitrogen Carlsbad, CA) with 2.5 μg /ml Actinomycin D (Calbiochem -Novabiochem San Diego, CA) and incubated at 37ºC for 20 minutes. At the end of 20 minutes the media was replaced with phosphate free media containing 2.5 μg /ml Actinomycin D, 2% dialyzed serum, and 0.5 mCi of $^{32}PO_4$ (ICN Irvine, CA) and incubated at 37ºC until syncytia enveloped 90-95% of the monolayer, usually 14-16 hours post infection. RNA was

extracted either with the RNeasy kit from Qiagen (Qiagen Valencia, CA) or by 8M guanidium HCL extraction and ethanol precipitation. Three to six μg of RNA was denatured in RNA loading buffer [final concentration 0.5X MOPS, 50.5% formamide (Sigma St. Louis, MO), 18% formaldehyde (EM Science Gibbstown, NJ), 5% glycerol (EM Science Gibbstown, NJ) and 0.02 μg ethidium bromide (Sigma St. Louis, MO)] onto a 1% SeaKem GTG (FMC Rockland ME) 18% formaldehyde (EM Science Gibbstown, NJ) 1X MOPS buffer gel and electrophoresed in 1X MOPS buffer which contained 18% formaldehyde for 6 hours at 120V constant voltage. Gels were exposed to UV light and photographed, fixed in 80% methanol (EM Science Gibbstown, NJs) dried and exposed to Biomax MS film (Kodak Rochester, NY). If DI RNA accumulated positive strand, as seen by a band which migrates between mRNA's 6 and 7, the DI RNA was quantitated using Molecular Dynamics Phosphorimager and Storm 8.2 software, three experiments for each set of mutants were used to generate an average (Amersham Pharmacia Piscataway NJ). The ethidium bromide stained gel was used to normalize to wild type B36 (set at 100%) to adjust for miniscule differences in quantitation and loading.

RT-PCR and sequencing. Total RNA of each culture underwent reverse transcription using Invitrogen Carlsbad, CA's Superscript II RT following the manufacturer protocol with one μg of total RNA from each DI RNA evaluated and 2 pmoles of primer B36n-1 (5'GGCTTCCTATTTACATCC) (Sigma Genosys The Woodlands,TX) which is specific to the negative strand B36 DI RNA. This ensured that only replicated DI B36 would be detected. No RT and no RNA controls were included in the RT step. The no RT control

used extracted RNA from the B36 DI RNA transfected culture to ensure that residual digested transcription template DNA was eliminated and not amplified by PCR. PCR reactions for each DI RNA was carried out with 31 cycles of 95°C for 30 seconds, 35°C for 60 seconds, 72°C for 90 seconds, followed by a fifteen-minute extension at 72°C using 200 nM primers B36n-1 and 17TG (5'TTTTTTTTTTTTTTTTTG) (Sigma Genosys The Woodlands, TX) with one unit of Taq DNA polymerase, 1X PCR buffer (Invitrogen Carlsbad, CA), 1.5mM $MgCl_2$ (Invitrogen Carlsbad, CA), 200 μM dNTP (Amersham Pharmacia Piscataway, NJ) mix, and1μl of RT product as template in a 50μl volume. PCR products were electrophoresed on a 1.0% 1X TAE Seakem LE (FMC Rockland ME) at 90 volts, stained with ethidium bromide, and photographed.

The RT products for each DI RNA were amplified further, using the conditions listed above, for sequencing. Four PCR reactions were combined and gel purified using the Wizard PCR preps (Promega Madison, WI). Purified cDNA was sequenced using the 3 pmoles of primer 5666 (5'GTAGTGCCAGATGGGTTA), 8μl of the Big Dye terminator kit (ABI Foster City, CA) and 600 ng of template using the following protocol in a 20μl reaction: 98°C for 30 seconds, 50°C for 15 seconds, and 60°C for 4 minutes for 24 cycles. Sequencing products were purified using a Bio-Spin 30 column (Bio-Rad Hercules, CA). Columns were prepared by warming to room temperature, letting resin settle for 1 hour, and centrifuged at 700xg for 2 minutes. After preparation of the column, the reaction was added and centrifuged again at 700xg for 2 minutes (Dr. David Needleman, UTMS-H personal communication). Samples were then dried and

analyzed by the Gene Technologies Lab at Texas A&M University using ABI (ABI Foster City, CA) 377 and 371 automated sequencing gels.

Semi-quantitative RT-PCR. Semi-quantitative RT-PCR was carried out to determine if the relative amount of negative strand produced was equal in the DI RNA's that maintained their mutations. Two micrograms of total RNA was incubated with 100 ng of random hexamers (Invitrogen Carlsbad, CA) and 5mM dNTP's (Amersham Pharmacia Piscataway, NJ) for 5 minutes at 65°C, followed by a 10 minute incubation at 25°C, then a reaction mixture consisting of 1X First-Strand Buffer (Invitrogen Carlsbad, CA), 10 mM DTT (Invitrogen Carlsbad, CA) was added in a final volume of 19 µl, and incubated for 1 minute at 42°C, finally 1 µl of Superscript II Reverse Transcriptase (200 units) (Invitrogen Carlsbad, CA) was added and incubated for 50 minutes at 42°C. Superscript II was heat inactivated at 70°C for 15 minutes, and reactions were stored at -20°C until needed.

PCR was carried out on 2 µl of each RT reaction using one unit of Taq DNA polymerase, 1.5mM $MgCl_2$ (Invitrogen Carlsbad, CA) at 1X PCR buffer concentration [diluted from 10X stock (Invitrogen Carlsbad, CA) with 200 nM each primer, and 200 µM dNTP (Amersham Pharmacia Piscataway, NJ) Primers B36n-1 and B36rev (5'ATTGCAGGAATAGTACCC) (Sigma Genosys The Woodlands TX) were used along with primers GAPDH-1 (5' GCCAAAAGGGTCATCATCTC) (Sigma Genosys The Woodlands, TX) and GAPDH-2 (5' GTAGAGGCAGGGATGATGTTC) (Sigma Genosys The Woodlands, TX) under the following conditions: 94°C 60 seconds, 55°C for 60 seconds, 72°C for 4 minutes for 30 cycles. Individual reactions were removed at

cycles, 14, 18, 22, 26 and 30, electrophoresed on 1.5% SeaKem LE (FMC Rockland ME) for 2 hours at 90 volts constant and stained with ethidium bromide (Sigma St. Louis, MO). RT-PCR products were analyzed by densitometry using the Storm 8.2 software package (Amersham Pharmacia Piscataway, NJ).

Results

DI RNA replication assays. DI RNA replication experiments were carried out as described in Materials and Methods. For simplicity, replication assays were performed in two groups, the first with the mutants involving the 11nt host protein binding motif. The second group consisted of the mutants which were based upon the more recent Mfold data, two of which, ATW and ATW3', formed RNP complexes at higher levels than wild type probe in gel mobility shift RNase T_1 protection assays.

The first set of mutants analyzed were MT2A, MT3C and M24C. Mutant MT2A was chosen because it was the mutant that had the greatest effect on host protein binding that also maintained wild type computer predicted secondary structure. MT3C was chosen because it had the greatest effect on RNP formation and the most drastic change in secondary structure of any of the mutants that were developed based upon Yu and Leibowitz's data (109). M24C was chosen because it carries the second site mutant of the deleterious MT3C mutant, this mutant increased binding activity to 74.1% of wild type probe from 6.3% and restored wild type computer predicted secondary structure, establishing a possible connection between secondary structure and RNP complex formation. Three complete experiments were used to determine an average DI RNA replication efficiency. A complete experiment was defined as one in which DI B36

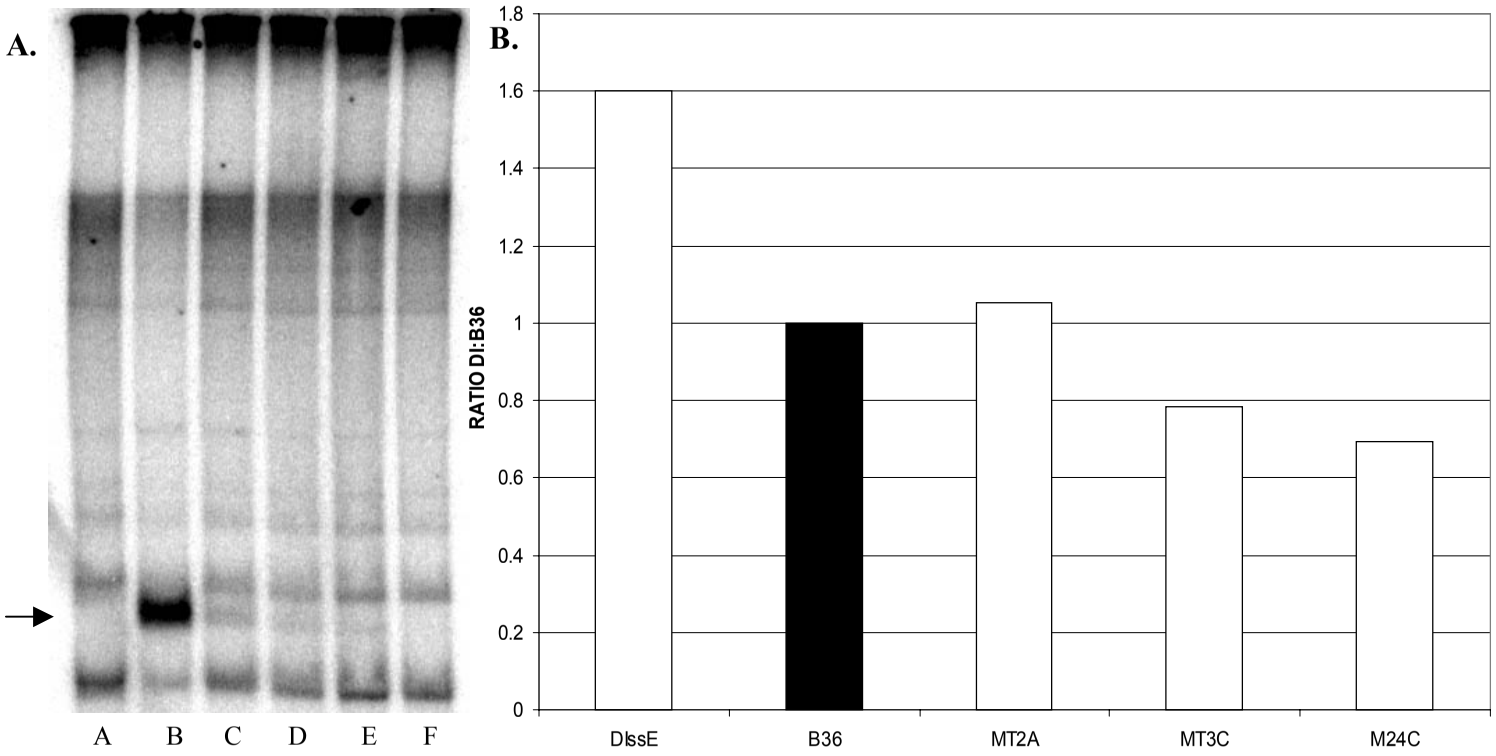

Figure 20. Panel A is a representative experiment for mutants MT2A, MT3C, and M24C. A=A59 mock transfected control, B=DIssE, C=B36, D=Mt2A, E=MT3C, and F=M24C, these mutants underwent a recombination event in all experiments that restored wild type B36 sequence. The arrow indicates the quantitated DI RNA band. Panel B indicates the average replication efficiency for 3 experiments using mutants MT2A, MT3C, and M24C. DIssE consistently replicate 1.6 fold of wild type B36 in these experiments.

RNA and DIssE RNA both replicated to detectable levels regardless of how well the mutant DI RNA's replicated, and time constants for all electroporations was 0.8, indicating that electroporation conditions were optimal. Mutants MT2A, MT3C, and M24C all appeared to produce positive strand DI RNA with varying efficiency compared to wild type DI B36 as detected by metabolic labeling. Quantitation by phosphorimager analysis revealed that MT2A replicated 5% better than B36, MT3C replicated 78% as well as B36, and M24C replicated 69% as efficiently as B36. See Figure 20. In order to determine if replicated DI RNA's had maintained the intended mutation, RT-PCR for negative strand RNA was carried out for DI RNA's MT2A, MT3C, and M24C. See Figure 21. Negative strand was amplified because positive strand DI RNA was transfected, so it becomes impossible to differentiate between input positive strand DI RNA and replicated positive strand DI RNA. Upon sequencing it was apparent that the mutant DI RNA's had undergone recombination events which restored the wild type sequence and the ability of the DI RNA to replicatein all three experiments. Recombination was not entirely unexpected since recombination to restore wild type sequence is a common occurrence in DI RNA replication experiments (33, 56, 109, 110).

The same conditions were used to test the replication efficiency of the second set of mutants ATW, ATW5', and ATW3'. In contrast to the first set of mutants ATW, ATW5', and ATW3' did not replicate nearly as efficiently as DI B36 and were generally undetectable by metabolic labeling. Sequencing was carried out by RT-PCR for negative strand DI RNA followed by sequencing of the PCR products to determine if the

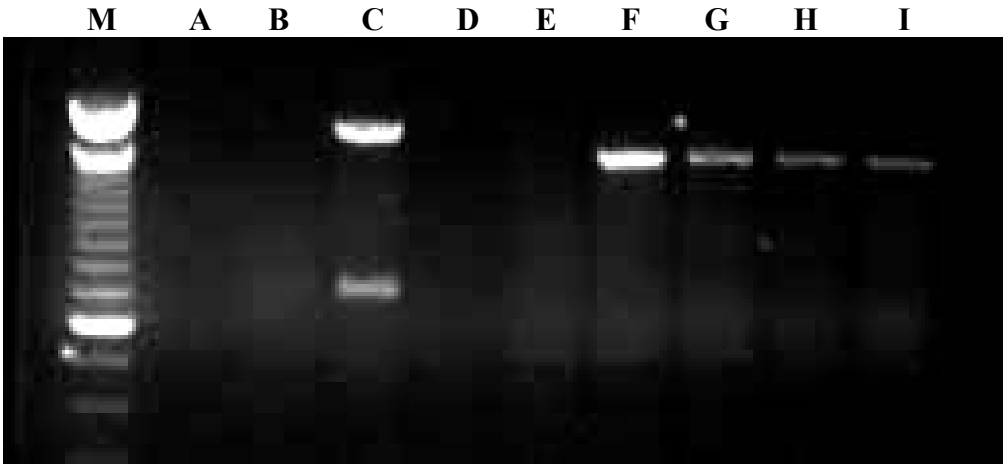

Figure 21. A representative RT-PCR for negative strand DI RNA. Lane M=100 bp marker, Lane A=No RT control, Lane B=No RNA control Lane C=pB36 PCR control, Lane D=A59 mock transfected, Lane E=DIssE, Lane F=B36 DI, Lane G=MT2A, Lane H=MT3C, Lane I=M24C. These products were amplified and used as sequencing templates.

intended mutations had been maintained. The results indicated that for the three complete experiments obtained, in two of the three experiments the mutations were maintained in ATW, ATW5', and ATW3'. In one of those two experiments ATW3' replicated at 4% of B36 levels and was undetectable in the other, while ATW and ATW5' were undetectable by phosphoimager analysis in both experiments. See Figure 22.

In the third experiment sequencing data indicated a mixed population of DI's. Some of the mutant nucleotides were reverted to wild type within the DI population, while part of the population had either a mutant or wild type base in a particular position. Sequencing was repeated for these DI's with the identical results. The double mutant ATW was supposed to carry the sequence 2U, 3G, 4A, 5U, 23A, 24U, 25C, 26A. Positions 2, 24, and 25 maintained their mutations. Position 3 was ambiguous for wild type C and mutant G, position 4 reverted to wild type, and position 5 was ambiguous for wild type A or mutant U. Positions 23 and 26 were ambiguous for mutant A or wild type U. With this nucleotide configuration the DI ATW population replicated 65% as well as wild type DI B36. Mutant DI ATW5' underwent a similar event which restored part of the wild type sequence and it replicated 71% as well as wild type DI. DI ATW5' has the mutations 23A, 24U, 25C, 26A from wild type 23U, 24A, 25G, and 26U, sequencing revealed that positions 24 and 25 maintained their mutations while positions 23 and 26 were ambiguous for mutant A or wild type U. DI ATW3' also restored part of its sequence to wild type. DI ATW3' has mutant nucleotides of 2U, 3G, 4A, 5U, sequencing revealed it restored wild type at positions 3 and 4 (A and C respectively),

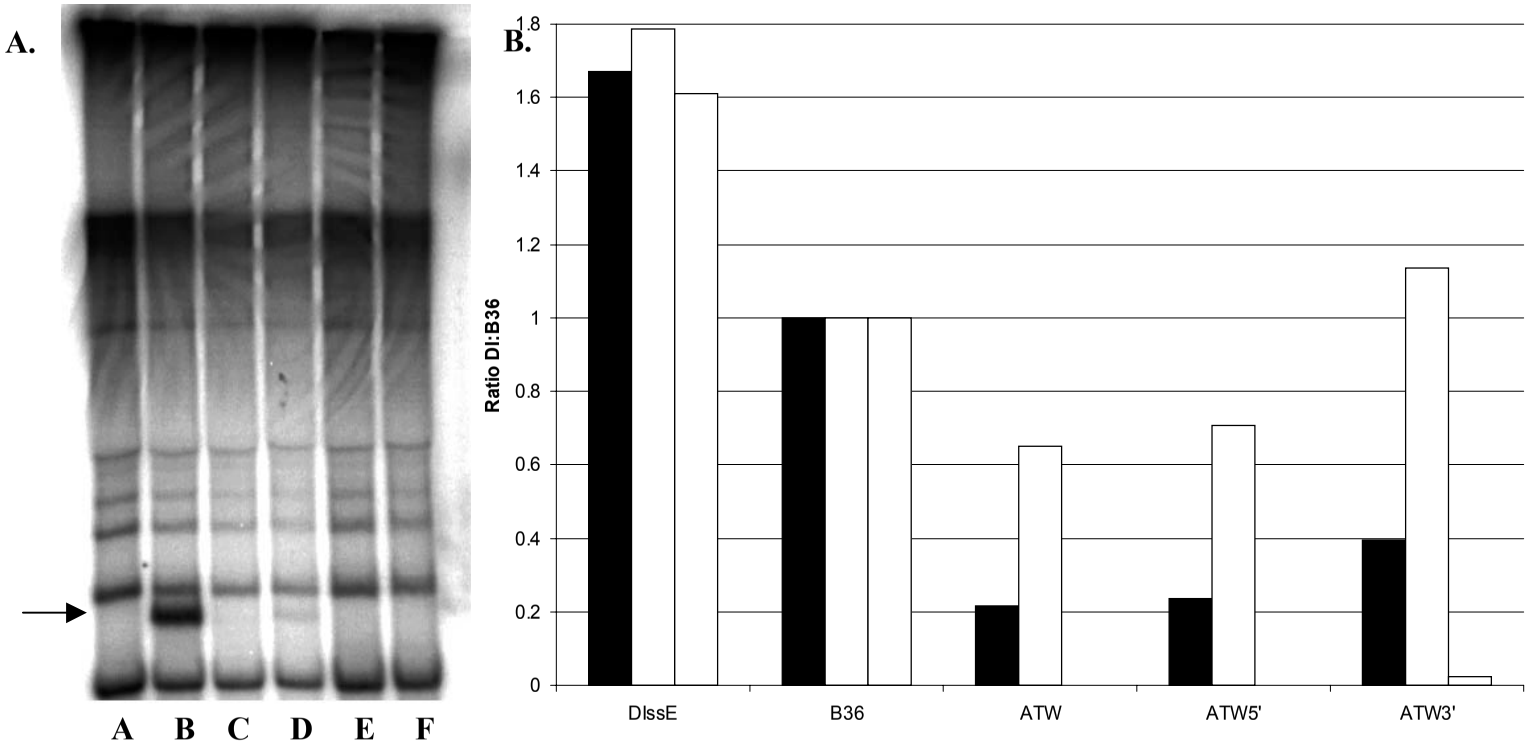

Figure 22. Panel A is a representative experiment for mutants ATW, ATW5', and ATW3'. A=A59 mock transfected, B=DIssE, C=ATW, D=B36, E=ATW5', F=ATW3'. In the two experiments that the mutants maintained their intended sequence only wild type DI's would replicate. DIssE was included as a control for DI replication and consistently replicated 1.8 fold of B36. The arrow indicates the quantitated DI band. Panel B is a summation of the DI replication data for these three mutants: the solid bar indicates an average replication efficiency of all 3 experiments, the dotted bar indicates the replication of sequence's with partial restoration of wild type sequence, and the gray bar indicates the average of the two experiments in which each DI maintained its intended mutation, see text for details.

maintained its mutant at position 2, was ambiguous at position 5 for wild type A or mutant U, and position 24 which was not targeted for mutation in this DI was ambiguous for A or U with A being the wild type nucleotide. In this experiment the ATW3' DI population replicated 13% better than wild type DI B36.

Semi-quantitative RT-PCR. Semi-quantitative RT-PCR was carried out for the 2 ATW, ATW5', and ATW3' DI RNA replication experiments in which positive strand was not detected and sequencing indicated that mutations were maintained. The results indicate that negative strand ATW5' mutants produced more negative strand RNA than B36 and ATW3' and ATW are produced below levels of B36. See Figure 23. Upon densitometric analysis of the data using the Storm software package indicates the differences in negative strand production is not as drastic as it appears on the ethidium stained gel and the negative strand produced by each mutant DI RNA is near to wild type DI B36 levels. Overzealous background correction by the software may account for this disparity.

Conclusions

Data for the first set of mutants MT2A, MT3C, and M24C are not unusual as recombination to wild type sequence occurs frequently in DI experiments (33, 56, 57, 109, 110). Recombinants indicate that the introduced mutations were selected against, and deleterious when compared to the wild type sequence. The intended mutant DI RNA could still be viable, but replicated at a much lower level than wild type. When the recombination event(s) that restores wild type sequence occurred, the wild type sequence is obviously replication competent and becomes the predominant species as seen in our

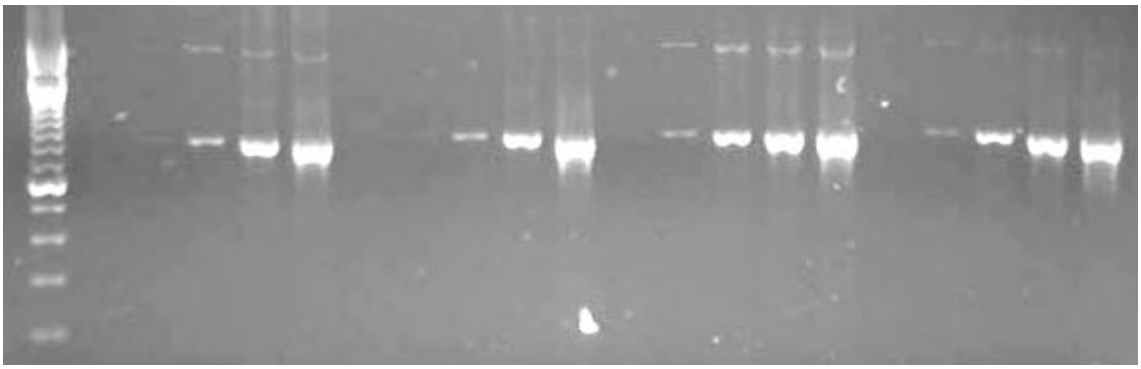

Figure 23. Semi-quantitative RT-PCR of negative strand B36, ATW, ATW3', and ATW5' DI's generated in DI replication assays. The upper bands are the DI negative strand specific bands, and the lower band indicate the GAPDH controls. Samples of each DI were removed at 14, 18, 22, 26, and 30 cycles of PCR and electrophoresed as described in Materials and Methods.

sequencing data. The differences in amount of wild type recombinant DI RNA produced is also not unusual, in Liu's recent work several recombinants with restored wild type sequence replicated at lower efficiencies than wild type DIssE (57). It is unknown if the lower replication efficiency observed for MT3C and M24C is relevant. It is possible that several recombination events took place and the lag between the time recombination started and the correct sequence was arrived at did not allow enough time for recombinant DI B36 to accumulate to wild type levels. It is also possible that there is an effect on host protein binding that is initial, deleterious, and short-lived and then recombination occurs after the initial effect is overcome, either by recognition of the polymerase complex by a signal within the 3' UTR, or use of a redundant system that allows replication to proceed after recombination has occurred.

Mutants ATW, ATW5', and ATW3' indicate that mutations in the 3' terminal 42 nucleotide host protein binding element disrupt positive strand synthesis. No positive strand synthesis could be detected by radiolabeling with $^{32}PO_4$ and exposure to a phosphoimager. Semi-quantitative RT-PCR indicates that negative strand synthesis is not significantly affected by introduced mutations. Data from Lin et al. suggest that the 3' terminal 55 nts plus poly (A) tail are essential for negative strand synthesis in DI constructs (55). The mutations we introduced into the region indicate did not significantly effect negative strand synthesis but had greatly decreased levels of positive strand synthesis. It is possible that our mutations were not in the proper location of the region to effect negative strand synthesis and that other mutations in the 3' terminal 55 nts might produce a phenotype that is negative strand defective.

The experiment in which partial restoration of wild type sequence was observed provides some evidence of which nucleotides are important for positive strand synthesis. The nucleotides that remained mutants probably have little effect on positive strand synthesis, those nucleotides are 2, 24, and 25. Nucleotide 4 was the only position that returned to wild type in the mutant DI RNA's carrying a 4A (ATW and ATW3'), suggesting that a wild type C at this position is necessary for positive strand synthesis. It is impossible to distinguish the contribution of individual nucleotides that were ambiguous (nucleotides 3, 5, 23, and 26) in positive strand synthesis from the data generated. The data from the partial sequence restoration experiment indicates that the sequence carried would restore DI positive strand replication, the ATW3' mutant actually replicated better than wild type B36 DI, and ATW and ATW5' replicated at lower efficiencies 65 and 71%, but this is one experiment so the data are not conclusive. In order to test the specific effects of each position a set of mutants will have to be developed that carry single point mutations or other combinations of the mutated nucleotides in question, instead of the arrangement of clustered point mutations used in this experiment.

CHAPTER V

DETERMINING THE ROLE OF THE 3' 42 NUCLEOTIDE HOST PROTEIN BINDING ELEMENT OF THE MHV 3' UTR USING THE cDNA INFECTIOUS CLONE

Introduction

DI replication experiments demonstrated that mutations in the 3' terminal 42 nucleotide host protein binding element had effects on replication of DI RNA's. Three of the mutants studied had deleterious effects on positive strand synthesis, while three other mutants recombined to restore functional wild type sequence. Recombination to wild type sequence essentially masked any mutant DI RNA that may have replicated poorly in the background of a normally replicating wild type DI population. Recombination also impaired our ability to construct mutant viruses using targeted recombination. In order to eliminate recombination, infectious cDNA clones carrying mutations explored in Chapters III and IVs were constructed using Ralph Baric's MHV-A59 infectious clone system (108).

Yount et al. recently described the construction of infectious cDNA clones for TGEV and MHV (107, 108). Their approach was to generate stable cDNA fragments of the genome, ligate them together in gene order so that reading frame of the MHV genome was intact. RNA is then transcribed from the assembled fragments, transfected into BHK cells, and isolate viruses from plaques generated. BHK cells were used because they are easier to manipulate and have been previously shown to produce MHV

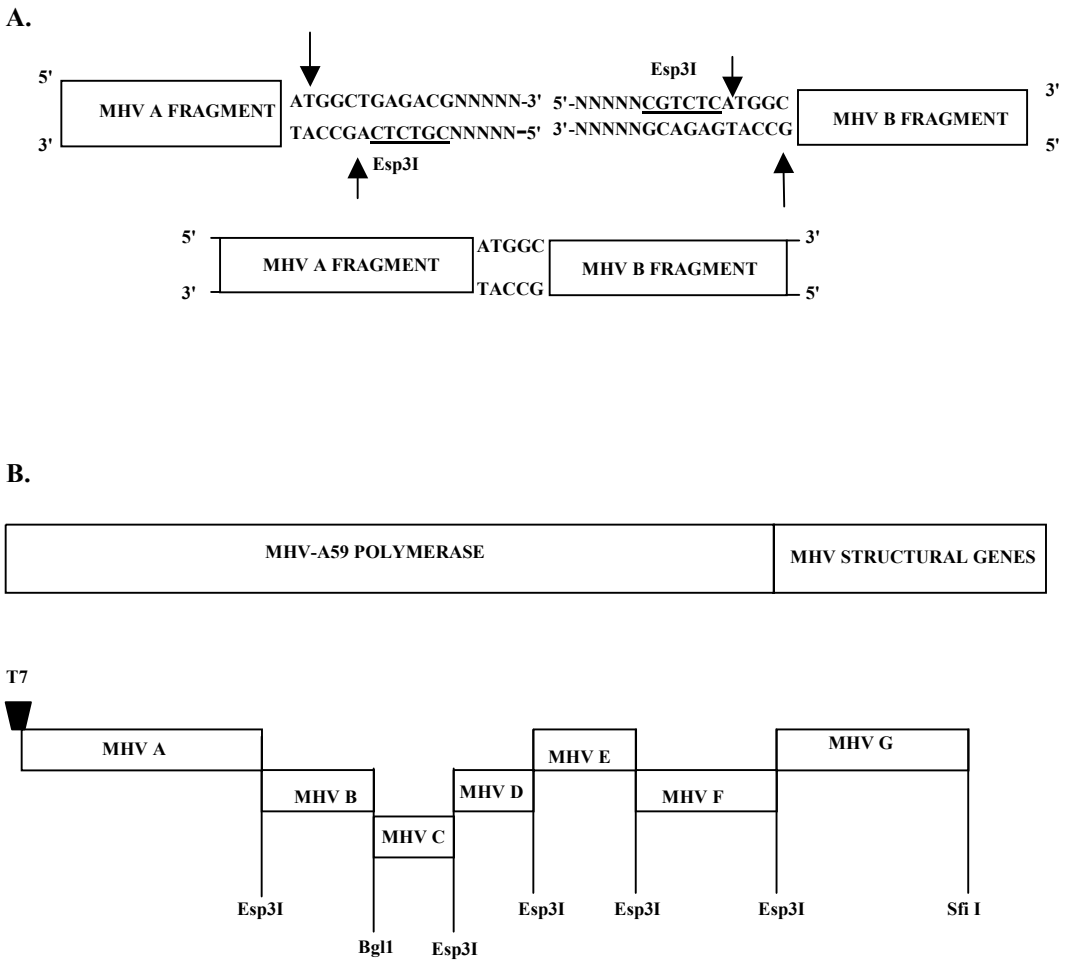

Figure 24. Panel A shows an example of construction of the template for infectious clone generation using the enzyme Esp3I. Esp3I recognizes a specific sequence 5'C GTCTC(N), cuts 3' to position (N) leaving a 4 nucleotide overhang that is non-palindromic when ligated with another similarly engineered Esp3I cut fragment. Panel B shows the arrangement of fragments and their restriction sites that allow for full length template assembly.

at equal levels to 17CL-1 and DBT cells when BHK cells express the MHV receptor (100).

A similar approach was used to generate the A59 infectious clone. Taking advantage of restriction enzymes that have specific recognition site but cut at a given position rather than nucleotide sequence within the restriction site, Baric's lab was able to generate 7 fragments that contain either a Bgl I or Esp 3I site for fragment assembly. We obtained fragment G which contains the 3' terminal 8.7 kb of the MHV A59 genome encompassing genes 2 through 7, the 3' UTR, and approximately 100 nucleotide poly (A) tail. The 5' end of fragment G contains an Esp3I site and the 3' end contains a Sfi I site, these sites are used to liberate the G fragment. G is then ligated to F fragment in a specific orientation due to the Esp3I site at the 3' end of F fragment. See Figure 24 for details. Fragment G was modified from pMH54 to introduce the Esp 3I site (108). Plasmid pMH54 was developed by Paul Masters for the FIPV spike protein based targeted recombination system (45). Our intent was to introduce our mutations into the G fragment by restriction fragment exchange between the unique Nru I site of the G fragment and pB36 and a Pac I site introduced into the Nsi I site just 3' to the poly (A) tail of pB36. Ideally, the mutants would be viable, but have unique phenotype when compared to wild type A59, but given the data from Chapter IV it is possible that mutants ATW, ATW5', and ATW3' would not produce a virus, and only accumulate negative strand viral RNA's, while mutants MT2A, MT3C, and M24C would not be viable.

Materials and Methods

Cells and virus. 17Cl-1 cells, a spontaneously transformed NIH 3T3 fibroblast cell line, were maintained at 37°C and 5% CO_2 in DMEM (Invitrogen Carlsbad, CA) supplemented with 10% calf serum (HyClone, Logan UT). DBT cells were maintained at 37°C and 5% CO_2 in DMEM supplemented with 10% calf serum (HyClone, Logan UT). Wild type MHV-A59 was used as a control for growth curves.

Plasmids. Ralph Baric kindly provided the plasmids carrying the appropriate fragments of the A59 infectious clone construct. The plasmid was introduced into TOP10F *E. coli* strain from Invitrogen Carlsbad, CA and grown in LB_{AMP} 50μg/ml for B, C, D, E, and G fragments or LB_{KAN} 50 μg/ml for A and F fragments and plasmid was purified using the Plasmid Mini Prep Kit (Bio-Rad Hercules, CA). Multiple colonies of each clone were selected and grown individually at 26ºC for 24 hours, fed with the proper media and grown an additional 24 hours and screened for the appropriate restriction pattern. Positive colonies were then pooled; this provided enough plasmid to carry out all manipulations.

Restriction fragment exchange. To generate a plasmid that contained compatible restriction sites five micrograms of DI B36 mutants generated in Chapter III, MT2A, MT3C, M24C, 24C, ATW, ATW5', and ATW3' were digested with 50 units of Nsi I (New England BioLabs Beverly, MA) and digested plasmid was purified from a 1.0% NuSeive GTG (FMC Rockland ME) 1X TAE agarose gel using the Qiaquick Gel Extraction Kit (Qiagen Valencia, CA) and quantitated by spectrophotometry. One-

hundred nanomoles of each oligonucleotide B36PacI3' (5'GCGCGCTTAATTAACGCGCCGGTGCA) (Sigma Genosys The Woodlands, TX) and B36PacI5' (5'CCGGCGCGTTAATTAAGCGCGCTGCA) (Sigma Genosys The Woodlands, TX) were annealed together by heating to 95°C for 30 seconds, cooling to 65°C for 30 seconds, then 2 minutes at 40°C, and then on ice until ligation to introduce a Pac I site into the Nsi I site, disrupting the Nsi I site. Ligations were assembled using 50 ng of each mutant plasmid and two μl of annealed oligo with 1X T4 ligation buffer (Invitrogen Carlsbad, CA), one unit T4 DNA ligase (Invitrogen Carlsbad, CA) in a 20 μl volume, incubated for 1 hour at 24°C. One microliter of each ligation reaction was electroporated into JM109's using the Gene Pulser II (Bio-Rad Hercules, CA) and 0.2 cm cuvettes (Bio-Rad Hercules, CA) recovered at 37°C and grown in LB_{AMP} at 37°C overnight. Putative Pac I positive plasmids were digested by Pac I (New England BioLabs Beverly, MA) and electrophoresed on 1.5% Seaplaque (FMC Rockland ME), 1X TAE agarose gels and stained with ethidium bromide. JM109's with the Pac I-B36 plasmids were grown and a glycerated stock was maintained at -70°C. Plasmids were purified using the Plasmid Midi Prep Kit (Bio-Rad Hercules, CA), and 10 μg of plasmid was digested with Nru I and Pac I, the resulting 178 bp fragment was gel purified from 1.0% NuSeive GTG (FMC Rockland ME) 1X TAE gels and extracted using the Qiaquick Gel Extraction Kit (Qiagen Valencia, CA). Nru I- Pac I fragments were quantitated by electrophoresis on 2.0% Seaplaque (FMC Rockland ME) 1X TAE ethidium bromide stained gels run with Low Mass DNA Marker (Invitrogen Carlsbad, CA) and quantitated by densitometry using the Alpha Imager 3.24 software (Alpha

Innotech San Leandro, CA). To receive the mutant sequence 10 μg of fragment G was digested with 50 units of Nru I and 50 units Pac I and gel purified from a 1.0% Metaphor (FMC Rockland ME) 1X TAE agarose gel using the Qiaquick Gel Extraction Kit (Qiagen Valencia, CA) and quantitated. Mutant Nru I-Pac I fragments were ligated into Sac I and Pac I digested G fragment using 50 ng G fragment and 2.4 ng of each mutant fragment in 1X T4 DNA ligase with 1 unit T4 DNA ligase (Invitrogen Carlsbad, CA) at 24°C for 1 hour and then transformed into TOP10F's. G fragment was grown at 29°C for 24 hours followed by colony screening by Esp 3I digestion. Plasmids which digested to produce a 9 kb fragment and 3 kb fragment were sequenced using primer 5666 (5'GTAGTGCCAGATGGGTTA) (Sigma Genosys The Woodlands, TX) using the same conditions as described in Chapter III. Primer 5666 is upstream of the Nru I site confirming the orientation and introduction of mutant sequence into the G fragment.

Production of the MHV-A59 infectious cDNA clone. Plasmids containing the A fragment of the MHV cDNA were digested with Mlu I (New England BioLabs Beverly, MA) and treated with 15 units of calf intestinal phosphatase (New England BioLabs Beverly, MA). BsmB I, an isoschizomer of Esp 3I, was used to liberate the A fragment. The B fragment was excised with Bgl I (New England BioLabs Beverly, MA). C, D, E and F fragments were digested from their parental plasmids using BsmB I. G fragment was digested with Sfi I (New England BioLabs Beverly, MA) treated with 15 units of calf intestinal phosphatase and digested with BsmB I. Fragments A, B, C, D, and G were electrophoresed on 0.8% Metaphor agarose 1X TAE gels, fragments E and F were electrophoresed on 1% Metaphor agarose 1X TAE gels. All gels were stained with

ethidium bromide visualized with Dark Reader technology (Claire Chemical Research Denver CO) and the appropriate fragment was excised and purified using the Qiaex II gel purification system. Recovered DNA was quantitated by spectrophotometry. 1.5 μg of total DNA composed of each of the fragments in equal molar ratios was ligated using 50 units T4 DNA ligase at 14°C overnight. The resulting full-length cDNA template was used in in-vitro transcription reactions with the mMessage mMachine T7 kit (Ambion Austin, TX) with a 1:1 GTP to cap ratio. To provide N transcript in trans N was amplified from the G fragment using the following primer (5' TCGGCCTCGATGGCCATTTAGGTGACACTATAGATGTCTTTTGTTCCTGGGCAAG) and primer a59Ng3'(-) (5' TCCGGA$(TTT)_8$ TTACACATTAGAGTCATCTTCTAACC). The PCR product was gel purified and used in in vitro transcription reactions with the mMessage mMachine SP6 kit (Ambion Austin, TX). The transcripts from the T7 and SP6 reactions were electroporated by 3 pulses at 0.85 kV, and 25μF into $8x10^6$ BHK-R cells. The electroporation reaction was allowed to recover for ten minutes at room temperature and then plated onto DBT cells that were 70% confluent in a T-75 flask.

Plaque isolation. After electroporation of the assembled infectious clone into MHV receptor expressing BHK cells, cultures were incubated for two days. The cells were then frozen at -80°C, thawed, refrozen twice, and sonicated on ice for 3 pulses of 30 seconds at 30% power in a cup probe using a Heat Systems Sonicators Ultrasonic Processor XL (Heat Systems Sonicators Farmingdale, NY). The resulting suspension was then centrifuged for 15 minutes at 2,500xg at 4°C. The supernatant was removed

and stored at -80°C for subsequent selection viruses. To isolate individual viruses an aliquot of each mutant was serially 10 fold diluted and incubated on DBT cells overlayed with 0.8% agarose and incubated at 37°C for 3 days. At the end of 3 days individual plaques were isolated using a plugged pasteur pipette and innoculated onto a 70% confluent monolayer of 17Cl-1 cells in a 65 mm tissue culture dish (Becton Dickinson and Company Franklin Lakes, NJ) until CPE enveloped 85% of the monolayer. At this point the media was removed and stored at –70°C.

RNA isolation and sequencing. RNA from the monolayer of 17Cl-1 cells infected with the mutant virus was isolated using the RNeasy RNA extraction kit (Qiagen Valencia, CA). RT was carried out using the primer 17TG with the sequence 5' TTTTTTTTTTTTTTTTTG, which should select any mRNA with a C residue 5' to the poly (A) tail, including viral RNA. RT reactions were carried out by following Invitrogen Carlsbad, CA's protocol for SuperScript II RNase H^- Reverse Transcriptase. Five hundred nanograms of 17TG was incubated with 1 μg of total RNA with 1.2mM dNTP's in a volume of 12 μl, incubated at 65°C for 5 minutes and chilled on ice for 2 minutes. Following the first incubation step, Invitrogen's 5X 1^{st} strand buffer (Invitrogen Carlsbad, CA) was added to 1X concentration with 10μM DTT and DEPC water in a volume of 19μl, this mix was incubated at 42°C for 2 minutes then 200 units (1μl) of SuperScript II was added and incubated at 42°C for 50 minutes (Invitrogen Carlsbad, CA). The RT was heat inactivated at 70°C for 15 minutes. PCR for sequencing reactions was carried out using the B36For (5'TAGTACTCTACCTGGTTTT) and 17TG primers under the conditions: 34 cycles of

95ºC for 30 seconds, 40ºC for 60 seconds and 72ºC for 60 seconds, followed by a final extension for 15 minutes at 72ºC. A total of 4 PCR reactions were combined and gel purified using the Wizard PCR purification kit (Promega Madison, WI) quantitated and sequenced using the primer 5666 (5'GTAGTGCCAGATGGGTTA), and the Big Dye Terminator kit (ABI Foster City, CA). Sequencing was performed on 600 ng of gel purified material under the following cycle conditions: preheat thermocycler to 96°C then 98°C for 30 seconds, 50°C for 15 seconds, 60°C for 4 minutes, repeated 24 times. Unincorporated nucleotides were removed using Micro-Spin 30 columns (Bio-Rad Hercules, CA). Columns were warmed to room temperature and tapping cleared any bubbles. The columns were allowed to settle for 30 minutes and the plug was removed from the bottom. The columns were then centrifuged at 100 xG for 2 minutes. Columns were removed and place in fresh tubes. The sequencing reaction was added and centrifuged again at 700 xG for two minutes. The columns were discarded and the reaction was dried completely and taken to the Gene Technologies Laboratory at Texas A&M University Department of Biology. The program Sequencher (Gene Codes Corporation Ann Arbor MI) was used to evaluate the sequences.

Growth curves. If mutant virus is obtained growth curves will be carried out in order to determine the effects of our mutations on viral replication. 17Cl-1 monolayers will be infected with an equivalent M.O.I. of each mutant was well as wild type A59 virus. At time points 2, 4, 6, 12, 24, and 48 hours. Virus production was quantitated by plaque assay on L2 monolayers overlayed with 0.8% agarose and stained with crystal violet 2 g

crystal violet (Sigma St. Louis, MO) 800 ml methanol (EM Science Gibbstown, NJ), and 200 ml water, and quantitated.

Results

To date we have successfully introduced the mutations MT2A, ATW5', ATW3', ATW, MT3C, M24C, and 24C into the MHV G fragment by restriction fragment exchange. Putative mutant positive plasmids were screened by Esp 3I (US Biological Swampscott MA), and by sequencing using the conditions described in Materials and Methods. Mutants ATW3' and MT3C have been constructed into the infectious clone system and were apparently viable. The viruses need to be plaque purified and sequenced to confirm the retention of the intended mutation. After the sequence of the 3' UTR has been established growth curves will be carried out as described in Materials and Methods.

CHAPTER VI

CONCLUSIONS

Discussion

The goal of this dissertation was to determine the structural requirements for the 3' terminal 42 nucleotide host protein binding element in MHV replication. A mutagenic study of the 3' terminal 42 nucleotide host protein binding element demonstrated that primary and secondary structure both play a role in host protein binding to viral RNA. Compensatory mutants that restored wild type computer predicted secondary structure were developed and restored host protein binding. Two mutants were developed that bound protein at elevated levels when compared to wild type probe.

Comparisons between the computer predicted RNA secondary structure models of the wild type 3' terminal 42 nucleotide and enzymatic probing data of the 3' terminal 166 nucleotides reveals that the 42 nucleotide model matches the digestion data more accurately than the computer predicted model for the 3' terminal 166 nucleotides, suggesting that the wild type secondary structure predicted for the 3' terminal 42 nucleotides may form in a larger RNA molecule.

In order to determine the biological effects of the mutants developed, targeted recombination was performed in an attempt to introduce these mutations into infectious virions. The results of targeted recombination indicate that the primary structure of the 3' terminal 42 nucleotide host protein binding element was strongly selected for. RNA molecules that recombined to restore wild type primary and secondary structure of the 3'

terminal 42 nucleotide host protein binding element were able to replicate and were selected.

Although we were unable to introduce these mutations into viruses by targeted recombination it was possible to examine their effect on RNA replication utilizing DI RNA's. DI RNA's carrying mutations within the 3' terminal 42 nucleotide host protein binding motif were unable to produce positive strand DI that could be detected in our assays. Negative strand DI RNA was sequenced in order to determine what replicated and three of the mutants that apparently replicated had recombined to restore wild type primary structure in all three experiments attempted. One of these mutants, MT3C, had been tested by Yu and Leibowitz in DIssE and it also recombined to restore wild type secondary structure and DI RNA positive strand synthesis (110). The other 3 mutants tested were also unable to produce detectable levels of positive strand DI B36. Sequencing demonstrated that the mutations were maintained and semi-quantitative RT-PCR demonstrated that negative strand synthesis was not adversely affected by the mutations introduced. It is worth noting that the DI RNA's that could synthesize negative strand only had one point mutation within the 11 nucleotide motif, and the other mutations in those mutants lay outside the region. These results indicate that conservation of primary structure in the 11 nucleotide motif is necessary for DI RNA replication. However in one experiment positive strand DI RNA did replicate, and upon sequencing it was discovered that partial restoration of primary structure occurred. Indicating that at least some of the point mutants introduced had no effect, while others were deleterious.

In order to establish the effect of the mutations on viral replication the MHV-A59 infectious cDNA clone developed by Baric's lab was mutated (108). Mutants of the 3' terminal 42 nucleotide host protein binding element that had the greatest decrease in host protein binding, and the greatest increase in host protein binding were engineered into the G fragment of the infectious clone. Mutant G fragment was assembled into the full-length cDNA, transcribed and introduced into cells that support MHV replication. Initially each mutant virus was viable, but sequence and titers of the cloned viruses have not been established.

Previous work on MHV has established the importance of host proteins interacting with the MHV genome. PTB binds to the leader RNA as well as the 5' end of the genome complement, data suggests PTB is important for MHV transcription (35, 52). It has recently been demonstrated that over-expression of PTB decreases viral mRNA transcription but not translation (17). PTB also alters RNA secondary structure and may help mediate 5' to 3' interactions of the MHV genome through PTB interactions with hnRNP-A1(36). hnRNP-A1 interacts with the TRS and 3' UTR; DI mutants with decreased hnRNPA-1 binding also had a decrease in transcription and replication (36, 36, 53)

Spagnolo and Hogue characterized an interaction between the poly A tail of DI's and PABP. PABP is a host cellular protein that is required for translation of eukaryotic mRNA's. PABP has been shown to interact with eIF4G in stimulating translation and circularization of mRNA's. Herold and Andino established that PABP interaction with the poly (A) tail of the poliovirus genome resulted in circularization of the genome that

resulted in the initiation of complementary strand RNA synthesis (32). It is likely that PABP binding to the MHV 3' UTR has a similar effect on virus replication as Spagnolo and Hogue hypothesize (93). Further work on PABP interactions with poliovirus genome suggests that the circularized genome is translationally active. Support for PABP mediated circularization of viral genomes comes from Svitkin et. al. who demonstrated that the PABP eIF4G interaction was essential for translation (97), another supporting study showed that cleavage of eIF4G by poliovirus proteins will stop translation of the poliovirus genome (65). For MHV it is possible that PABP, PTB, and hnRNP-A1 all interact to form the protein-protein bridge necessary for viral complementary strand synthesis.

To date, no interaction between PABP, PTB, and hnRNP-A1 has been established in MHV although there is support for PTB and hnRNP-A1 interactions. If it were found that PABP binds to either PTB or hnRNP-A1 it would help establish the circularization of MHV as an essential step for virus replication. In order to test if PTB, hnRNP-A1, and PABP interact co-immunoprecipitation assays could be performed. If an interaction is established then the poliovirus 3C protease that cleaves PABP could be selectively expressed in MHV infected cells. If the interaction results in cessation of translation then cleavage of PABP would result in a deleterious phenotype and the effects could be measured by western blot for MHV proteins. If PABP plays another role in the MHV lifecycle cells expressing 3C protease could be used to determine if PABP influences replication or negative strand synthesis.

Nanda and Leibowitz established the identity of four proteins that specifically interact with the MHV 3' terminal 42 nucleotide host protein binding element as mitochondrial aconitase, mitochondrial HSP70, HSP60, and HSP40 (68). They also established that metabolic regulation of the RNA binding activity of mitochondrial aconitase did influence viral growth. Mitochondrial aconitase has a cytosolic counterpart that is a conditional RNA binding protein, iron regulatory protein (IRP). IRP regulates the translation of ferritin and transferrin through specific interactions with the 5' and 3' UTR's of each mRNA depending upon the iron concentration of the cell. By increasing iron concentration of the cell Nanda and Leibowitz were able to increase the amount of mitochondrial aconitase in the cell which may have influenced the RNA binding properties of mitochondrial aconitase and increased viral titer compared to virus infected cells that did not receive iron treatment at early times post infection.

The results described here demonstrate the role of the 3' terminal 42 nucleotide host protein binding element in viral RNA replication. Mutants of the 3' terminal 42 nucleotide host protein binding element were readily selected against in targeted recombination experiments, and again in DI replication experiments. Three of the mutants generated were maintained in DI replication assays, but these mutants were defective in positive strand synthesis. The positive strand defective phenotype explains the inability to isolate mutant virus from targeted recombination. It is also possible that the 11 nucleotide motif is required for initiation of negative strand synthesis. Mutations outside the region accumulated negative strand, while mutations within the 11 nucleotide motif were recombined back to wild type. Although in the infectious cDNA construct

the mutants generated virus, but these viruses have not yet been sequenced or compared to wild type virus in growth curve experiments.

The exact mechanism for the host protein interaction has not been characterized, but it is possible that binding of the mitochondrial aconitase complex to the 11 nucleotide motif is a necessary signal for another complex of proteins to interact and begin negative strand synthesis. It is possible that the other proteins which bind the 5' and 3' UTR's interacted as proposed, the genome circularized as predicted, but the initiation signal for negative strand synthesis did not occur due to the missing mitochondrial aconitase complex. Another possibility is that the mitochondrial aconitase complex binding initiates a conformational change in concert with the secondary structure change described for PTB (35). Since the mitochondrial aconitase complex did not bind, the proper RNA conformation for negative strand synthesis was not achieved. Without the proper conglomeration of RNA, host proteins, and viral proteins the appropriate signal for negative strand synthesis was absent so no negative strand synthesis occurred.

Results from Lin et. al. identified the signal for complementary strand synthesis as the 3' terminal 55 nucleotides (55). The complementary strand synthesis signal was identified by a deletion mutant of the 3' terminal 55 nucleotides, not a mutagenic study of the same region. Obviously the 3' terminal 42 nucleotide element resides within the 3' terminal 55 nucleotides and the 11 nucleotide motif is present therein. It is likely that by deleting the 3' terminal 42 nucleotide element of the 3' UTR Lin et al. removed signals for positive and negative strand synthesis. Had the 11 nucleotide motif remained intact

it is possible that they would have seen complementary strand synthesis. Lin et al demonstrate that the upstream 11 nucleotide motif was not sufficient for negative strand synthesis, if the upstream sequence was sufficient the 55 3' terminal deletion would have generated complementary strand RNA.

It is possible that the 11 nucleotide motif is the initiation signal for complementary strand synthesis and that a cis-acting sequence composed of the nucleotides from the end of the 11 nucleotide motif to the beginning of the poly (A) tail contain the signal for genomic RNA synthesis. DI replication assays ascertained that mutations outside of the 11 nucleotide motif did not effect complementary strand synthesis but only effected positive strand synthesis. Suggesting a role for other motifs in the 3' terminal 42 nucleotide host protein binding element as necessary signals for positive strand synthesis.

In order to investigate the possible mechanisms of initiation of negative strand synthesis the infectious clone could be used to develop a panel of mutants with single point mutations to precisely define the structural requirements for viral replication. If mutants that did not replicate were developed then strand specific northern blot analyses could be performed to determine if complementary strand RNA was produced. In order to establish a specific interaction between the protein in question and the RNA probes containing the same mutations introduced into the cDNA infectious clone could be assayed by gel shift. Another approach to show a specific interaction inside an infected cell would be to establish a time-course of host protein interacting with the 3' terminal 42 nucleotide element with mitochondrial aconitase or one of the other proteins of the

complex. Immunoprecipitation-RT-PCR and sequencing to determine the origin of the RNA captured could be applied. Another approach would be to expose radiolabeled mutant virus infected cells to UV light, cross-linking any protein:nucleic acid interaction and immunoprecipitate with antibodies to mitochondrial aconitase. If a viral RNA:protein interaction occurred then the immunoprecipitation product would be readily detectable. This data could be matched kinetically by appearance of complementary strand RNA, mRNA, or genomic RNA as detected by strand specific northern blot or RPA on an identical time course.

An approach to determine a specific protein's role in virus replication is to use siRNAs and block specific host proteins at translation, infect cells and perform growth curves to establish roles in virus growth. If effective deletion of a specific protein resulted in the impedance of replication, then real time PCR could be used to determine if the effect was on transcription, negative strand synthesis or positive strand synthesis. If it was found that the effect was not on viral replication or transcription then western Blot could be used to determine a role in translation. It is also possible that the protein binding plays a role in packaging of the viral genome, so EM studies could be used to identify the build up of viral RNA's.

Since the roles of the proteins identified in MHV replication have not been precisely identified it is possible that many of the proteins that bind to the 5' and 3' UTR's could act to protect viral RNA from degradation. Spangberg et. al. used an in vitro protection system to establish the role of La antigen in binding to the HCV 3' UTR

(95). Such a system could be used to define the role of PABP, hnRNP-A1, PTB, and the mitochondrial aconitase complex.

Another uncharacterized aspect of host protein binding to specific RNA secondary structures in the 3' terminal 42 nucleotide host protein binding element is whether the secondary structure forms first or if the protein binding forces a conformational change. A study of poly (C) binding protein, demonstrated that the HCV IRES must take shape first then poly (C) binding protein will attach. Poly(C) binding proteins role in HCV replication is unknown at this time (94). Conversely, PTB binding to the 3' UTR is thought to mediate a conformational change in MHV (35). If binding forces an RNA conformational change in order to initiate negative strand synthesis, it is possible that the change in conformation drives not only RNA:protein interactions but RNA:RNA interactions as well. Binding of the mitochondrial aconitase complex may open up an RNA binding site for a helicase. The helicase then initiates unfolding of the positive strand which in turn allows the replicase proteins to bind resulting in production of the strand full-length complementary strand RNA.

REFERENCES

1. **Ali, N., G. J. Prujin, D. J. Kennan, J. D. Keene, and A. Siddiqui.** 2000. Human La antigen is required for the hepatitis C virus internal ribosome entry site-mediated translation. Journal of Biological Chemistry **275:** 27531-27540.

2. **Ali, N. and A. Siddiqui,** 1995. Interaction of polypyrimidine tract-binding protein (PTB) with the 5' noncoding region of the hepatitis C virus RNA genome and its functional requirement in internal initiation of translation. Journal of Virology **69:** 6367-6375.

3. **Almazan, F., J. M. Gonzalez, Z. Penzes, I. E. Calvo, and L. Enjuanes.** 2000. Engineering the largest RNA virus genome as an infectious bacterial artificial chromosome. Proc Natl Acad Sci USA **97:** 5516-5521.

4. **An, S., C. Chen, X. Yu, J. L. Leibowitz, and S. Makino.** 1999. Induction of apoptosis in murine coronavirus-infected cultured cells and demonstration of E protein as an apoptosis inducer. Journal of Virology **73:** 7853-7859.

5. **An, S. and S. Makino.** 1998. Characterizations of coronavirus *cis*-acting RNA elements and the transcription step affecting its transcription efficiency. Virology **243:** 198-207.

6. **Andino, R., N. Boddeker, D. Silvera, and Gamarnik. A. V.** 1999. Intracellular determinants of picornavirus replication. Trends in Microbiology **7:** 76-82.

7. **Baric, R. S., S. A. Stohlman, M. K. Razavi, and M. M. C. Lai.** 1985. Characterization of the leader-related small RNAs in coronavirus-infected cells: further evidence for leader-primed mechanism of transcription. Virus Research **3:** 19-33.

8. **Bernstein, H. D., P. Sarnow, and D. Baltimore.** 1986. Genetic complementation among poliovirus mutants derived from an infectious cDNA clone. Journal of Virology **60:** 1040-1049.

9. **Blyn, L. B., J. S. Towner, B. L. Semler, and E. Ehrenfeld.** 2003.Requirement of poly(rC) binding protein 2 for translation of poliovirus RNA. Journal of Virology **71:** 6243-6246.

10. **Bonilla, P., A. Gorbalenya, and S. R. Weiss.** 1994. Mouse hepatitis virus strain A59 RNA polymerase gene ORF 1a: heterogeneity among MHV strains. Virology **198:** 736-740.

11. **Bredenbeek, P. J., A. F. H. Noten, M. C. Horzinek, and W. J. M. Spaan.** 1990. Identification and stability of a 30-kDA nonstructural protein encoded by mRNA 2 of mouse hepatitis virus in infected cells. Virology **175:** 303-306.

12. **Bredenbeek, P. J., C. J. Pachuk, A. F. H. Noten, J. Charite, W. Luytjes, S. R. Weiss, and W. J. M. Spaan.** 1990. The primary structure and expression of the second open reading frame of the polymerase gene of the coronavirus MHV-A59. Nucleic Acids Research **18:** 1825-1832.

13. **Burk, J., B. Devald, L. Jankovsky, and J. Gerdes.** 1980. Two coronaviruses isolated from central nervous system tissue of two multiple sclerosis patients. Science **209:** 933-934.

14. **Carstens, E. B., M. K. Estes, S. M. Lemon, J. Maniloff, M. A. Mayo, D. J McGeoch, C. R. Pringle, and R. B. Wickner.** 2000. Coronaviridae, p.835-849 *In* M. H. V. van Regenmortel, C. M., Fauquet, and J.-L Bodmer (ed.), Virus taxonomy., 7th ed. Academic Press, San Diego, California.

15. **Casias, R., V. Thiel, S. G. Siddell, D. Cavanagh, and P. Britton.** 2001. Reverse Genetics System for the Avian Coronavirus Infectious Bronchitis Virus. Journal of Virology **75:** 12359-12369.

16. **Chambers, P., C. R. Pringle, and A. J. Easton.** 1990. Heptad repeat sequences are located adjacent to hydrophobic regions in several types of virus fusion glycoproteins. Journal of General Virology **71:** 3075-3080.

17. **Choi, K. S., P.Huang, and M. M. C. Lai.** 2002. Polypyrimidine-tract-binding protein affects transcription but not translation of mouse hepatitis virus RNA. Virology **303:** 58-68.

18. **de Groot, R. J., W. Luytjes, M. C. Horzinek, B. A. M. van der Zeijst, W. J. M. Spaan, and J. A. Lenstra.** 1987. Evidence for a coiled-coil structure in the spike protein of coronaviruses. Journal of Molecular Biology **196:** 963-966.

19. **de Haan, C. A. M., P. S. Masters, X. Shen, S. R. Weiss, and P. M. J. Rottier.** 2002. The group-specific murine coronavirus genes are not essential, but their deletion, by reverse genetics, is attenuating in the natural host. Virology **296:** 177-189.

20. **de Vries, A. A. F., M. C. Horzinek, P. M. J. Rottier, and R. J. de Groot.** 1997. The genome organization of the nidovirales: similarities and differences between arteri-,toro-, and coronaviruses. Seminars in Virology **8:** 33-47.

21. **Denison, M. R., W. J. M. Spaan, Y. van der Meer, C. A. Gibson, A. C. Sims, E. Prentice, and X. T. Lu.** 1999. The putative helicase of the coronavirus mouse

hepatitis virus is processed from the replicase gene polyprotein and localizes in complexes that are active in viral RNA synthesis. Journal of Virology **73:** 6862-6871.

22. **Fazakerley, J. K., S. Amor, and A. A. Nash.** 1997 Animal model systems of MS, p.255-273. *In* W. C. Russell (ed.), Molecular biology of multiple sclerosis, John Wiley & Sons, Ltd. Chichester, New York.

23. **Fischer, F. D., D. Peng, S. T. Hingley, S. R. Weiss, and P. S. Masters.** 1997. The internal open reading frame within the nucleocapsid gene of mouse hepatitis virus encodes a structural protein that is not essential for replication. Journal of Virology **71:** 7567-7578.

24. **Fischer, F. D., C. F. Stegen, P. S. Masters, and W. A. Samsonoff.** 1998. Analysis of constructed E gene mutants of mouse hepatitis virus confirms a pivotal role for E protein in coronavirus assembly. Journal of Virology **72:** 7885-7894.

25. **Fleming, J., R. Shubin, M. Sussman, N. Casteel, and S.A.Stohlman.** 1989. Monoclonal antibodies to the matrix (E1) glycoprotein of mouse hepatitis virus protect mice from encephalitis. Virology **168:** 162-167.

26. **Frana, M. F., J. N. Behnke, L. S. Sturman, and K. V. Holmes.** 1985. Proteolytic cleavage of E2 glycoprotein of murine coronavirus: host-dependent differences in proteolytic cleavage and cell fusion. Journal of Virology **56:** 912-920.

27. **Gamarink, A. V. and R. Andino.** 2000. Interactions of viral protein 3CD and poly(rC) binding protein with the 5' untranslated region of the poliovirus genome. Journal of Virology **74:** 2219-2226.

28. **Gebhard, J. R. and E. Ehrenfeld.** 1992. Specific interactions of HeLa cell proteins with proposed translation domains of the poliovirus 5' noncoding region. Journal of Virology **66:** 3101-3109.

29. **Gontarek, R. R., L. L. Gutshall, K. M. Herold, J. Tsai, J. G. M. Sathe, C. Mao, Prescott, and A. M Del Vecchio.** 1999. hnRNP C and polypyrimidine tract-binding protein specifically interact with the pyrimidine-rich region within the 3'NTR of the HCV RNA genome. Nucleic Acids Research **27:** 1457-1463.

30. **Gonzalez, J. M., Z. Penzes, F. Almazan, E. Calvo, and L.Enjuanes.** 2002. Stabilization of a full-length infectious cDNA clone of transmissible gastroenteritis coronavirus by insertion of an intron. Journal of Virology **76:** 46551-4661.

31. **Graff, J., J. Cha, L. B. Blyn, and E. Ehrenfeld.** 1998. Interaction of poly(rC) binding protein 2 with the 5' noncoding region of hepatitis A virus RNA and its effects on translation. Journal of Virology **73:** 6015-6023.

32. **Herold, J. and R. Andino.** 2001.Poliovirus RNA replication require genome circularization through a protein-protein bridge. Molecular Cell **7:** 582-591.

33. **Hsue, B., T. Hartshorne, and P. S. Masters.** 2000. Characterization of an essential RNA secondary structure in the 3'untranslated region of the murine coronavirus genome. Journal of Virology **74:** 6911-6921.

34. **Hsue, B. and P. S. Masters.** 1997.A bulged stem-loop structure in the 3' untranslated region of the genome of the coronavirus mouse hepatitis virus is essential for replication. Journal of Virology **71:** 7567-7578.

35. **Huang, P.and M. M. C. Lai.** 1999. Polypyrimidine tract-binding protein binds to the complementary strand of the mouse hepatitis virus 3' untranslated region, thereby altering RNA conformation. Journal of Virology **73:** 9110-9116.

36. **Huang, P. and M. M. Lai.** 2001. Hetereogeneous nuclear ribonucleoprotein A1 binds to the 3' untranslated region and mediates potential 5'-3-end cross talks of mouse hepatitis virus RNA. Journal of Virology **75:** 5009-5017.

37. **Kalicharran, K. & Dales, S**. 1995. Dephosporylation of the nucleocapsid protein of inoculum JHMV may be essential for initiating replication. Advances in Experimental Medicine and Biology **380:** 485-489.

38. **Kappor, M., L., Zhang, P. M. Mohan, and R. Padmanabhan**, 2002. Synthesis and characterization of an infectious dengue virus type-2 RNA genome (New Guinea C strain). Gene **162:** 175-180.

39. **Kennedy, M. C., L. Mende-Mueller, G. A. Blondin, and J.Beinert.** 1992. Purification and characterization of cytosolic aconitase from beef liver and its relationship to the iron-responsive element binding protein. Proc Natl Acad Sci USA **89:** 11730-11734.

40. **Kim, Y., Y. S. Jeong, and S. Makino.** 1993. Analysis of *cis*-acting sequences essential for coronavirus defective interfering RNA replication. Virology **197:** 53-63.

41. **Kim, Y. and S. Makino.** 1995. Characterization of a murine coronavirus defective interfering RNA internal *cis*-acting replication signal. Journal of Virology **69:** 4963-4971.

42. **Koetzner, C. A., M. M. Parker, C. S. Ricard, L. S. Sturman, and P. S. Masters.** 1992. Repair and mutagenesis of the genome of a deletion mutant of the coronavirus mouse hepatitis virus by targeted RNA recombination. Journal of Virology **66:** 1841-1848.

43. **Kolykhalov, A. A., K. Mihalik, S. M. Feinstone, and Rice, C. M.** 2000.Hepatitis C virus-encoded enzymatic activities and conserved RNA elements in the 3' nontranslated region are essential for virus replication in vivo. Journal of Virology **74:** 2046-2051.

44. **Kubo, H., Y. K. Yamada, and F. Taguchi.** 1994. Localization of neutralizing epitopes and the receptor binding site within the amino-terminal 330 amino acids of the murine coronavirus spike protein. Journal of Virology **68:** 5404-5410.

45. **Kuo, L., G.-J., Godeke M. J. B. Raamsman, P. S. Masters, and P. M. J. Rottier**. 2000. Retargeting of coronavirus by substitution of the spike glycoprotein ectodomain: crossing the host cell species barrier. Journal of Virology **74:** 1393-1406.

46. **Kuo, L. and P. S. Masters.** 2002. Genetic evidence for a structural interaction between the carboxy termini of the membrane and nucleocapsid proteins of mouse hepatitis virus. Journal of Virology **76:** 4987-4999.

47. **Kuyumcu-Martinez, N. M., M. Joachims, and R. E. Lloyd.** 2002.Efficient cleavage of ribosome-associated poly(A)-binding protein by enterovirus 3C protease. Journal of Virology **76:** 2062-2074.

48. **Lampert, P. W., J. K. Sims, and A. J. Kniazeff.** 1973. Mechanism of demyelination in JHM virus encephalomyelitis. Acta Neuropathologica **24:** 79-85.

49. **Lanford, R. E., H. Lee, D. Chavez, B. Guerra, and K. M. Brasky.** 2001. Infectious cDNA clone of the hepatitis C virus genotype 1 prototype sequence. Journal of General Virology **82:** 1291-1297.

50. **Lee, H.-J., C.-K., Shieh. A., Gorbalenya. E. V. Koonin, N. Lamonica, J.Tuler, A. Bagdzhadzhyan, and M. M. C. Lai.** 1989. The complete sequence (22 kilobases) of murine coronavirus gene-1 encoding the putative protease and RNA polymerase. Virology **180:** 567-582.

51. **Leparc-Goffart, I., S. T., Hingley. M. M. Chau. J. Phillips, E. Lavi, and S. R. Weiss.** 1998. Targeted recombination within the spike gene of murine coronavirus mouse hepatitis virus-A59: Q159 is a determinant of hepatotropism. Journal of Virology **72:** 9628-9636.

52. **Li, H., P. Huang, S. Park, and M. M. C. Lai.** 1999 Polypyrimidine tract-binding protein binds to the leader RNA of mouse hepatitis virus and serves as a regulator of viral transcription. Journal of Virology **73:** 772-777.

53. **Li, H., X. Zhang, R. Duncan, L. Comai, and M. M. C. Lai.**. 1997. Heterogeneous Nuclear Ribonucleoprotein A1 Binds to the Transcription-Regulatory Region of Mouse Hepatitis Virus RNA. Proc Natl Acad Sci USA **94:** 9544-9549.

54. **Li, W. and M. A**. **Brinton.** 2001. The 3' stem loop of the West Nile virus genomic RNA can suppress translation of chimeric mRNAs. Virology **287:** 49-61 .

55. **Lin, Y., C. Liao, and M. M. C. Lai.** 1994.Identification of the *cis*-acting signal for minus-strand RNA synthesis of murine coronavirus: implications for the role of minus-strand RNA in replication and transcription. Journal of Virology **68:** 8131-8140.

56. **Liu, Q., R. F. Johnson, and J. L. Leibowitz.** 2002.Secondary structural elements within the 3' untranslated region of mouse hepatitis virus strain JHM genomic RNA. Journal of Virology **75:** 12105-12113.

57. **Liu, Q., W. Yu, and J. L. Leibowitz.** 1997. A specific host cellular protein binding element near the 3' end of mouse hepatitis virus genomic RNA. Virology **232:** 74-85.

58. **Luytjes, W**. 1995. Coronavirus gene expression. Advances in Experimental Medicine and Biology **380**: 33-54.

59. **Luytjes, W., L. Sturman, P. J. Bredenbeek, J. Charite, B. A. M. van der Zeijst, M. C. Horzinek, and W. J. M. Spaan.** 1987. Primary structure of the glycoprotein E2 of coronavirus MHV-A59 and identification of the trypsin cleavage site. Virology **161:** 479-487.

60. **Maeda, J., J. F. Repass, A. Maeda, and S. Makino.** 2001. Membrane topology of coronavirus E protein. Virology **281:** 163-169.

61. **Makino, S., C.-K. Shieh, L. H. Soe, S. R. Weiss, and M. M. C. Lai.** 1989. Primary structure and translation of a defective interfering RNA of murine coronavirus. Virology **166:** 550-560.

62. **Makino, S., S. A. Stohlman, and M. M. C**. **Lai.** 1986. Leader sequences of murine coronavirus mRNAs can be freely reassorted: evidence for the role of free leader RNA in transcription. Proc Natl Acad Sci USA **83:** 4204-4208.

63. **Masters, P. S., C. A. Koetzner, C. A. Kerr, and H. Yong.** 1994. Optimization of targeted RNA recombination and mapping of a novel nucleocapsid gene mutation in the coronavirus, mouse hepatitis virus. Journal of Virology **68:** 328-337.

64. **Mellits, K., J. M., Meredith, J. B Rohil, D. J. Evans, and J. W. Almond.** 1998.Binding of cellular factor to the 3' untranslated region of the RNA genomes of entero- and rhinoviruses plays a role in virus replication. Journal of General Virology **79:** 1715-1723.

65. **Michel, Y. M., A. M. Borman, S. Paulous, and K. M. Kean.** 2001. Eukaryotic initiation factor 4G -poly(A) binding protein interaction is required for poly(A) tail-mediated stimulation of picornavirus internal ribosome entry segment-driven translation but not for X-mediated stimulation of hepatitis C virus translation. Molecular and Cellular Biology **21:** 4097-4109.

66. **Moorman, R. J. M., H. G. P. van Gennip, G. K. W. Miedema, M. M. Hulst, and P. A. van Rijn,** 1996. Infectious RNA transcribed from an engineered full-length cDNA template of the genome of a pestivirus. Journal of Virology **70:** 763-770.

67. **Nanda, S. K., R. F. Johnson, Q. Liu, and J. L. Leibowitz.** 2003. Mitochondrial HSP70, HSP40 and HSP60 bind to the 3' Untranslated region of the mouse hepatitis virus genome. Personal collection, R. Johnson

68. **Nanda, S. K. and J. L. Leibowitz.** 2001. Mitochondrial aconitase binds to the 3' untranslated region of the mouse hepatitis virus genome. Journal of Virology **75:** 3352-3362.

69. **Narayanan, K., A. Maeda, J. Maeda, and S. Makino.** 2000.Characterization of the coronavirus M protein and nucleocapsid interaction in infected cells. Journal of Virology **74:** 8127-8134.

70. **Nguyen, V. and B. G. Hogue.** 1997. Protein interactions during coronavirus assembly. Journal of Virology **71:** 9278-9284.

71. **Ochs, K., L. Saleh, G. Bassili, V. J. Sonntag, A. Zeller, and M. Niepmann.** 2002. Interaction of translation initiation factor eIF4B with the poliovirus internal ribosome entry site. Journal of Virology **76:** 2113-2122.

72. **Odreman-Macchioli, F. E., S. G. Tisiminetzky, M. Zotti, F. E. Baralle, and E. Buratti.** 2000. Influence of the correct secondary structure and tertiary RNA folding on the binding of cellular factors to the HCV IRES. Nucleic Acids Research **28:** 875-885.

73. **Ontiveros, E., Kuo, L., Masters, P. S. and Perlman, S.** 2001. Inactivation of expression of gene 4 of mouse hepatitis virus strain JHM does not affect virulence in the murine CNS. Journal of Virology **289:** 230-238.

74. **Pasternak, A. O., A. P. Gultyaev, W. J. M. Spaan, and E. J. Snijder.** 2000. Genetic manipulation of arterivirus alternative mRNA leader-body junction sites reveals tight regulation of structural protein expression. Journal of Virology **74:** 11642-11653.

75. **Proutski, V., M. W. Gaunt, E. A. Gould, and E. C. Holmes.** 1997. Secondary structure of the 3' untranslated region of yellow fever virus: implications for virulence, attenuation and vaccine development. Journal of General Virology **78:** 1543-1549.

76. **Proutski, V., E. A. Gould, and E. C. Holmes,** 1997.Secondary structure of the 3' untranslated region of flaviviruses:similarities and differences. Nucleic Acids Research **25:** 1194-1202.

77. **Racaniello, V. R. and D. Baltimore.** 1981. Cloned poliovirus complementary DNA is infectious in mammalian cells. Science **214:** 916-919.

78. **Repass, J. F. and S. Makino.** 1999. Importance of the positive-strand RNA secondary structure of a murine coronavirus defective interfering RNA internal replication signal in positive-strand RNA synthesis. Journal of Virology **72:** 7926-7933.

79. **Rettig, P. J. and G. P. Altshuler.** 1985. Fatal gastroentieritis associated with coronavirus-like particles. American Journal of Diseases of Children **139:** 245-248.

80. **Rice, C. M., A. Grakoui, R. Galler, and T. J. Chambers.** 1989. Transcription of infectious yellow fever RNA from full-length cDNA templates produced by in vitro ligation. New Biology **1:** 285-296.

81. **Rousset, S., P. Moscovici, P. Lebon, J. P. Barbet, P. Helardot, B. Mace, L. T. Vinh, and C. Chany.** 1984. Intestinal lesions containing coronavirus-like particles in neonatal necrotizing enterocolitis: an ultrastructural analysis. Pediatrics **73:** 218-224.

82. **Satyanarayan, T., M. Bar-Joseph, M. Mawassi, M. R. Albiach-Marti, M. A. Ayllon, S. Gowda, M. E. Hilf, P. Poreno, S. M. Garnsey, and W. O. Dawson.** 2001. Amplification of citrus tristeza virus from a cDNA clone and infection of citrus trees. Virology **280:** 87-96.

83. **Sawicki, S. G. and D. L. Sawicki.** 1990. Coronavirus transcription: subgenomic mouse hepatitis virus replicative intermediates function in RNA synthesis. Journal of Virology **64:** 1050-1056.

84. **Sawicki, S. G. and D. L. Sawicki.** 1995. Coronaviruses use discontinuous extension for synthesis of subgenome-length negative stands. Advances in Experimental Medicine and Biology **380:** 499-506.

85. **Schaad, M. C. & R. S. Baric.** 1994. Genetics of mouse hepatitis virus transcription: evidence that subgenomic negative strands are functional templates. Journal of Virology **68:** 8169-8179.

86. **Schuster, C., Isel, C., Imbert, I., Ehresmann, C., R. Marquet, and M. P. Kieny.** 2002. Secondary structure of the 3' terminus of hepatitis C virus minus-strand RNA. Journal of Virology **76:** 8058-8068.

87. **Sehtna, P. B., S. Hung, and D. A. Brian.** Coronavirus subgenomic minus-strand RNAs and the potential for mRNA replicons. Proc Natl Acad Sci USA **86:** 5626-5630. 1991.

88. **Shen, X. and P. S. Masters.** 2001. Evaluation of the role of heterogeneous nuclear ribonucleoprotein A1 as a host factor in murine coronavirus discontinuous transcription and genome replication. Proc Natl Acad Sci USA **98:**2717-2722

89. **Shi, P.-Y., M. Tilgner, M. K. Lo, K. A. Kent, and K. A. Bernard.** 2002. Infectious cDNA clone of the epidemic West Nile virus from New York City. Journal of Virology **76:** 5847-5856.

90. **Shi, S. T., P. Huang, , H.-P. Li, and M. M. C. Lai.** 2000. Heterogeneous nuclear ribonucleoprotein A1 regulates RNA synthesis of a cytoplasmic virus. EMBO Journal **19:** 4701-4711.

91. **Shimoike, T., S. Mimori, H. Tani, Y. Matsuura, and Miyamura, T.** 1999. Interaction of hepatitis C virus core protein with viral sense RNA and suppression of its translation. Journal of Virology **73:** 9718-9725.

92. **Siddell, S., H. Wege, and V. ter Meulen.** 1983. The biology of coronaviruses. Journal of General Virology **64:** 761-776.

93. **Spagnolo, J. F. and B. G. Hogue.** 2000. Host protein interactions with the 3' end of bovine coronavirus RNA and the requirement of the poly(A) tail for coronavirus defective genome replication. Journal of Virology **74:** 5053-5065.

94. **Spangberg, K. and S. Schwartz.** 1999. Poly(C)-binding protein interacts with the hepatitis C virus 5' untranslated region. Journal of General Virology **80:** 1371-1376.

95. **Spangberg, K., L. Wiklund, and S. Schwartz.** 2001. Binding of the La autoantigen to the hepatitis C virus 3' untranslated region protects the RNA from rapid degradation in vitro. Journal of General Virology **82:** 113-120.

96. **Stalcup, R. P., R. S. Baric, and J. L. Leibowitz.** 1998. Genetic complementation amongst three panels of mouse hepatitis virus gene 1 mutants. Virology **241:** 112-121.

97. **Svitkin, Y. V., H. Imataka, K. Khaleghpour, A. Kahvejian, H. D. Liebig, and N. Sonenberg.** 2001. Poly(A)-binding protein interaction with eIF4G stimulates picornavirus IRES-dependent translation. RNA **7:** 1743-1752.

98. **Thiel, V., J. Herold, B. Schelle, and S. G. Siddell.** 2001. Infectious RNA transcribed in vitro from a cDNA copy of the human coronavirus genome cloned in vaccinia virus. Journal of General Virology **82:** 1273-1281.

99. **Todd, S., J. S. Towner, D. M. Brown, and B. L. Semler,** 1997. Replication-competent picornaviruses with complete genomic RNA 3' noncoding region deletions. Journal of Virology **71:** 8868-8874.

100. **Tresnan, D. B., R. Levis, and K. V. Holmes.** 1996. Feline aminopepetidase N serves as a receptor for feline, canine, porcine, and human coronavirus in serogroup I. Journal of Virology **70:** 8669-8674.

101. **van der Most, R. G. and W. J. M. Spaan.** 1995. Coronavirus replication, transcription and RNA recombination. Advances in Experimental Medicine and Biology **380:** 11-31.

102. **van Dinten, L. C., J. A. den Boon, A. L. M. Wassenaar, W. J. M. Spaan, and E. J. Snijder.** 1997. An infectious arterivirus cDNA clone: identification of a replicase point mutation that abolishes discontinuous mRNA transcription. Proc Natl Acad Sci USA **94:** 991-996.

103. **Vaucher, Y. E., C. G. Ray, L. L. Minich, C. M. Payne, D. Beck, and P. Lowe.** 1982. Pleomorphic, enveloped virus-like particles associated with gastrointestinal illness in neonates. Journal of Infectious Disease **145:** 27-36.

104. **Whelan, S. P. J., A. Ball, J. N. Barr, and G. T. W. Wertz.** 1995. Efficient recovery of infectious vesicular stomatitis virus entirely from cDNA clones. Proc Natl Acad Sci USA **95:** 8388-8392.

105. **Williams, G. D., R.-Y. Chang, and D. A. Brian.** 1999. A phylogenetically conserved hairpin-type 3' untranslated region pseudoknot functions in coronavirus RNA replication. Journal of Virology **73:** 8349-8355.

106. **Yanagi, M., M. St. Claire, S. U., Emerson, R. H. Purcell, and J. Bukh.** 1999. In vivo analysis of the 3' untranslated region of the hepatitis C virus after in vitro mutagenesis of an infectious cDNA clone. Proc Natl Acad Sci USA **96:** 2291-2295.

107. **Yount, B., K. M. Curtis, and R. S. Baric.** 2000. Strategy for systematic assembly of large RNA and DNA genomes: transmissible gastroenteritis virus model. Journal of Virology **74:** 10600-10611.

108. **Yount, B., M. R. Denison, S. R. Weiss, and Baric, R. S.** 2002. Systematic assembly of a full-length infectious cDNA of mouse hepatitis virus strain A59. Journal of Virology **76:** 11065-11078.

109. **Yu, W. and J. L Leibowitz.** 1995. Specific binding of host cellular proteins to multiple sites within the 3' end of mouse hepatitis virus genomic RNA. Journal of Virology **69:** 2016-2023.

110. **Yu, W. and J. L. Leibowitz.** 1995. A conserved motif at the 3' end of mouse hepatitis virus genomic RNA required for host protein binding and viral RNA replication. Virology **214:** 129-138.

111. **Yu, X., W. Bi, S. R. Weiss, and Leibowitz, J. L.** 1994. Mouse hepatitis virus gene 5B protein is a new virion envelope protein. Virology **202:** 1018-1023.

112. **Zuker, M., D.H. Mathews & D.H. Turner.** 1999. Algorithms and thermodynamics for RNA secondary structure prediction: a practical guide, p.11-43. *In*. J. Barciszewski and B.F.C. Clark, (ed.), RNA biochemistry and biotechnology 1st ed. NATO ASI Series, Kluwer Academic Publishers, San Diego, California.

VITA

Reed F. Johnson

Current Address 1616 St. Andrews Dr.
Lawrence KS, 66046

Education:

B.S. Biology Kansas State University, Manhattan, KS, 1996

Ph.D. Medical Sciences Texas A&M University, College Station, TX, 2003

Publications:

Johnson, R.F. and J.L. Leibowitz. Mutagenesis of the 3'42 nucleotide host protein binding element of the MHV 3'UTR. Adv. Exp. Med. Biol., in press.

Liu, Q., R.F. Johnson, and J.L. Leibowitz. 2002. Secondary structural elements within the 3' untranslated region of mouse hepatitis virus strain JHM genomic RNA. Journal of Virology. **75:** 12105-12113.

Nanda, Santosh K., R.F. Johnson, Q. Liu, and J. L. Leibowitz. Mitochondrial HSP70 phosphorylation enhances protein binding to mouse hepatitis virus RNA. Submitted.